

**DEVELOPMENT OF ENERGY-EFFICIENT
PERSONALIZED THERMAL COMFORT DRIVEN
CONTROL IN HVAC SYSTEMS**

**A Thesis Submitted to the
Graduate School of Engineering and Sciences of
İzmir Institute of Technology
in Partial Fulfillment of the Requirements for the Degree of**

DOCTOR OF PHILOSOPHY

in Mechanical Engineering

**by
Cihan TURHAN**

**December 2018
İZMİR**

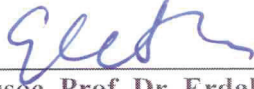
We approve the thesis of **Cihan TURHAN**

Examining Committee Members:



Prof. Dr. Gülden GÖKÇEN AKKURT

Department of Energy Systems Engineering, İzmir Institute of Technology



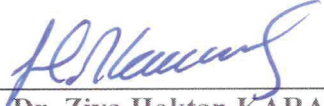
Assoc. Prof. Dr. Erdal ÇETKİN

Department of Mechanical Engineering, İzmir Institute of Technology



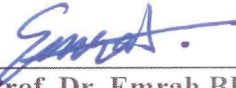
Assist. Prof. Dr. Barbaros ÖZDEMİREL

Department of Electrical and Electronics Engineering, İzmir Institute of Technology



Assist. Prof. Dr. Ziya Haktan KARADENİZ

Department of Mechanical Engineering, İzmir Katip Çelebi University



Assist. Prof. Dr. Emrah BIYIK

Department of Energy Systems Engineering, Yaşar University

28 December 2018



Prof. Dr. Gülden GÖKÇEN AKKURT

Supervisor

Department of Energy

Systems Engineering

İzmir Institute of Technology



Assoc. Prof. Dr. Silvio SIMANI

Co-Supervisor

Department of Engineering

University of Ferrara

Prof. Dr. Metin TANOĞLU

Head of the Department of

Mechanical Engineering

Prof. Dr. Aysun SOFUOĞLU

Dean of the Graduate School of

Engineering and Sciences

ACKNOWLEDGEMENTS

As the author of this thesis, I would like to express my deepest gratitude to my supervisor Prof. Dr. Gülden Gökçen Akkurt for her continuous enthusiasm and encouragement. I am also deeply grateful to my co-advisor Assoc. Prof. Dr. Silvio Simani for his invaluable input and patience during the thesis work and my visit in Italy.

I am very grateful to Assist. Prof. Dr. Barbaros Özdemirel and Enes Elmas for their valuable help in establishing an air-conditioner controller interface. I am also thankful for the feedback given by Assoc. Prof. Dr. Erdal Çetkin during my thesis process.

I would like to thank all my colleagues at Izmir Institute of Technology who have been supporting me during my research and the writing process. I also would like to thank my dear parents Yüksel and Müyesser Turhan for giving me a loving childhood and raising me up to believe in my skills. Last but definitely not least, I heartily thank my dear wife Emel Turhan for her love and patience during the long writing process.

ABSTRACT

DEVELOPMENT OF ENERGY-EFFICIENT PERSONALIZED THERMAL COMFORT DRIVEN CONTROL IN HVAC SYSTEMS

Increasing thermal comfort and reducing energy consumption are two main objectives of advanced HVAC control systems. Studies conducted in the last decade show that intelligent HVAC systems can greatly affect thermal comfort, health, satisfaction, and productivity of building occupants while decreasing the energy consumption. Also, personalized thermal comfort driven control of the HVAC systems is the most effective way of saving energy and maintaining thermal comfort.

In this thesis, an energy-efficient personalized thermal comfort control algorithm is developed to improve HVAC control system. The thesis presents a complete system to control algorithm which includes the deployment of wireless sensor network. First, a novel control algorithm is developed to perceived comfort conditions of occupants and to save energy. Then, a prototype of the personalized thermal comfort driven controller (PTC-DC) is manufactured and tested in a case building at Izmir Institute of Technology Campus, Izmir/Turkey. The proposed control strategy is tested between July 3rd, 2017 and November 1st, 2018, and compared with conventional controller in terms of energy savings and both energetic and exergetic approaches of thermal comfort.

The results showed that PTC-DC satisfies neutral thermal comfort for 92% of total measurements days while AMV=0 for only 6% of total measurement days for conventional controller. From energy consumption point of view, PTC-DC decreased energy consumption by 13.2% compared to conventional controller.

ÖZET

KİŞİSELLEŞTİRİLMİŞ ENERJİ ETKİN ISIL KONFOR BAZLI HVAC KONTROL SİSTEMLERİNİN GELİŞTİRİLMESİ

Akıllı HVAC sistemlerinin iki önemli amacı ısı konforu iyileştirmek ve enerji tüketimini azaltmaktır. Son yıllarda yapılan çalışmalar, akıllı HVAC sistemlerinin enerji tüketimini düşürdüğü gibi insan sağlığını, ısı konforu, memnuniyeti ve bina sakinlerinin verimliliğinin gelişimini doğrudan etkilediğini göstermektedir. Bunun yanısıra, kişiselleştirilmiş ısı konfor bazlı HVAC kontrol sistemleri ısı konforu ve enerji tasarrufunu sağlamakta en etkili yöntemdir.

Bu tezde, HVAC kontrol sistemlerini iyileştirmek amacıyla kişiselleştirilmiş ısı konfor bazlı HVAC kontrol algoritması geliştirilmiştir. Çalışmada kablosuz alıcı ağı oluşturularak bütünleşik bir kontrol sistemi sunulmuştur. Çalışmada öncelikle, kullanıcıların tercih ettiği konfor koşullarını ile birlikte enerji tasarrufunu sağlayan bir kontrol algoritması geliştirilmiştir. Daha sonra, bu yeni kontrol algoritmasını kullanan kişiselleştirilmiş enerji-etkin ısı konfor bazlı kontrolcü (PTC-DC) prototipi geliştirilmiş ve İzmir Yüksek Teknoloji Enstitüsü Kampüsü'nde bulunan bir binada test edilmiştir. Testler 03.07.2017- 01.11.2018 tarihleri arasında gerçekleştirilmiş ve binada mevcut bulunan konvansiyonel kontrolcü ile enerji tasarrufu ve hem enerjetik hem de ekserjetik ısı konfor yaklaşımları açısından karşılaştırılmıştır.

Konvansiyonel kontrolcü nötr ısı konforu toplam test günlerinin sadece %6'sında sağlarken, PTC-DC toplam test günlerinin %92'sinde sağlamaktadır. Enerji tüketimi açısından, PTC-DC konvansiyonel kontrolcüye göre %13,2 enerji tasarrufu sağlamıştır.

TABLE OF CONTENTS

LIST OF FIGURES.....	ix
LIST OF TABLES.....	xii
LIST OF SYMBOLS.....	xiii
CHAPTER 1. INTRODUCTION.....	1
1.1. Thermal Comfort.....	3
1.1.1. Energetic Approach.....	3
1.1.2. Exergetic Approach.....	5
1.2. Energy Consumption of HVAC Systems.....	5
1.3. HVAC System Control.....	7
1.4. Motivation.....	9
1.5. Aim of the Thesis.....	11
CHAPTER 2. HVAC CONTROL SYSTEMS.....	12
2.1. Conventional HVAC Control Systems.....	12
2.1.1. On/off Control.....	12
2.1.2. PID-type Controllers.....	13
2.2. Advanced HVAC Controllers.....	14
2.2.1. Artificial Neural Network Controllers.....	14
2.2.2. Fuzzy Logic Controllers.....	14
2.2.3. Adaptive Neuro-Fuzzy Inference System Controllers.....	18
2.2.4. Model Predictive Controllers.....	19
CHAPTER 3. THERMAL COMFORT APPROACHES.....	20
3.1. Energetic Approach of Thermal Comfort.....	21
3.1.1. Environmental Parameters.....	21
3.1.2. Personal Parameters.....	24
3.1.3. Indoor Air Quality (IAQ) Parameters.....	26

3.2. Exergetic Approach for Thermal Comfort	26
3.3. Actual Mean Vote (AMV).....	30
CHAPTER 4. LITERATURE REVIEW.....	32
4.1. Conventional HVAC Control Systems.....	32
4.2. Advanced HVAC Controllers.....	35
4.2.1. Artificial Neural Network Controllers	35
4.2.2. Fuzzy Logic Controllers	36
4.2.3. Adaptive Neuro-Fuzzy Inference System Controllers.....	38
4.2.4. Model Predictive Controllers.....	39
4.3. Personalized Thermal Comfort Controllers.....	42
4.4. Studies on Exergetic Thermal Comfort	51
CHAPTER 5. METATERIALS AND METHODS.....	53
5.1. Case Building	55
5.2. Development of PTC-DC	58
5.2.1. Development of PTC-DC software.....	59
5.2.2. Mobile application development	62
5.2.3. Development of PTC-DC hardware	62
5.3. Measurements.....	68
5.4. Assessment of PTC-DC.....	70
CHAPTER 6. RESULTS AND DISCUSSION.....	72
6.1. PTC-DC Software Development	72
6.2. Mobile Application Development	75
6.3. PTC-DC Hardware Development.....	76
6.4. Assessment of PTC-DC.....	79
6.4.1. Evaluation of energy consumption	80
6.4.2. Evaluation of thermal comfort	83
CHAPTER 7. CONCLUSIONS.....	94
REFERENCES	97

APPENDICES

APPENDIX A. THE WIRE DIAGRAM OF PTC-DC 112

LIST OF FIGURES

<u>Figure</u>	<u>Page</u>
Figure 1.1. A simple HVAC system	1
Figure 1.2. Schematic of AHU unit	2
Figure 1.3. Refrigeration cycle used in air-conditioner	2
Figure 1.4. HVAC control system	3
Figure 1.5. Energy consumption by sector in EU	6
Figure 1.6. Energy consumption by sector in Turkey	6
Figure 1.7. Share of total energy consumption in EU buildings	7
Figure 1.8. Classification of control methods in HVAC systems	9
Figure 2.1. On/off controller feedback for temperature control	12
Figure 2.2. Block diagram of a PID controller	13
Figure 2.3. The phrase of FL estimation model	15
Figure 2.4. A graphical explanation of two fuzzy sets and their union, intersection, and complement	17
Figure 2.5. An adaptive network	18
Figure 3.1. Fanger's PMV Model	20
Figure 3.2. Modelling of human body system	27
Figure 3.3. Human body system and its interactions with indoor environment	29
Figure 3.4. An example of survey to obtain AMV	31
Figure 4.1. PID controller for HVAC systems in buildings	33
Figure 4.2. Block diagram of thermal comfort control with ANN regulator	35
Figure 4.3. Prediction model of PMV index neural network	36
Figure 4.4. Co-simulation example for thermal comfort control	37
Figure 4.5. Architecture of the proposed FL controller	38
Figure 4.6. ANFIS structure for water mass flow rate	39
Figure 4.7. Comparison of PID and fuzzy-MPC of an AHU system	40
Figure 4.8. MPC scheme for HVAC systems	41
Figure 4.9. MPC control system for thermal comfort	41
Figure 4.10. Sensors worn by an occupant	44
Figure 4.11. Personalized thermal comfort controller as a chair	45
Figure 4.12. PIR sensors used for occupancy detection	46

Figure 4.13. Wireless sensors for thermal comfort measurement	46
Figure 4.14. Components of user interface and thermal preference scale	47
Figure 4.15. Thermographic data collection points	48
Figure 4.16. Sensor placement for personalized thermal comfort controllers.....	48
Figure 4.17. The infrared sensing system installed on an eyeglass frame.....	49
Figure 4.18. Learning thermostats	50
Figure 4.19. Personal wristband thermostat.....	50
Figure 5.1. Overview of the methodology	54
Figure 5.2. Location of Izmir (left) and case building (right).....	55
Figure 5.3. Surroundings of the case building (left) and case building-outer view (right)	56
Figure 5.4. The configuration of door (left) and windows (right)	56
Figure 5.5. Inside of case building (left) and split type air-conditioner used in the case building (right)	58
Figure 5.6. Algorithm of PTC-DC.....	58
Figure 5.7. Membership functions used for the development of PTC-DC.....	61
Figure 5.8. Microcontroller for PTC-DC.....	67
Figure 5.9. The PMV sensor used for measuring the PMV.....	69
Figure 5.10. Power analyser to measure energy consumption of air-conditioner	69
Figure 6.1. Schema of the developed PTC-DC software.....	72
Figure 6.2. Screenshot of PTC-DC programming	74
Figure 6.3. Screenshots of mobile application used by PTC-DC	75
Figure 6.4. Technical drawing of PTC-DC, front (left), back (right)	76
Figure 6.5. Three-view drawing of PTC-DC.....	77
Figure 6.6. Front view of the prototype of PTC-DC	77
Figure 6.7. Back view of the prototype of PTC-DC.....	78
Figure 6.8. The main screen of PTC-DC	78
Figure 6.9. Power consumption profile of transition and steady-state conditions.....	81
Figure 6.10. Comparison of energy consumption for PID controller and PTC-DC (v.1).....	81
Figure 6.11. Comparison of energy consumption for PID controller and PTC-DC (v.2).....	82
Figure 6.12. AMV comparison for PID controller and PTC-DC (v.1).....	84

Figure 6.13. APD comparison for PID controller and PTC-DC (v.1) for the total measurement period.....	85
Figure 6.14. AMV comparison for PID controller and PTC-DC (v.2).....	85
Figure 6.15. APD comparison for PID controller and PTC-DC (v.2) for the total measurement period	86
Figure 6.16. AMV value in dependence on T_i and MRT	87
Figure 6.17. The effect of carbon dioxide concentration on AMV for PID controller...	87
Figure 6.18. The effect of carbon dioxide concentration on AMV for PTC-DC (v.2)...	88
Figure 6.19. Comparison of PID and PTC-DC with respect to HBexC and MRT.....	90
Figure 6.20. HBexC rate-heating period.....	91
Figure 6.21. HBexC rate-cooling period	91
Figure 6.22. Variation of outgoing exergy calculated for the conditions of $T_i=21.8^\circ\text{C}$ and $\text{RH}_i=55\%$ on 12 th of June, 2018	92

LIST OF TABLES

<u>Table</u>	<u>Page</u>
Table 1.1 Thermal sensation scale	4
Table 2.1 Comparison between fuzzy and classical operations.....	16
Table 2.2. Representing the correspondences between fuzzy set and fuzzy logic	16
Table 3.1. Metabolic rates at different activities	25
Table 3.2. Insulating value of clothing elements	25
Table 3.3. Effects of O ₂ concentration on occupants.....	26
Table 3.4. Exergy balance for human body system.....	28
Table 4.1. Comparison of HVAC control systems	42
Table 5.1. Overall heat transfer coefficients and thicknesses of the walls, floor, doors and windows of the case building	57
Table 5.2. Specifications of air-conditioner.....	57
Table 5.3. Division of thermal perception index range into fuzzy sets membership function.....	60
Table 5.4. Specifications of all components used for PTC-DC hardware.....	65
Table 5.5. Minimum requirements for PTC-DC.....	68
Table 5.6. Physical data of the occupant	68
Table 5.7. Specifications of power analyser	70
Table 6.1. An example set of 135 fuzzy rules	73
Table 6.2. Comparison of Version 1 and 2 of PTC-DC	74
Table 6.3. Total measurement, outdoor and preferred temperatures for measurement period.	79
Table 6.4. Training dates for PTC-DC	80
Table 6.5. Summary of energy consumption saving of PTC-DC compared to PID controller (excluding the first one hour)	83
Table 6.6. Decrease in APD values compared to PID controller	86
Table 6.7. Calculated and measured parameters which give minimum HBexC rates...	89

LIST OF SYMBOLS

A	Area	m^2
ANFIS	Adaptive neuro fuzzy inference system	
ANN	Artificial neural network	
AMV	Actual mean vote	
APD	Actual percentage of dissatisfied	%
clo	Clothing insulation	
CO ₂	Carbon dioxide	
e	Specific exergy consumption rate	$W/m^2.kg$
f	Ratio of clothed body surface area to nude body surface area	
FL	Fuzzy logic	
h	Convective heat transfer coefficient	$W/m^2.K$
HBexC	Human body exergy consumption	W/m^2
I	Thermal resistance	m^2K/W
IAQ	Indoor air quality	
\dot{m}	Mass flow rate	kg/s
M	Metabolism	W/m^2
met	Metabolic rate	
MPC	Model predictive controller	
MRT	Mean radiant temperature	$^{\circ}C$
O ₂	Oxygen	
P	Partial water vapor	Pa
PID	Proportional-integral-derivative	
PMV	Predicted mean vote	
PPD	Predicted percentage of dissatisfied	%
PTC-DC	Personalized thermal comfort driven controller	
Q	Heat transfer rate	W
R	Gas constant	$J/kg.K$
R ²	Determination of multiple coefficient	
RH	Relative humidity	%
T	Air temperature	$^{\circ}C$

v	Air velocity	m/s
W	External work	W/m ²
X	Exergy rate	W
\hat{y}	Fuzzy logic estimation model results	
y	Standart deviation	
y_i	Measurement results	

Subscripts

a	Air
bl	blood
c	Convection
cl	Clothing
cr	Body core
dht22	DHT22 sensor results
Du	DuBois
e	Evaporative
hobo	HOBO sensor results
i	Indoor
n	Surface
o	Outdoor
p	Person
r	Reference state
rd	Radiation
sk	Skin
w	Water, water vapour

Greek letters

φ	Humidity ratio
σ	Stefan–Boltzmann constant
ε	Emissivity

CHAPTER 1

INTRODUCTION

Heating, Ventilating and Air Conditioning (HVAC) systems maintain thermal comfort for occupants of residential, commercial and industrial buildings. HVAC systems comprise of an inside unit, air handling unit (AHU), ducts (air distribution system) and an outside unit.

A HVAC system provides heating and/or cooling for a space by controlling temperature and relative humidity (Fig. 1.1).

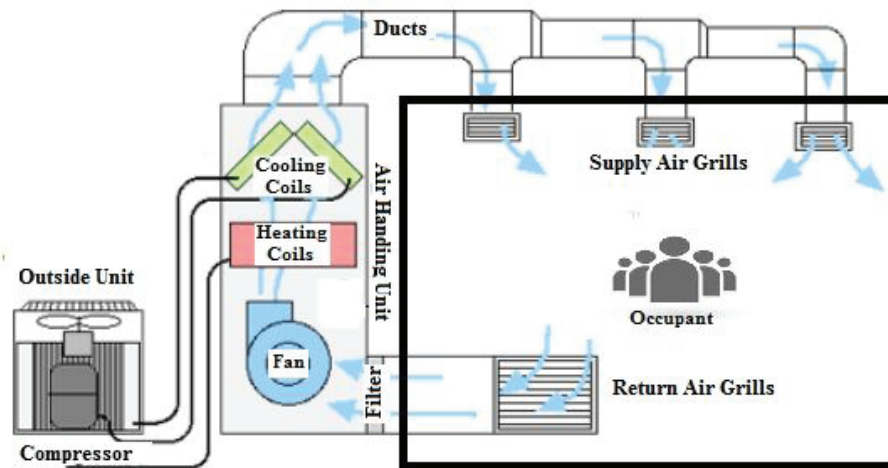


Figure 1.1. A simple HVAC system
(Source: Lightfootmechanical, 2018)

The AHU is an integrated piece of equipment that consists of a fan, heating and cooling coils, air-control dampers, filters and silencers (Fig. 1.2). The outside air is cooled or heated, after which it is discharged into the building space through a duct system. A fan is an air pump that creates a pressure difference and causes airflow whilst filters are to remove particles and contaminants of various sizes from the air. Cooling coil is used to cool and dehumidify the air while heating coil sends warm air into the space. Finally, the dampers move the air through the air-handling unit and out into the spaces.

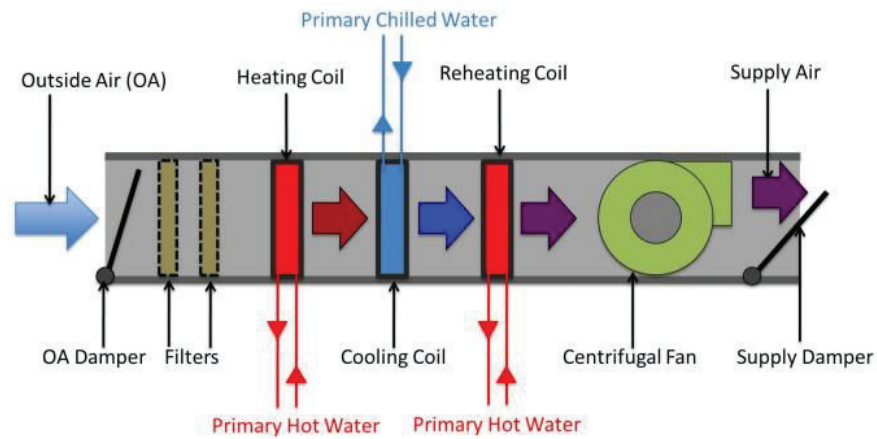


Figure 1.2. Schematic of AHU unit
(Source: Cooper, 2018)

An air-conditioner is a kind of AHU which treats air in an enclosed space via refrigeration cycle (Fig. 1.3). Compression, condensation, expansion and evaporation are four components of refrigeration cycle which is used by all air-conditioners. The most commonly used refrigeration cycle is vapor-compression cycle. Briefly, for a cooling function, refrigerant enters the compressor as saturated vapor while low pressure is increased to high pressure. Then, the refrigerant is cooled to the saturated liquid in condenser as a result of heat rejection to the surroundings. The refrigerant is throttled to low pressure for evaporator and finally vaporizes absorbing heat from refrigerated space (Çengel and Bowles, 2005).

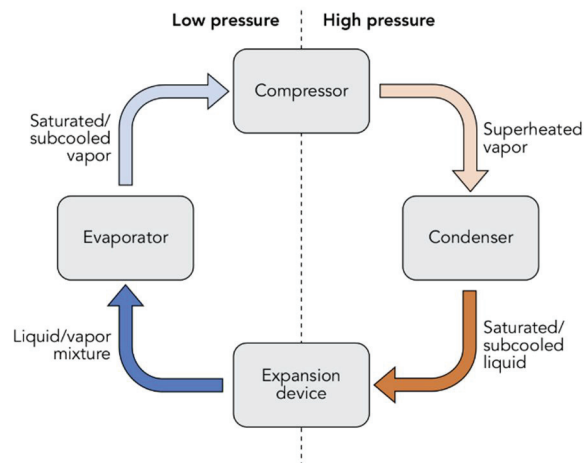


Figure 1.3. Refrigeration cycle used in air-conditioner
(Source: Çengel and Boles, 2015)

A typical HVAC control system is depicted in Fig. 1.4. The supply air temperature is controlled by controller C1 while the duct static pressure is controlled by controller C2. Additionally, the zone air temperature is controlled by controller C3.

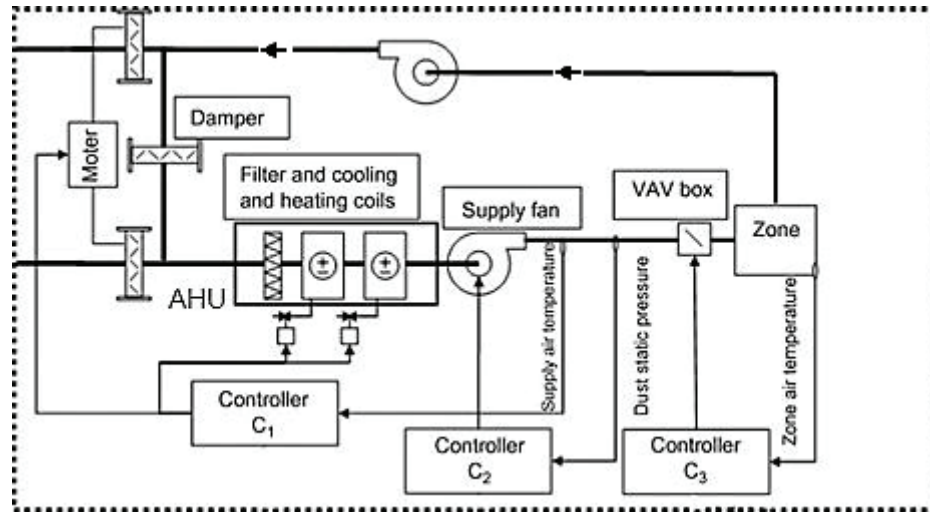


Figure 1.4. HVAC control system
(Source: Nassif et al., 2008)

1.1. Thermal Comfort

Thermal comfort is investigated based on energetic approach and exergetic approach which use the First and Second Law of Thermodynamics, respectively.

1.1.1. Energetic Approach

The American Society of Heating, Refrigerating and Air-Conditioning Engineers (ASHRAE) defined “Thermal Comfort” as “*the condition of the mind in which satisfaction is expressed with the thermal environment*” (ASHRAE, 2017). Thermal comfort is dependent upon whole body sensation which is the function of six variables: air temperature, humidity, air velocity, clothing insulation, metabolic rate and mean radiant temperature. Obviously, thermal comfort can be measured directly by the surveys or can be estimated by measuring the quantities of the thermal environment. The Predicted Mean Vote (PMV) is an empirical fit to the human sensation of thermal comfort. It is the most common metric to estimate the thermal comfort as presented in

ISO 7730 (2005a). The variables for PMV calculation are the user’s activity level (met) and clothing insulation (clo-value), indoor air temperature (T_i), mean radiant temperature (MRT), relative air velocity (v_a) and humidity (RH_i). The PMV refers to a thermal scale that runs from cold (-3) to hot (+3), originally developed by Fanger (1970). The scale uses thermal sensation codes as given in Table 1.1 as -3 for cold, -2 for cool, -1 for slightly cool, 0 for neutral, +1 for slightly warm, +2 for warm and +3 for hot. According to the ISO 7730 (2005a) the values of PMV is 0 with a tolerance of ± 0.5 as 90% of the occupants feel thermally satisfied. In a conditioned environment, $PMV = 0 \pm 0.5$ is the target to be achieved by a HVAC system.

Table 1.1 Thermal sensation scale
(Source: ISO 7730, 2005a)

Thermal sensations	PMV
Hot	+3
Warm	+2
Slightly warm	+1
Neutral	0
Slightly cool	-1
Cool	-2
Cold	-3

The second thermal comfort index is the Predicted Percentage of Dissatisfied (PPD). The PPD, which is defined in terms of PMV, predicts the percentage of occupants that will be dissatisfied with the thermal conditions and adds no information to that already available in PMV. An indoor environment is assumed as “thermally comfortable” when 90% of the occupants are satisfied (or 10% dissatisfied) with their thermal environment (ASHRAE, 2017). The PMV/PPD model calculates the thermal comfort by using six variables listed above; nevertheless, the calculation method is complex.

In 1998, the adaptive thermal comfort model (Brager and de Dear, 1998) was adopted in ASHRAE 55 (2017) for naturally ventilated buildings, alongside the PMV/PPD index for buildings using HVAC equipment. Adaptive comfort model added a little more human behavior to the thermal sensation models. The model assumes that,

if changes occur in the thermal environment to produce discomfort, the occupants generally change their behavior and act in a way that the occupants restore their comfort (Nicol and Humphreys, 2002). These actions include taking off clothing, reducing activity levels or even opening a window. The main effect of such models is to increase the range of conditions that designers can consider as comfortable, especially in naturally ventilated buildings where the occupants have a greater degree of control over their thermal environment. In order to consider adaptive comfort, the space must have operable windows and no mechanical cooling system. Furthermore, occupants must have the option of adding or removing clothing to adapt to the thermal conditions

1.1.2. Exergetic Approach

The ISO 7730 (2005a) uses PMV method which was developed based on the First Law of Thermodynamics. As discussed in Section 1.1.1., the method uses six parameters (air temperature, humidity, air velocity, clothing insulation, metabolic rate and mean radiant temperature) for the calculation and refers to a thermal scale in Table 1.1 and the body is believed to be thermally satisfied at $PMV = 0 \pm 0.5$ (Fanger, 1970). Zero PMV value (0) is accepted as thermal neutrality. However, there are many combinations of the thermal comfort parameters that give the thermal neutrality. Shukuya (2009) suggested another approach which is based on the Second Law of Thermodynamics. This approach considers human body system as a complex model with circular nodes and uses outdoor air temperature (T_o) and relative humidity (RH_o) as well as indoor environmental conditions; indoor air temperature (T_i) and relative humidity (RH_i), mean radiant temperature (MRT) and air velocity (v_a) and then calculates the human body exergy consumption (HBexC) rate. Consequently, Shukuya (2009) indicated that there are limited combinations of thermal comfort parameters that give the minimum HBexC rate value and thermal neutrality.

1.2. Energy Consumption of HVAC Systems

Energy consumption of the building sector over total final energy consumption was 40% and 32% in 2016 for EU and Turkey, respectively (Fig. 1.5 and 1.6)

(Cucchiella et al., 2018; TUIK, 2016). Final energy consumption in residential buildings in EU decreased by 9% between 2001 and 2015. However, in this period, 48% of increase is recorded in the energy consumption by residential buildings in Turkey (Atmaca, 2016).

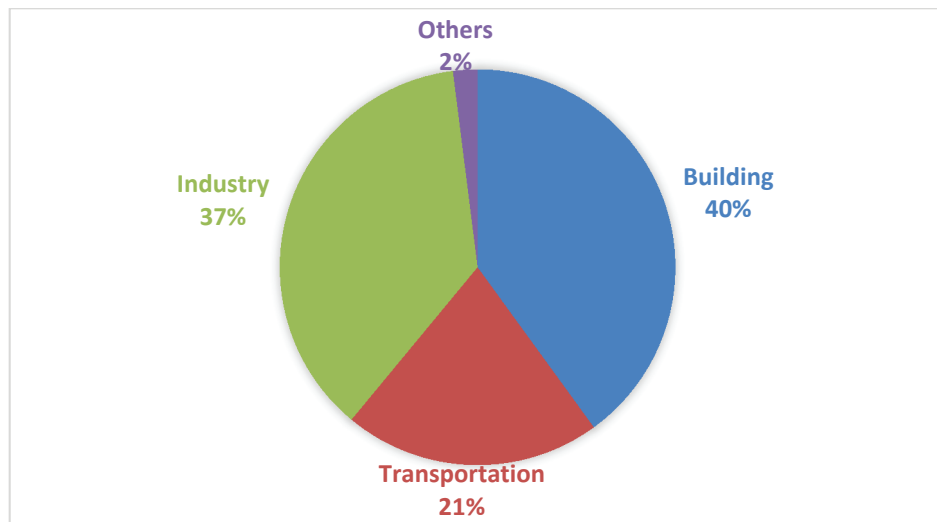


Figure 1.5. Energy consumption by sector in EU
(Source: Cucchiella *et al.*, 2018)

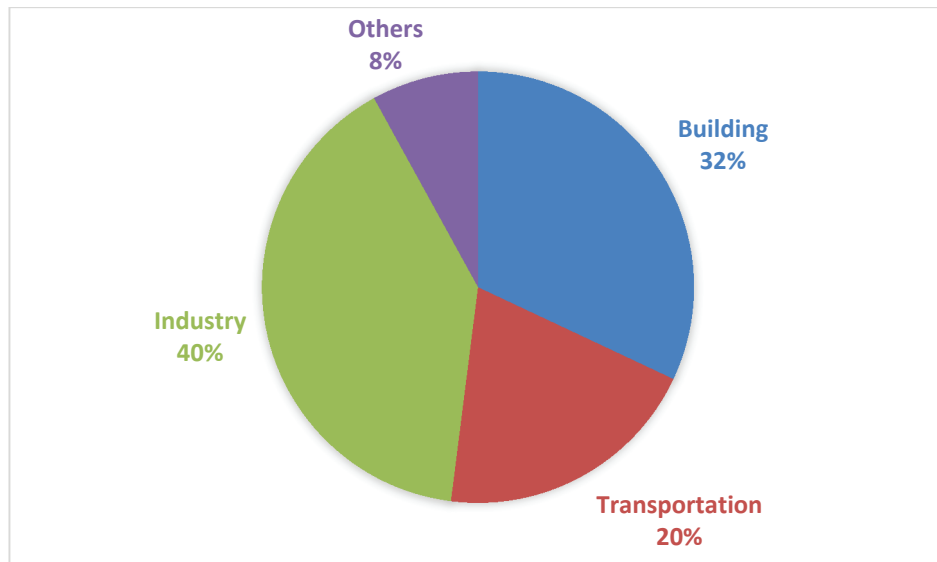


Figure 1.6. Energy consumption by sector in Turkey
(Source: Atmaca, 2016)

HVAC systems consume 30-50% of the building's energy share in Europe (Ferreira et al., 2012; E.U.Parliament, 2017) as shown in Fig. 1.7. However, 40% of energy consumption can be saved by applying energy-efficient HVAC control systems (Dai et al., 2016).

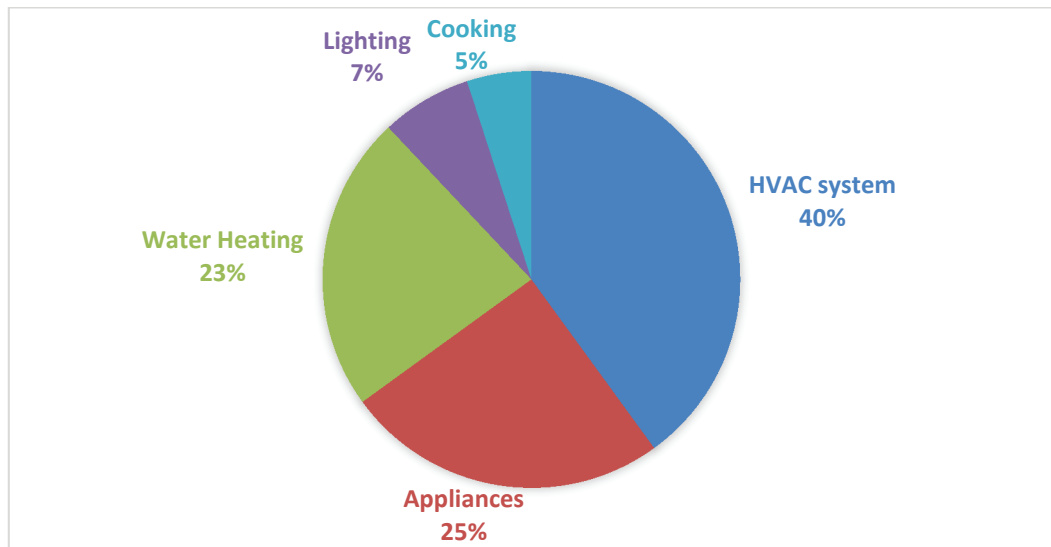


Figure 1.7. Share of total energy consumption in EU buildings
(Source: E.U. Parliament, 2017)

Energy consumption of HVAC systems can be decreased by using proper control strategy such as control systems which detect occupant-building interactions (Hang et al., 2016).

1.3. HVAC System Control

HVAC systems are typical nonlinear time-dependent multivariable systems with inter-related variables like T_i and v_a as well as disturbances like occupants' behavior, T_o and RH_o (Mirinejad et al., 2012; Dar et al., 2015; Dong et al., 2014; Chen et al., 2016).

Historically, the oldest prototype of a HVAC system control emerged in the 1930s. The developed on/off control provided only two outputs; maximum (on) or zero (off). In the early 1980s, standard PID (proportional-integral-derivative) regulators were commonly used as feedback controllers. The control logic is based on the computation of the error $e(t)$ between the desired and the measured values of the output, i.e. $e(t) = r(t) - y(t)$, which is fed back to the system after proportional, integral and derivative operations. By the 1990s, computerized controllers became popular. Some of the controllers used computer programs and could be accessed even by a web browser. Then, many advanced control systems were introduced which used Artificial Neural Network (ANN), Fuzzy Logic (FL), Artificial Neuro-Fuzzy Inference System (ANFIS) and Model Predictive Control (MPC) algorithms.

Many HVAC control systems use air temperature regulators to control the thermal environment. However, thermostatic control of a HVAC system is not aware of occupant comfort, instead, it concentrates only on controlling room temperature. The limitations of the traditional approach to HVAC system control have led many researchers to design personalized HVAC control systems (Feldmeier, 2009; Jazizadeh et al., 2014; Hossein Sagheby, 2018). Participation of the buildings' occupants is essential in learning their comfort profiles for personalized and comfort-driven HVAC operations (Jazizadeh et al., 2014; Jazizadeh et al., 2018). To this aim, personalized thermal comfort controllers deal with individual thermal sensation instead of calculating PMV value. The role of the personalized thermal control system is to control the HVAC system automatically to maintain the comfort level of individual occupants when they are actually present.

In general, HVAC control systems could be classified into two categories: conventional controllers (on/off, PID type controllers etc.) and advanced controllers (Fig. 1.8). PID type controllers include P, PI and PID regulators. Advanced controllers are based on detection of nonlinear and dynamic systems. The advantage of advanced HVAC controllers is the adaptation to the changing climate and indoor thermal conditions of the buildings (Holland, 1975). This category of controllers includes ANN, FL, ANFIS and MPCs.

Advanced HVAC control systems can understand the complex structure of occupant thermal comfort. For this purpose, intelligent controllers started to be developed in 1990s. To address the preferred thermal comfort and indoor conditions, the authors studied ANN controllers (Guillemin and Morel, 2002; Liang and Du, 2005; Reena et al., 2018), FL controllers (Hamdi and Lachiver, 1998; Calvino et al., 2010; Nowak and Urbaniak, 2011; Anastasiadi and Dounis, 2018), adaptive controllers (Morel et al., 2000; Kolokotsa et al., 2005; Jazizadeh and Jung, 2018) and MPCs (Privera et al., 2011; May-Ostendorp et al., 2011; Garnier et al., 2014; Dong and Lam, 2014; Hilliard et al., 2017; Yang et al., 2018).

Due to the fuzzy nature of thermal comfort, several studies concluded that FL controllers can be used to obtain thermal comfort better than other advanced controllers (Kolokotsa et al., 2005; Barmejo et al., 2012; Ghahramani et al., 2018). Some researchers developed thermal comfort sensing systems and advanced HVAC controllers together (Scheatzle, 1991; Kang and Park, 2000; Wang et al., 2007; Ghahramani et al., 2018).

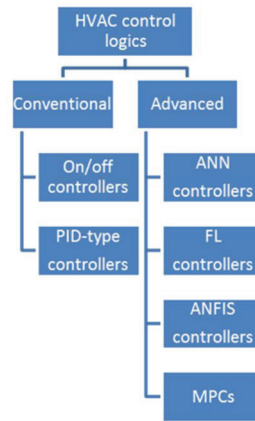


Figure 1.8. Classification of control methods in HVAC systems
(Source: Dar et al., 2015)

1.4. Motivation

In the 21st century, HVAC systems still use conventional controls such as simple on/off and/or conventional PID controllers. However, these systems regulate only air temperature to control the thermal environment. Thermal comfort of the occupants and energy savings are not parameters. Moreover, conventional control logics can not detect the presence of the occupants in a room. Hence, adjusting the set points for unoccupied times leads to higher energy consumption. Although control algorithms of conventional HVAC systems are simple, satisfaction of thermal comfort is the problem. While advanced HVAC controllers offer better performance than conventional ones (Hang et al., 2016), many advanced HVAC controllers require extra effort to develop a suitable dynamic model. First, a proper nonlinear mathematical model of HVAC system and thermal sensation model must be derived. This procedure requires a great knowledge of mathematics. In particular, ANN and FL controllers rely on the learning accumulated from off-line simulations but it is time consuming to train the model properly. For instance, when modelling of the dynamic system can be taken into account, the MPC is preferred; however, MPC requires an optimization procedure. For this reason, in the last ten years, development of new generation building monitoring systems and personalized thermal comfort control tools has accelerated (E.U. Commission, 2016). The revised Energy Performance of Buildings Directive (EPBD, 2018) aims to accelerate the use of smart and energy-efficient technologies in the building sector across Europe. It

introduces a "smartness indicator" which will measure the buildings' capacity to use new technologies and electronic systems to optimize their operation and interact with the grid. An increase of smart technologies has potential to decrease energy consumption as well as to improve occupant's thermal comfort via adjusting control parameters in the building according to the needs of the occupant. However, smart personalized control systems are still expensive because of the high number of pricey sensors and optimizing the existing control system equations is computationally-heavy burden. Moreover, the response time of these controllers is still long. Many sensing systems are not easy-to-use by the occupants. Dense sensing systems make personalized thermal comfort controllers complicated. Moreover, the programming of such a large sensor network becomes the most complicating issue.

This thesis offers a solution to the problems stated above by developing a novel energy-efficient personalized thermal comfort control system. The major contributions of the thesis are;

- to develop a novel personalized thermal comfort control algorithm that aims increasing thermal comfort as well as saving energy.
- to use simple fuzzy logic rules for easy-understanding of the algorithm by occupants.
- to develop a personalized thermal comfort controller, which uses the novel control algorithm.
- to test the developed control system in an office building by deploying a prototype.
- to operate HVAC system by changing set-temperature and fan speed according to thermal preferences of the occupant (AMV) instead of Fanger's PMV method.
- to monitor and use indoor air quality parameters as well as thermal comfort parameters in the controller.
- to evaluate results by exergetic approach of thermal comfort as well as energetic approach.

1.5. Aim of the Thesis

The aim of this thesis is to develop a novel personalized thermal comfort driven control algorithm with simple fuzzy logic rules in order to increase thermal comfort while decreasing energy consumption without any retrofitting on HVAC system. For this aim, a prototype of an energy-efficient personalized thermal comfort driven controller (PTC-DC) is developed with minimum cost of sensors and maximum efficiency in order to obtain better thermal comfort. Additionally, the PTC-DC takes air quality parameters into the algorithm i.e warning the occupant by easy- to- understand signals in order to prevent poor indoor air quality and to improve thermal comfort.

The remainder of the thesis is organized as follows. Chapter 2 presents a review of HVAC control systems. In Chapter 3, both energetic and exergetic approaches of thermal comfort are given in detail. A detailed literature survey on HVAC controllers is presented in Chapter 4 along with examples of personalized thermal comfort controllers. Chapter 5 presents materials and methods for the thesis. First, development of PTC-DC is shown, then, the case building and measurement system is introduced. In Chapter 6, prototype of PTC-DC and the tests are presented. Comparison of proposed algorithm with conventional controller is also given in this Chapter. Finally, Chapter 7 concludes the thesis.

CHAPTER 2

HVAC CONTROL SYSTEMS

HVAC control systems have been investigated by various techniques such as standard on/off control, PID-type control and advanced control methods like Artificial Neural Network (ANN), Adaptive Neuro-Fuzzy Inference System (ANFIS), Fuzzy Logic (FL) and Model Predictive Control (MPC) approaches.

2.1. Conventional HVAC Control Systems

Several control strategies for HVAC systems still use on/off and conventional PID (proportional, integrative and derivative) methods (Calvino et al., 2010; Mirinejad et al., 2012).

2.1.1. On/off Control

Simplest and common control of HVAC systems is on/off control. As a common control, fixed-speed compressor on-off operations are used to modulate the capacity provided to some enclosed space. On/off control provides only two outputs, maximum (on) or zero (off). The control sensor usually takes the form of an on/off thermostat, pressure switch, humidistat, etc. and operates so that when the controlled variable is below the set point, the contacts close or contacts made when the controlled variable is above the setting (Harrold and Lush, 1988).

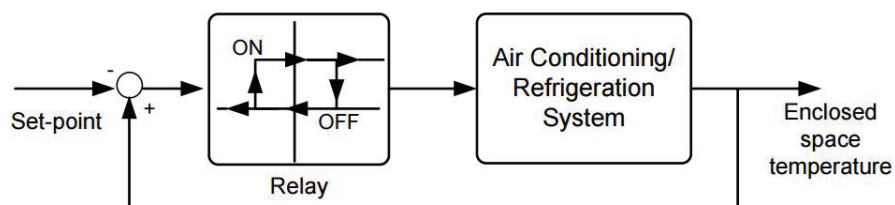


Figure 2.1. On/off controller feedback for temperature control
(Source: Harrold and Lush, 1988)

This process can be simply expressed as (2.1).

$$\text{Switch off when } T \geq T_u \text{ and on when } T \leq T_l \quad (2.1)$$

Where T is the desired temperature and T_u and T_l are the upper and lower bound for the controller.

2.1.2. PID-type Controllers

Standard PID (proportional-plus-integral-plus-derivative) regulators are the most commonly used feedback controllers since the oldest prototype of a PID controller emerged in the 1930s. PID controllers are usually understandable and reliable for the HVAC system operators. The control logic is based on the calculation of the error $e(t)$ between the desired $r(t)$ and the measured $y(t)$ values of the output, i.e. $e(t) = r(t) - y(t)$, which is computed after proportional, integral and derivative operations. The proportional action adjusts the controller output according to the size of the error, the integral action eliminates the steady state offset and the future is anticipated via derivative action. A typical equation that describes a PID regulator, is (2.2).

$$u(t) = K_p e(t) + K_i \int_0^t e(t) dt + K_d \frac{de(t)}{dt} \quad (2.2)$$

where K_p , K_i , K_d are the PID proportional, integral and derivative gains, respectively. The PID controller produces promising outputs based on the computation of the error $e(t)$.

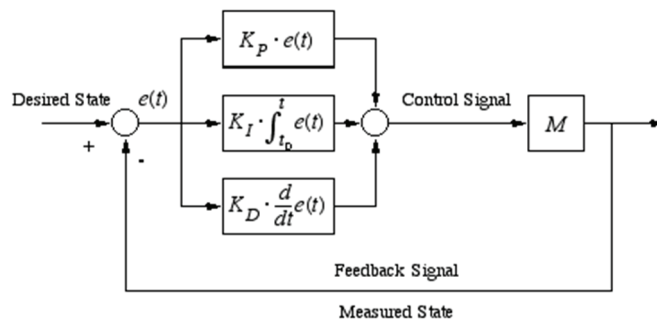


Figure 2.2. Block diagram of a PID controller
(Source: Mohsenizadeh et al., 2011)

2.2. Advanced HVAC Controllers

Advanced HVAC control systems are Artificial Intelligence (AI) based controllers, namely, ANN controllers, FL controllers, ANFIS controllers and MPCs (Krarti, 2003; He et al., 2005; Soyguder and Alli, 2009; Dounis and Caraiskos, 2009; Ferriera et al. 2012; Kumar and Sigh, 2013; Abdo-Allah et al., 2018).

2.2.1. Artificial Neural Network Controllers

ANNs have been accepted as an alternative technology offering a way to tackle complex and ill-defined, specially nonlinear and dynamic system control, since 1990s. They are not programmed in a traditional way but they are trained using past history data representing the behavior of a system (Moon et al., 2011; Kumar et al., 2013; Turhan et al., 2014). The ANN controllers are practical and they do not require the identification of the HVAC model. As an example, thermal comfort control equations based on PMV values of ANN regulator is shown in (2.3-5) (Ferreira et al., 2012).

$$v = w_{11}e + w_{12}e + w_{13}b \quad (2.3)$$

$$u = \frac{1}{1 + \exp(-v^2)} \quad (2.4)$$

$$\Delta w_{ij} = -\eta \frac{\partial E}{\partial w_{ij}} = -\eta \frac{\partial E}{\partial PMV} * \frac{\partial PMV}{\partial u} * \frac{\partial u}{\partial w_{ij}} \quad (2.5)$$

Here, v is the input, w_{ij} are the synaptic weights, u is summation of the weights, E is the error, b is the bias and η is the learning rate.

2.2.2. Fuzzy Logic Controllers

The FL is a system that formulates approximate reasoning which was developed by Loutfi A. Zadeh (Zadeh, 1965). It is defined with grade of membership by

characterizing objects with a membership function. Controlling parameters like temperature, air velocity, electric current and machine control are some of the application areas of FL (Munataka, 1998). The main structure of FL modeling is depicted in Fig. 2.3.

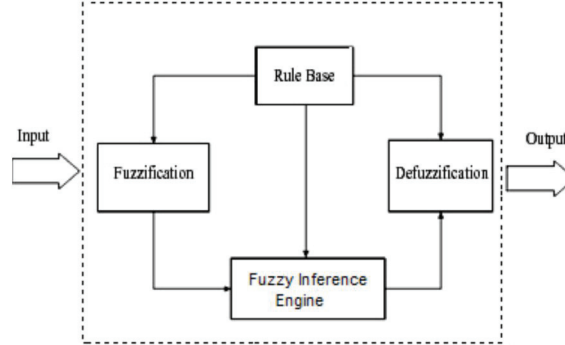


Figure 2.3. The phrase of FL estimation model
(Source: Zadeh, 1965)

A fuzzy set is a class of ordinary set by allowing members to have degrees of membership. The degree of membership is indicated by a number between 0 and 1. If the degree is 0, the object is not in the set, and if 1, the object belongs 100% to the set.

In the fuzzy set, every object is represented by a degree of membership. The membership function has values between 0 and 1 which is formally written as (2.6).

$$\mu_a(x) : X \rightarrow [0, 1] \quad (2.6)$$

Relationship between fuzzy sets are similar to the ordinary sets. In fuzzy operation concept, there are four operations including union, intersection, complement, binary relations and composition of relations as classical operations. Table 2.1 shows three operations for fuzzy and classical sets.

In Table 2.1, α indicates the membership of subsets A and B. A graphical explanation of two fuzzy sets and fuzzy operations is indicated in Fig. 2.4. Fuzzy logic can be represented as fuzzy set theory. Table 2.2 indicates correspondences between fuzzy logic and fuzzy set theory.

The basic lingual If-Then rule is shown as (2.7).

$$\text{If “}\alpha\text{” is A and “}\beta\text{” is B, then “}\gamma\text{” is C} \quad (2.7)$$

Here, A, B and C are corresponding linguistic values while α , β and γ are the inputs of the model.

Table 2.1 Comparison between fuzzy and classical operations
(Source: Luger, 2009; Tayfur, 2012)

	Intersection	Union	Complement
	$\alpha_{A \cap B}(x) =$	$\alpha_{A \cup B}(x) =$	$\alpha_{\bar{A}}(x) =$
Classical	$\begin{cases} 1 & (x) \in A \cap B \\ 0 & (x) \notin A \cap B \end{cases}$	$\begin{cases} 1 & (x) \in A \cup B \\ 0 & (x) \notin A \cup B \end{cases}$	$\begin{cases} 1 & (x) \notin A \\ 0 & (x) \in A \end{cases}$
Fuzzy	$\min(\alpha_A(x), \alpha_B(x))$	$\max(\alpha_A(x), \alpha_B(x))$	$1 - \alpha_A(x)$
Operator	AND	OR	NOT

Table 2.2. Representing the correspondences between fuzzy set and fuzzy logic

Fuzzy set	Fuzzy logic
Degree of membership	Truth value of proposition
\cap	AND
\cup	OR
Complement	NOT

(2.7) can be re-written as (2.8) for any thermal comfort controller.

If the air temperature is “LOW” and clothing value is “LOW” the PMV is “-2” (2.8)

Four components are included in fuzzy logic: fuzzification, fuzzy rule base, fuzzy output engine, and defuzzification (Zadeh, 1965). First, each input and output variable is represented by degrees of membership via fuzzification. All fuzzy inputs and outputs are theoretically shown as a number between 0 and 1 (Zadeh, 1965). Fuzzy rule base is used for the basis of fuzzy logic to obtain output. Fuzzy rules are written between all inputs and outputs. Fuzzy rules are operated using a series of if-then statements given by IF ascendant, THEN consequent (Luger, 2009; Tayfur, 2012).

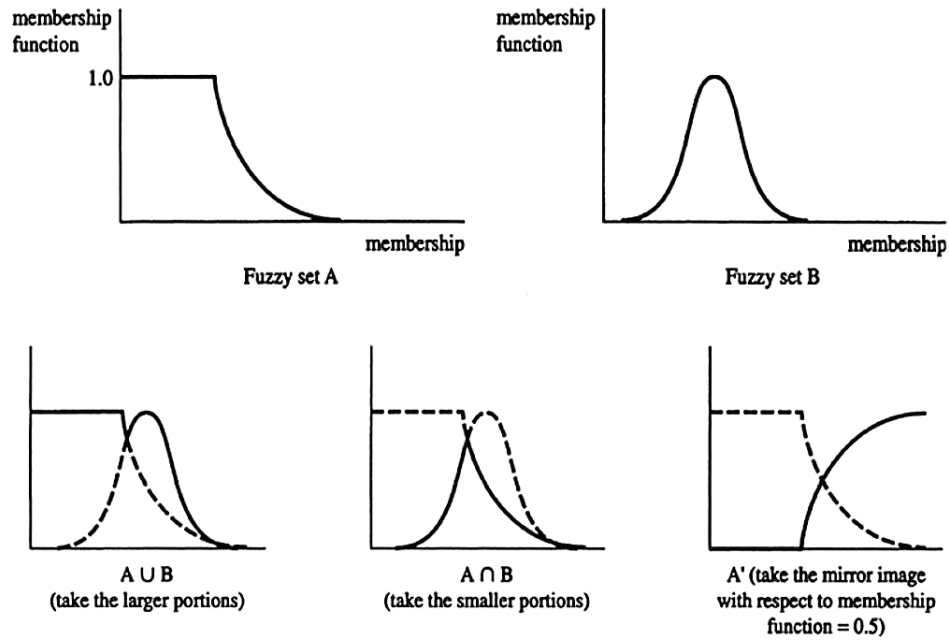


Figure 2.4. A graphical explanation of two fuzzy sets and their union, intersection, and complement (Source: Munakata, 1998)

Each fuzzy rule gives a representation of the truth-value of that rule. Fuzzy inference engine uses fuzzy rules in the fuzzy rule base based on concepts of fuzzy set theorem, fuzzy if-then rules, and fuzzy reasoning. Conventional fuzzy inference systems are typically constructed by experts and have been used in automatic control, decision analysis and advanced systems. Defuzzification extracts a crisp value that best represents the fuzzy set (Hirota and Pedrycz, 1991). Two methods are used in FL; the minimum and the product operation methods. If “ \circ ” is the operator that indicates rule of inference, (2.9) can be written in terms of membership function for minimum operator.

$$\circ B(y) = \text{MAX} [\text{MIN} (\circ A(x), \circ R(x,y))] \quad x \in EI \quad (2.9)$$

Similarly, (2.10) shows a membership function for product operator.

$$\circ B(y) = \text{MAX} [\circ A(x), \circ R(x,y)] \quad x \in EI \quad (2.10)$$

Defuzzification so called rounding off is the process of producing a quantifiable result in crisp logic, given fuzzy sets and corresponding membership degrees (Metcalf and Reid, 1992). In literature, many defuzzification methods are used such as mean of

maxima (MOM), center of gravity (COG)(centroid), leftmost maximum (LM), rightmost maximum (RM), bisector of area (BOA), centre of sums and weighted average method (Munataka, 1998; Tayfur, 2012). Centroid method is the most widely used method as expressed in (2.11).

$$K_x^* = \frac{[\sum_i \mu(K_{xi})K_{xi}]}{[\sum_i \mu(K_{xi})]} \quad (2.11)$$

where K_x^* is the defuzzified output value, K_{xi} is the output value in the i^{th} subset, and $\mu(K_{xi})$ is the membership value of the output value in the i^{th} subset (Tayfur, 2012).

2.2.3. Adaptive Neuro-Fuzzy Inference System Controllers

The ANFIS is a hybrid algorithm that applies the combination of ANN and FL approach. The advantages of ANFIS are self-learning ability like ANNs and simple structure of the FL rules (Chua et al., 2007; Soyguder and Alli, 2009; Işık and Inallı, 2018). The ANFIS method uses first order Sugeno (Takagi and Sugeno, 1985) fuzzy inference systems and its architecture is given in Fig. 2.5 (Jian and Wenjian, 2000). The node functions in the same layer are of the same function family and the network has totally five layers.

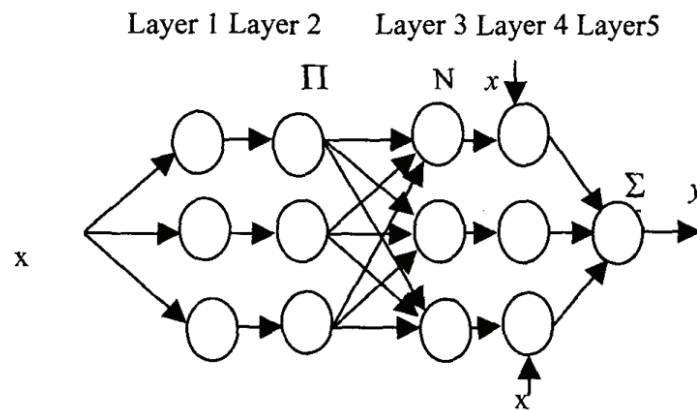


Figure 2.5. An adaptive network
(Source: Jian and Wenjian, 2000)

Layer 1 represents the input variables for the model. Node functions are used to obtain membership functions in this layer. In Layer 2, the rules are determined with the weight of corresponding layer. Additionally, this layer generates output. Layer 3 calculates the ratio of the rule's strength. The output of each rule is calculated in Layer 4. This layer acts as a defuzzifier. Finally, Layer 5 gives an output from the sum of each rule (Jang, 1993; Işık and Inallı, 2018).

2.2.4. Model Predictive Controllers

The MPCs rely on dynamic and linear models of HVAC systems; however, the models are obtained by system identification or linearization of a nonlinear plant (Ascione et al., 2016). MPC is not a single strategy; it consists of a class of control methods to obtain a control signal by minimizing an objective function (Sirocky et al. 2011). An example of a cost function J for optimization is given by (2.12).

$$J = \sum_k^{k+N_p} w_{y_k} (r_k - y_k)^2 + \sum_k^{k+N_c} w_{u_k} \Delta u_k^2 \quad (2.12)$$

Here, w_{y_k} is the weighting coefficient reflecting the relative importance of the monitored output, w_{u_k} is the weighting coefficient penalizing relative big changes in u_k , Δu_k is the difference between u_k and u_{k-1} , N_p represents the prediction horizon whilst N_c is the control horizon.

The MPC approach uses dynamic model of a process to predict future evaluation while optimizing control horizon. Further details of MPC approach can be found e.g. in Rossiter (2005).

CHAPTER 3

THERMAL COMFORT APPROACHES

Thermal comfort, as discussed in Chapter 1, is a subjective sensation in which satisfaction is expressed with the thermal environment (ASHRAE, 2017). Fanger (1970) developed the PMV index to estimate the thermal comfort as presented in ISO 7730 (2005a). The PMV uses six parameters as given in Fig. 3.1 and refers to a thermal scale from -3 (cold) to +3 (hot) (Fanger, 1970).

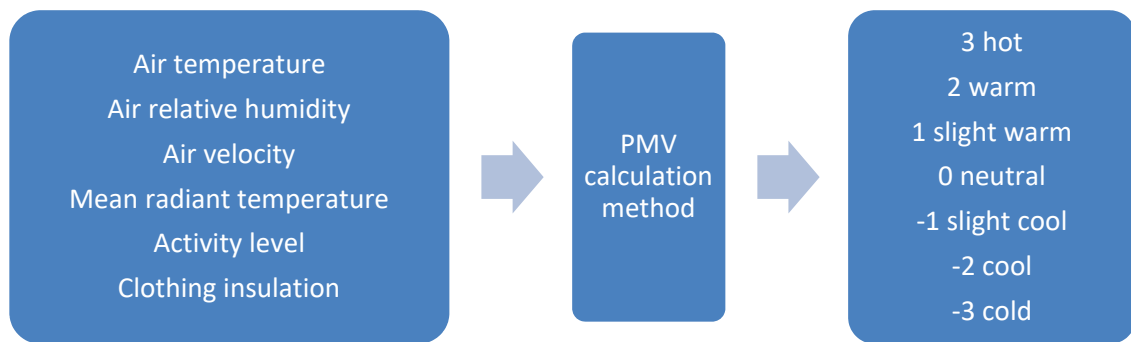


Figure 3.1. Fanger's PMV Model
(Source: Fanger, 1970)

The thermal sensation model based on Fanger's PMV formula can be used to calculate PMV value as shown in (3.1) (Fanger, 1970).

$$PMV = (0.028 + 0.3033e^{-0.036M}) \times \{ (M-W) - 3.05 [5.733 - 0.000699 (M-W) - P_a] - 0.42 [(M-W) - 58.15] - 0.0173M (5.867 - P_a) - 0.0014M (34 - T_a) - 3.96 \times 10^8 \times f_{cl} [(T_{cl} + 273)^4 - (T_{mrt} + 273)^4] - f_{cl} \times h_c (T_{cl} - T_a) \} \quad (3.1)$$

Here,

$$T_{cl} = 35.7 - 0.028 (M-W) - 0.155 I_{cl} \{ 3.96 \times 10^8 \times f_{cl} [(T_{cl} + 273)^4 - (T_{mrt} + 273)^4] - f_{cl} \times h_c (T_{cl} - T_a) \} \quad (3.2)$$

and

$$H_c = \begin{cases} 2.38 (T_{cl} - T_a)^{0.25} & \text{for } 2.38(T_{cl} - T_a)^{0.25} \geq 12.1\sqrt{V_{air}} \\ 12.1\sqrt{V_{air}} & \text{for } 2.38(T_{cl} - T_a)^{0.25} \leq 12.1\sqrt{V_{air}} \end{cases} \quad (3.3)$$

where M is metabolism (W/m^2), W is external work (W/m^2), P_a is partial water vapor pressure (Pa), f_{cl} is ratio of clothed body surface area to nude body surface area, T_{cl} is surface temperature of clothing (K), I_{cl} is thermal resistance of clothing (clo), h_c is convective heat transfer coefficient (W/m^2K).

The second thermal comfort index is the PPD which predicts the percentage of occupants that will be dissatisfied with the thermal conditions. PPD is incorporated into the PMV index. The PPD equation is given in (3.4) (Fanger, 1970).

$$PPD = 100 - 0.95 \times e^{-0.03353 \times PMV^4 + 0.2179 \times PMV^2} \quad (3.4)$$

3.1. Energetic Approach of Thermal Comfort

Fanger (1970) defines thermal comfort in the PMV/PPD model by using six parameters which can be classified into two categories: environmental and personal parameters. These parameters may be independent of each other, but together they contribute to an occupant's thermal comfort (McIntyre, 1980).

Environmental parameters are air temperature, radiant temperature, air velocity and relative humidity while personal parameters are clothing insulation and metabolic activity. However, gender, age or body mass are omitted in the PMV/PPD model. In addition, indoor air quality parameters were not included in this model. The most commonly used parameter is air temperature since it is easy to measure. However, air temperature alone is not an indicator of thermal comfort which must always be considered in relation to other environmental and personal parameters.

3.1.1. Environmental Parameters

The environmental parameters are air temperature (T_i), relative humidity (RH), mean radiant temperature (MRT) and air velocity.

Air Temperature (T_i)

Air temperature is a measure of the heat which surrounds an occupant (person) with respect to location and time. Numerous field and laboratory investigations have proven the relationship between air temperature and thermal comfort (Berglund et al., 1990; Seppänen et al., 1999; Lan et al., 2011; Nall, 2014). Air temperature is commonly measured by dry bulb thermometers. Based on ASHRAE 55 (2017), dry bulb temperature must be measured on the head, waist and ankle levels of the occupant.

Relative humidity (RH)

The RH is the ratio between the actual amount of water vapour in the air and the maximum amount of water vapour that the air can hold at a given temperature. It affects the heat balance of the body by determining the amount of evaporation on the skin (Çengel and Bowles, 2005).

RH can be calculated by (3.5) (Kim, 2004; Spengler et al., 2001).

$$RH (\%) = \frac{\text{vapor partial pressure in the air}}{\text{saturation vapor partial pressure in the air}} \times 100 \quad (3.5)$$

RH has greater effect on thermal comfort than air temperature. Occupants may feel discomfort in the higher RH at the same air temperature.

Mean radiant temperature (MRT)

MRT is defined as heat radiated by any material which depends on the temperature and emissivity of the surrounding surfaces as well as the view factor or the amount of the surface which is “seen” by the object (ASHRAE, 2017). Measuring the temperature of all surfaces in a space is time consuming, requires several sensors and calculation of the corresponding angle factors is quite difficult. Instead, MRT can be approximated by globe temperature measurements.

(3.6) can be used to calculate MRT (ASHRAE, 2017).

$$\text{MRT}^4 = T_1^4 F_{p-1} + T_2^4 F_{p-2} + \dots + T_n^4 F_{p-n} \quad (3.6)$$

where MRT refers mean radiant temperature whilst T_n shows the temperature of surface “n” in Kelvins. F_{p-n} is angle factor between a person and surface "n". If relatively small temperature differences occur between surfaces of the enclosure, Eq.3.6 can be simplified to a linear form as given in (3.7).

$$T_r = T_1 F_{p-1} + T_2 F_{p-2} + \dots + T_n F_{p-n} \quad (3.7)$$

However, angle factors are usually difficult to determine. Nagano and Mochida (2004) estimated the MRT by using (3.8).

$$\text{MRT} = 0.99 T_a - 0.01; R^2 = 0.99 \quad (3.8)$$

Where T_a is air temperature.

The MRT is one of the essential parameters that affects thermal comfort. Occupants can feel discomfort even with the comfortable T_i values, when they are surrounded by cold surfaces.

Air velocity (v_a)

In HVAC systems, air velocity is defined as the rate of air movement at a point, regardless from the direction. According to ASHRAE 55 (2017), it is the average velocity of the air to which the body is exposed, with respect to location and time. Air velocity is measured by an omni-directional anemometer. Air velocity, in general, is preferred to be around 0 to 0.5 m/s in a mechanically controlled space.

High air velocities cause discomfort due to dryness in the respiratory system of human. On the other hand, proper air movement reduces the heat stress through the evaporation on the skin in a space of low RH (Spengler et al., 2001).

3.1.2. Personal Parameters

Personal parameters are generally combined psychological parameters which are the factors depending on the occupant.

Metabolic rate (met)

Metabolism is a set of physico-chemical processes which take place at cellular level for the production of thermal and mechanical energy, replication, and elimination of waste material (Nall, 2004; Spengler et al., 2001). Metabolism can be divided into two categories; basal metabolism and actual metabolism. Basal metabolism is required in order to maintain blood circulation, respiration, and nerve transmissions in an organism. Every person shows different metabolic rates. According to age and activity, overall metabolic energy release-rate in humans ranges from 0.5 W/kg in elders to 2 W/kg in children, with a typical 1 W/kg in adults. On the other hand, actual metabolism involves muscular work. Actual metabolic rate can be measured by gas analysis in respiration, either by oxygen consumption or by CO₂ generation (and breath rate), or estimated by heart rate. As a result, heat is generated inside the body and may be dissipated to the environment in the form of radiation, conduction and convection (ASHRAE, 2017). The unit of metabolic rate is W/m² or met. ASHRAE 55 (2017) provides metabolic rates for a variety of activities as shown in Table 3.1.

Clothing Insulation (clo)

One of the thermal comfort parameters is insulating effect of clothing on the occupant. Clothing protects heat loss by acting as the body's insulation and helps the skin maintain a stabilized temperature. Depending on period and place, the clothing insulation varies. Clothing is expressed in terms of a unit called "*clo*" for the

calculation of thermal comfort. 1 *clo* corresponds to insulating cover over the body (ASHRAE, 2017).

Table 3.1. Metabolic rates at different activities
(Source: ASHRAE 55, 2017)

Activity	met	W/m²
Sleeping	0.7	40
Seated, at rest	1.0	58
Very light work (shopping, cooking, light industry)	1.6	93
Medium light work (house~, machine tool ~)	2.0	116
Steady medium work (jackhammer, social dancing)	3.0	175
Heavy work (sawing, planing by hand, tennis) up to	6.0	350
Very heavy work (squash, furnace work) up to	7.0	414

Table 3.2. Insulating value of clothing elements
(Source: ASHRAE, 2017)

Clothing	clo	m²K/W
Naked	00	0
Shorts	0.1	0.016
Typical tropical unit	0.3	0.047
Light summer clothing	0.5	0.078
Working clothes	0.8	0.124
Winter indoor clothing	1	0.155
Traditional business suit	1.5	0.233

3.1.3. Indoor Air Quality (IAQ) Parameters

Providing a good IAQ is important for thermal comfort. Many factors affect IAQ such as the type and the amount of the contaminants (CO, NO₂, Rn and SO₂) and the concentration of CO₂ or O₂ which can be measured by simple sensors.

The normal O₂ concentration in the air is 20.9% whilst the acceptable highest and lowest bound of O₂ concentration in a space is 23.5% and 19.5%, respectively. Table 3.3. shows effects of O₂ concentration on occupants.

Table 3.3. Effects of O₂ concentration on occupants

O ₂ concentration (%)	Effects on occupant
20.9	Normal O ₂ concentration in air
17 -19	Increased heartbeat, accelerated breathing
14-16	Rapid fatigue, poor muscular coordination
6-10	Vomiting, unconsciousness
<6	Spasmodic breathing, death

O₂ and CO₂ are both present in the atmosphere and when CO₂ concentration increases, O₂ concentration decreases. The upper limit of CO₂ concentration for indoor environments is accepted as 1000 ppm (Toksoy, 2015; Hossein Sagheby, 2018). Elevated CO₂ concentration stimulates human respiratory system and increases the met values.

3.2. Exergetic Approach for Thermal Comfort

The ISO 7730 (2005a) uses PMV method (as discussed in Section 3.1.) which was developed based on the First Law of Thermodynamics. However, in the PMV method, there are many combinations of the thermal comfort parameters that give the neutral environment (zero value). Shukuya (2013) suggested another approach which is

based on the Second Law of Thermodynamics. The approach considers human body system as a complex model with circular nodes developed by Gagge et al. (1986) and calculates the human body exergy consumption (HBexC) rate (Fig. 3.2) (Shukuya,2013). The exergetic approach indicates that there are limited combinations of thermal comfort parameters that give the minimum HBexC rate and thermal neutrality.

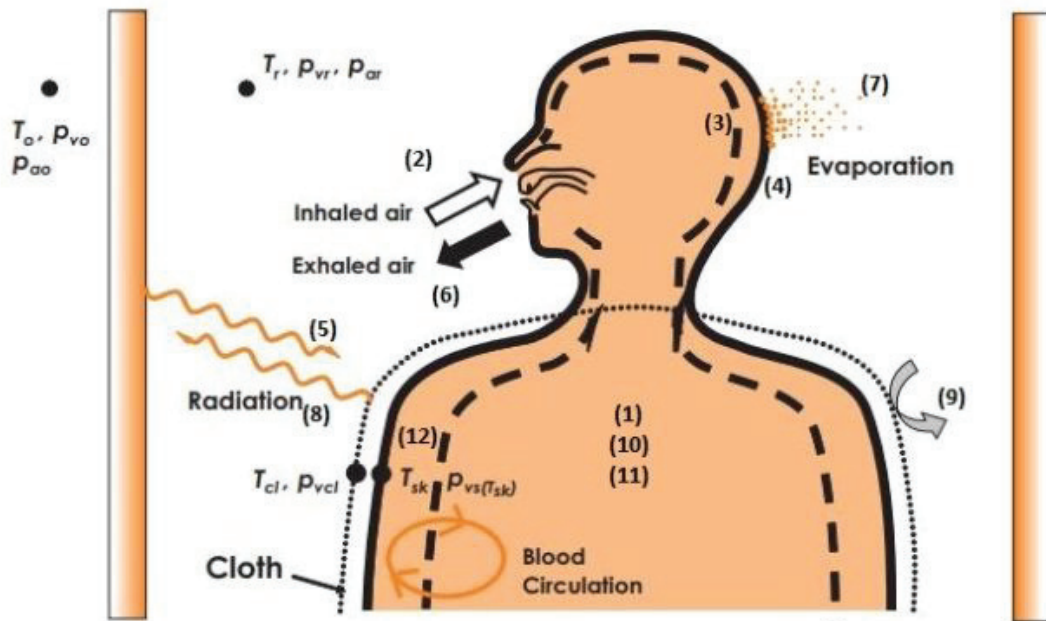


Figure 3.2. Modelling of human body system
(Source: Shukuya, 2013)

Exergy is the capacity of energy to do physical work (Shukuya et al., 2009; Shukuya, 2013). Energy is conservative and cannot be created/destroyed (1st Law of Thermodynamics), while exergy is non-conservative due to the irreversibility of exergy transfer process (2nd Law of Thermodynamics). The exergy balance is shown as in (3.9) (Shukuya, 2013).

$$X_{in} - X_{out} - X_{consumed} = X_{stored} \quad (3.9)$$

where X_{in} and X_{out} are input and output exergies, respectively. $X_{consumed}$ is exergy consumption whilst X_{stored} indicates stored exergy in the system.

The exergy concept can also be applied to the human body system. The human body works to convert energy for metabolism into other forms using personal parameters (body mass, skin surface, activity, clothing value etc.) to provide the desired

thermal comfort value. Taking into account the human body system, the terms in the (3.9) are given in Table 3.4. Since main purpose of the human body system is to keep body core temperature constant, X_{stored} term is very small compared to the other terms. Exergetic approach for thermal comfort takes into account the conditioned space along with the human body system (Fig. 3.3).

Table 3.4. Exergy balance for human body system

Terms	X_{in}	X_{out}	X_{consumed}	X_{stored}
Explanations	(1) exergy generated by metabolism	(6) exergy contained in the exhaled humid air	(10) exergy consumed by human body	(11) exergy stored in the core
	(2) exergy contained in the inhaled humid air	(7) exergy contained in the humid air leaving the body surface (evaporated water from the sweat)		(12) exergy stored in the skin
	(3) exergy contained in the liquid water generated in the body core by metabolism	(8) radiant exergy discharged through the surface (skin and clothing)		
	(4) exergy contained in sum of liquid water generated in the shell by metabolism (sweat)	(9) exergy transferred by convection from the surface to the surrounding air		
	(5) radiant exergy absorbed through the surface (skin and clothing).			

Thermal comfort of human body is the sum of the heat and mass transfer processes entering or leaving the body. Heat flow leaves the human body because of heat transmission (exhaled air), water diffusion, and sweat evaporation which cause the evaporative mass transfer.

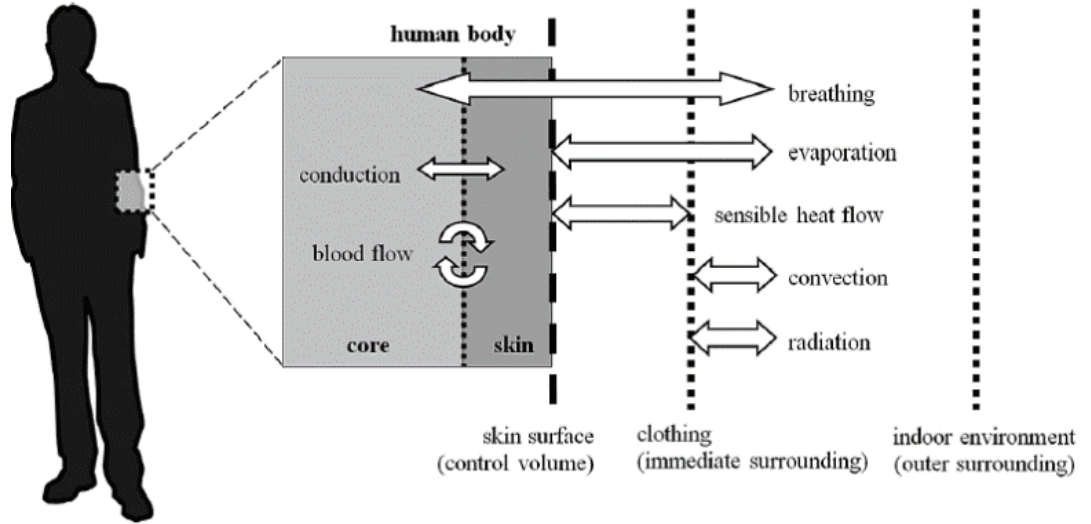


Figure 3.3. Human body system and its interactions with indoor environment
(Source: Prek and Butala, 2017)

On the other hand, energy flow leaves the skin via blood flow and then returns to the body core. Thus, exergy is transferred into the environment and controlled by the environmental conditions via heat and mass exchange. Exergy balance of the human body is calculated for given environmental conditions by assuming heat storage is negligible. In this case, (3.10) is written according to the steady-state conditions;

$$X_{in} + \dot{m}_{a,in} \times e_{a,in} + \dot{m}_{w,in} \times e_{w,in} - X_{consumed} = X_{out} + \dot{m}_{a,out} \times e_{a,out} + \dot{m}_{w,out} \times e_{w,out} \quad (3.10)$$

where ;

$$X_{in} = \left(1 - \frac{T_r}{T_{cr}}\right) \times M + R_w \times T_r \times \ln(\phi) \times \dot{m}_e \quad (3.11)$$

Similarly, the human body exergy output can be calculated. Dry and evaporative heat transfer and water dispersion into the air caused by skin diffusion, air humidifying by breathing and sweating are included in exergy output calculation.

The exergy transfer rates are related to the convection and radiation heat transfers, which are shown in (3.12) and (3.13).

$$X_c = \left(1 - \frac{T_r}{T_{sk}}\right) \times Q_c \quad (3.12)$$

$$X_{rd} = \left(1 - \frac{T_r}{T_{sk}}\right) \times Q_{rd} \quad (3.13)$$

Convective and radiative heat transfer between the human body and environment (room) is included in (3.14):

$$\begin{aligned} X_{consumed} = & c_{bl} \times \dot{m}_{bl} \times (T_{cr} - T_r - T_r \times \ln\left(\frac{T_{cr}}{T_r}\right)) + A_{Du} \times \varepsilon \times \sigma \times \left[T_{cr}^4 - T_r^4 - \frac{4}{3} \times T_r (T_{cr}^3 - T_r^3)\right] + \\ & A_{Du} \times \varepsilon \times \sigma \times \left[T_{sk}^4 - T_r^4 - \frac{4}{3} \times T_r (T_{sk}^3 - T_r^3)\right] + \\ & A_{Du} \times h_c \times (T_{sk} - T_a) \times \frac{(T_{sk} - T_r)}{T_{sk}} + \end{aligned} \quad (3.14)$$

Recalling that the First Law of Thermodynamics refers to the rate of heat generation equals the rate of heat loss; (3.14) implies that exergy input minus exergy consumption equals the exergy output. By using exergy balance equation, HBexC rate is determined. HBexC occurs to maintain body temperature as constant (Shukuya, 2013).

Human body exergy balance calculation needs eight parameters as inputs; T_o , RH_o , T_i , MRT , RH_i , v_a , met and clo . The calculation method uses Gagge's model described in Gagge et al. (1986). Following the exergy balance equation solution, the HBexC rate can be found which satisfies (3.9).

3.3. Actual Mean Vote (AMV)

The AMV is the subjective value of occupant's actual thermal sensation votes by using ASHRAE seven-point scale (Table 1.1). Subjective measurements are conducted via a survey or a mobile application which is designed as an occupant sensing application for smartphones according to ISO 10551 (1995) to obtain AMV (Fig. 3.4). In the thermal assessment studies, a number of thermal comfort sensation scales have been used for assessment of occupant's perceptions including ASHRAE thermal sensation scale (ASHRAE, 2017), Bedford comfort scale (Bedford et al., 1990), McIntyre 3-point preference scale (Griffiths and McIntyre, 1974) and acceptability scale (Brager et al., 1993).

THERMAL ENVIRONMENT SURVEY

This survey is part of a study to evaluate the current thermal conditions of the selected building. We appreciate your feedback in this evaluation. Please tick at the square box where applicable.

1. Gender:	Male <input type="checkbox"/>	Female <input type="checkbox"/>
2. Age :		
3. Occupant location:		
4. Occupant's Clothing <i>Please refer to the attached Table 1. Place a check mark next to the articles of clothing that you are currently wearing as you fill out this sheet. If you are wearing articles of clothing not listed in the table, please enter them into the space provided below.</i>		
Clothing:		
5. Occupant Activity Level (<i>Tick the one that is most suitable</i>)		
Seated quiet/writing, 1.0met	<input type="checkbox"/>	Walking about, 1.7met <input type="checkbox"/>
Typing, 1.1met	<input type="checkbox"/>	Lifting/packing, 2.1met <input type="checkbox"/>
Standing relaxed/Filing(seated), 1.2met	<input type="checkbox"/>	Light machine work, 2.2met <input type="checkbox"/>
Filing(standing), 1.4met	<input type="checkbox"/>	Heavy machine work, 4.0met <input type="checkbox"/>
6. How would you describe your typical level of thermal comfort?		
+3 Hot <input type="checkbox"/>		-1 Slightly Cool <input type="checkbox"/>
+2 Warm <input type="checkbox"/>		-2 Cool <input type="checkbox"/>
+1 Slightly Warm <input type="checkbox"/>		-3 Cold <input type="checkbox"/>
0 Neutral <input type="checkbox"/>		

Table 1
Clothing Ensembles

Description	
Trousers, short-sleeve shirt	
Trousers, long-sleeve shirt	
Trousers, long-sleeve shirt plus suit jacket	
Trousers, long-sleeve shirt plus suit jacket, vest, T-shirt	
Trousers, long-sleeve shirt plus long sleeve sweater, T-shirt	
Trousers, long-sleeve shirt plus long sleeve sweater, T-shirt plus suit jacket, long underwear bottoms	
Knee-length skirt, short sleeve-shirt (sandals)	
Knee-length skirt, long sleeve-shirt, full slip	
Knee-length skirt, long sleeve-shirt, half slip, long-sleeve sweater	
Angle-length skirt, long-sleeve shirt, suit jacket	
Walking-shorts, short-sleeve shirt	
Long-sleeve coveralls, T-shirt	
Overalls, long-sleeve shirt, T-shirt	
Insulated coveralls, long-sleeve thermal underwear tops and bottoms	
Sweat pants, sweat shirt	

Figure 3.4. An example of survey to obtain AMV

Actual Percentage of Dissatisfied (APD) is calculated based on the PPD definition used in ASHRAE 55 (2017) as a function of AMV bu using (3.15).

$$APD = 100 - 0.95 \times e^{-0.03353AMV^4 + 0.2179AMV^2} \quad (3.15)$$

CHAPTER 4

LITERATURE REVIEW

In this section, HVAC control systems are reviewed based on conventional, advanced and personalized thermal comfort controllers.

4.1. Conventional HVAC Control Systems

Conventional HVAC control systems use simple on/off controllers and PID-type controllers. Chinnakani et al. (2011) studied traditional on/off controller for HVAC systems. The authors stated that there is a dead zone between the upper and lower values where the controller stays off position. In addition, the controller does not take sensor delays and inertia of the HVAC system into consideration which cause tracking errors. In another work by Erham et al. (2018), the reason of the inefficiency of the on/off controller was given as the absence of differential values which influences both of human thermal comfort and energy saving.

Many studies showed that the conventional control algorithms using PID-type controllers could provide thermal comfort as well as decreasing the energy consumption in the early 2000's (Kulkarni and Hong, 2004; Bai and Zhang, 2007; Baia et al., 2008; Homod, 2018). Masato et al. (1994) investigated the application of a robust PID controller to HVAC systems for a single-zone environmental space cooling system (Fig. 4.1). The authors proposed to control temperature and they achieved to control the set-point $\pm 0.3^{\circ}\text{C}$. Geng and Geary (1993) carried out an experimental study to investigate the effects of disturbances and process time delays on a PID control performance. The authors also demonstrated some of the typical nonlinear behavior of AHUs. The results revealed that disturbances of the AHU caused mainly by inlet air temperature.

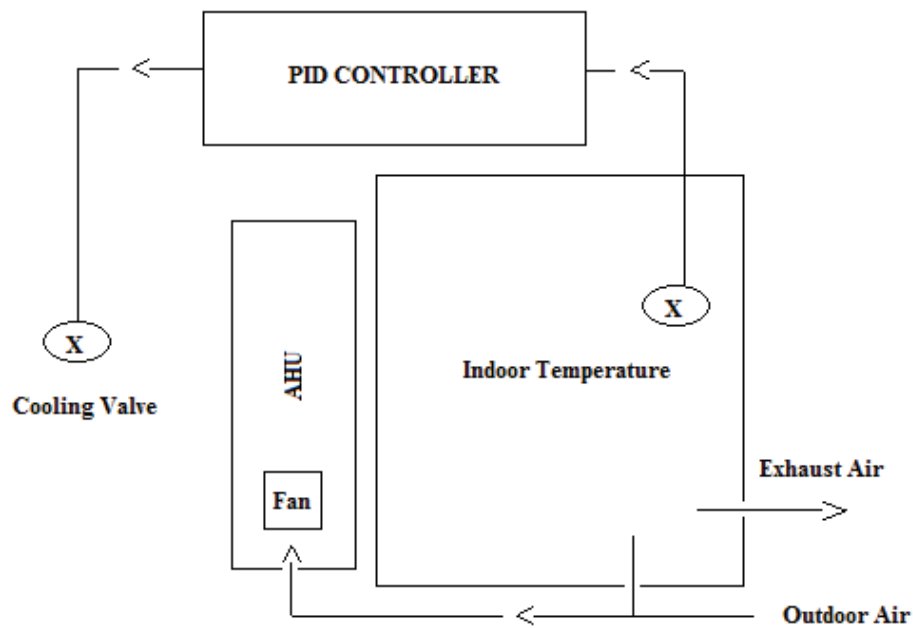


Figure 4.1. PID controller for HVAC systems in buildings
(Source: Masato et al.,1994)

In another study by Bi et al. (2000), an advanced PID application for both single- and multi-variable processes of HVAC system were presented. The control algorithms were written in C++, the graphic user interface (GUI) was used in Java and control system could be monitored through a Web browser. The auto-tuner was tested on an HVAC pilot plant and a commercial building. The authors also demonstrated that tuning a PID controller requires an effective controller design rule but can be a time-consuming, expensive and difficult task. In the last decades, the authors have preferred to compare the conventional controllers with advanced HVAC control systems (Zhou et al., 2000; Craig and Russell, 2001; Ahn et al., 2017; Zhang et al., 2018). For instance, Craig and Russell (2001) compared the PID controller with adaptive controllers. The authors proved that PID controllers are not efficient for all processes and adaptive controllers can be used for complex dynamic structures. On the other hand, adaptive controllers can not be simply trained and require experts to develop a proper dynamic model. Zhou et al. (2000) compared FL controller and traditional PI controller for an inverter air-conditioner. Similarly, Wang and Dai (2004) simulated three controllers including PID controller, FL controller and ANN controller for a central air-conditioning system. The authors proved that PID controllers could be replaced with more advanced HVAC controllers. Anastasiadi and Dounis (2018) developed a FL

controller for HVAC systems to regulate thermal comfort and compared with conventional on/off controller. The advanced controller reduced the annual mean percentage of dissatisfaction by 33%. In another study by Afram and Sharifi (2017), a supervisory controller which uses MPC strategy compared with conventional controllers on a sustainable house in Toronto. The MPC saved 50% of energy compared to conventional controller.

Another group of researchers studied hybrid systems such as advanced HVAC controllers with conventional ones (Wang et al., 2007, Soyguder et al., 2009; Ramteke and Parvat, 2015). Wang et al. (2007) studied the ANN and PID controllers together. The authors exhibited that the advantages of the ANN-PID controller is the capability of self-study and self-adaptation; however, the ANN-PID control system has disadvantages of having static error. In another study by Soyguder et al. (2009), a self-tuning PID-type fuzzy adaptive controller for an expert HVAC system was designed and tested. The proposed controller had no steady-state error compared to conventional ones; however, it had longer settling time compared to advanced HVAC controllers. Dehghani and Khodadadi (2017) designed a neuro-fuzzy PID controller for a heating system. The developed controller had lower overshoot, rise and settling time compared to conventional system.

Although traditional PID controllers have been commonly used in HVAC systems, sometimes it has been difficult to fully compensate for measurement noise and to keep controlled variables close to set point values within the prescribed range. This control objective often fails in achieving the primary goal of HVAC systems: a thermally comfortable environment. Another problem is the necessity of multi-criteria control since traditional HVAC control systems focus only on temperature control. The main reason is that the body thermal state not only depends on indoor air temperature, but also other environmental variables (e.g. mean radiant temperature, air velocity, relative humidity) and personal factors such as clothing insulation and metabolic rate. These parameters are combined in the well-known PMV comfort index developed by Fanger (Fanger, 1970) and was discussed in the previous chapter. Additionally, conventional controllers do not always produce fast response and have large settling times (Turhan et al., 2017).

4.2. Advanced HVAC Controllers

Advanced HVAC controllers have been studied by various artificial intelligence techniques such as ANN, FL, ANFIS and MPCs in the literature.

4.2.1. Artificial Neural Network Controllers

ANN controllers were used as an alternative regulator in both thermal comfort and temperature control of HVAC systems (Gou and Zhou, 2009; Jawed et al., 2017; Erfani et al., 2018; Reena et al., 2018). Magnier and Haghghat (2010) used ANNs to optimize thermal comfort and energy consumption together. PMV and heating and cooling loads were predicted continually by a feed-forward ANN controller which succeeded to predict with average relative error of <1% for the total energy consumption and <4% for the average PMV. Similarly, Macarulla et al. (2017) performed ANN controller in energy management of a commercial building (Fig. 4.2). The inputs of predictive controller were indoor and outdoor temperatures and water heating system temperature so that the controller easily predicted the time when boiler turned on. The proposed ANN controller decreased energy consumption by 19.7% without compromising thermal comfort of occupants.

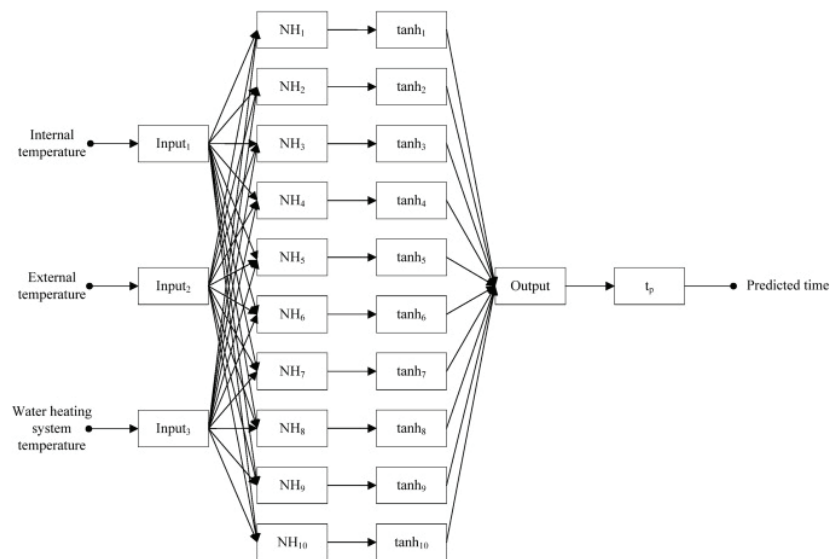


Figure 4.2. Block diagram of thermal comfort control with ANN regulator (Source: Macarulla et al., 2017)

The control of central air-conditioning systems mostly control indoor air temperature but the thermal comfort is affected not only indoor air temperature and but also air velocity, clothing insulation, occupant's gender, health and age. The PMV index takes all influencing factors into account comprehensively. However, the calculation of the PMV value is not easy. Researchers have to predict PMV values by taking constants for rate of body heat production and clothing level. For this purpose, Dong and Xinhua (2004) optimized the control for HVAC system based on ANNs (Fig. 4.3). The PMV index was easily estimated by ANN regulator. The result showed that prediction of PMV index based on ANN control could achieve better result than PID control.

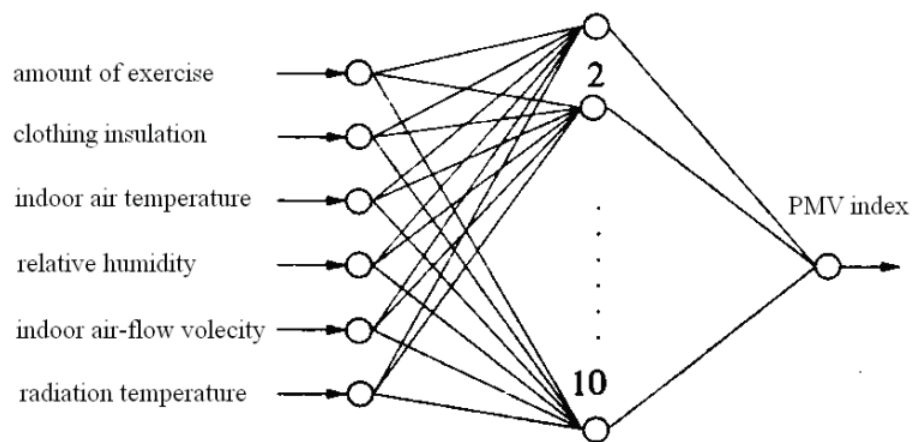


Figure 4.3. Prediction model of PMV index neural network
(Source: Dong and Xinhua, 2004)

Some of the researchers used ANN method in HVAC control systems for energy saving and thermal comfort optimization (Hagras, 2008; Nassif, 2014; Macarulla et al., 2017). Nassif (2014) carried out an experimental study to test self-tuning HVAC component models based on ANNs. The testing results indicated that the optimization process can provide a cooling energy saving of 11% compared to traditional PID controller. In another work by Macarulla et al. (2017), a building energy management system was used to regulate operation time of a boiler with the help of ANNs. The authors succeeded to save 19% energy.

4.2.2. Fuzzy Logic Controllers

The FL controllers are extensively used in complex non-linear processes (Soyguder and Alli, 2009; Tayfur, 2012; Turhan et al., 2015; Ahn et al., 2017). Alcal'a

et al. (2013) implemented a FL controller to maintain thermal comfort and tested the controller in an experimental building in 2013. The study showed that FL controller matched the thermal comfort level and reduced energy consumption by over 10% compared to the traditional controllers. In 2014, Hussain et al. (2014) studied a new method to moderate energy use and thermal comfort in a hotel. The authors used co-simulation tool for optimizing the building control and occupant thermal comfort (Fig. 4.4). The method used a building energy simulation tool EnergyPlus (2011) to evaluate PMV values while the controller was using SIMULINK (MATLAB, 2016). In co-simulation algorithm, EnergyPlus (2011) exports ambient temperature, mean radiant temperature and relative humidity to FL controller which is designed in SIMULINK (MATLAB, 2016). The FL controller processes these data and provides heating and cooling set point temperatures to the HVAC system. Additionally, genetic algorithm is used for optimization process which calculates total energy used and thermal comfort for each combination of the parameters. The FL controller decreased overall energy consumption by 16.1% and 18.1% in case of cooling and heating, respectively.

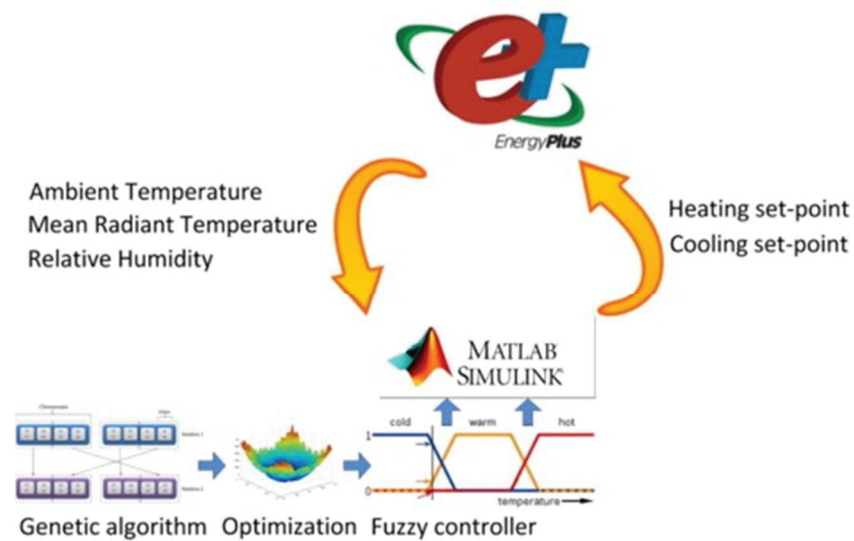


Figure 4.4. Co-simulation example for thermal comfort control
(Source: Hussain et al., 2014)

Yan et al. (2018) developed a FL controller which regulates PMV as output parameter (Fig. 4.5). The proposed controller used temperature, humidity and local air velocity as inputs and the FL controller achieved 7.6% of energy savings compared to conventional controllers. In addition to this work, Hang and Kim (2018) used an

innovative FL controller considering both PMV index and outdoor environmental data such as T_o and RH_o . The authors compared proposed FL controller with conventional controller which does not consider outdoor environmental data. The results of FL controller showed very stable behavior, allowing effective and fast control of the indoor thermal comfort condition.

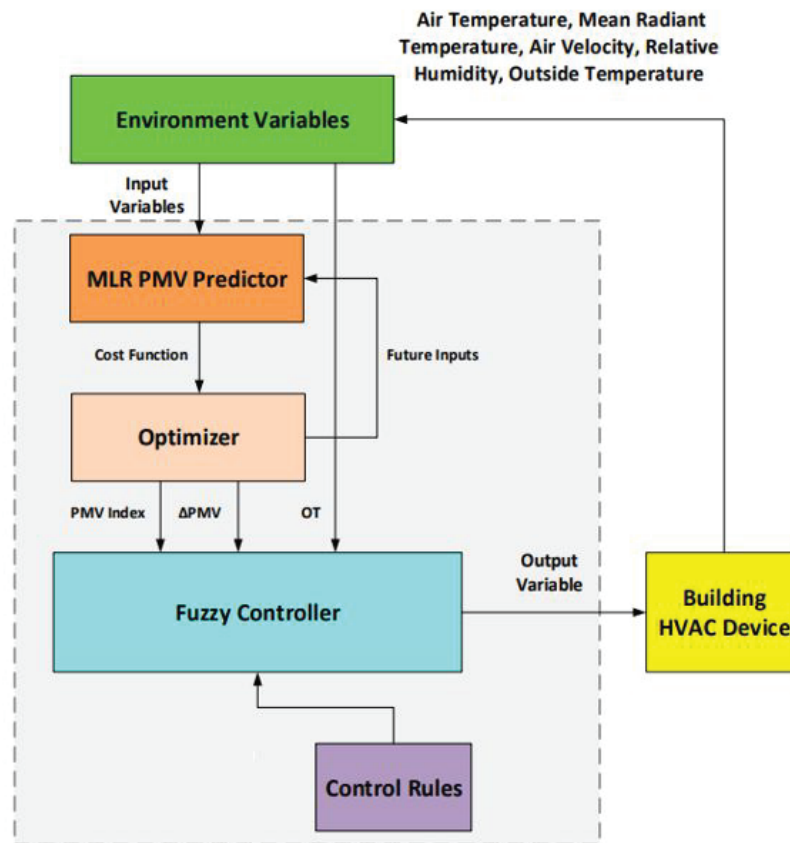


Figure 4.5. Architecture of the proposed FL controller (Source: Hang and Kim, 2018)

Fuzzy regulators can control non-linear processes like HVAC systems and time-delay processes significantly better than traditional controllers. Moreover, FL controllers do not require complex mathematical model of HVAC system. In terms of thermal comfort, FL controllers are more effective due to the fuzzy nature of thermal comfort indices.

4.2.3. Adaptive Neuro-Fuzzy Inference System Controllers

ANFIS is widely used in dynamic systems for prediction of thermal parameters; however, the application of the ANFIS controllers is very limited (Kulkarni, 2001). In a

paper by Al-Jarrah and Al-Jarrah (2013), ANFIS controller was used to control air-conditioning system at different pressures (60 kPa, 120 kPa and 1 atm). Heat transfer rate and water mass flow rate at inlet/outlet of the system was estimated by fuzzy If-Then rules. Then, the fuzzy rules are tuned by ANFIS. Three inputs (pressure, inlet air temperature and relative humidity) and two outputs (heat transfer rate and water mass flow rate) were used for the ANFIS controller (Fig. 4.6).

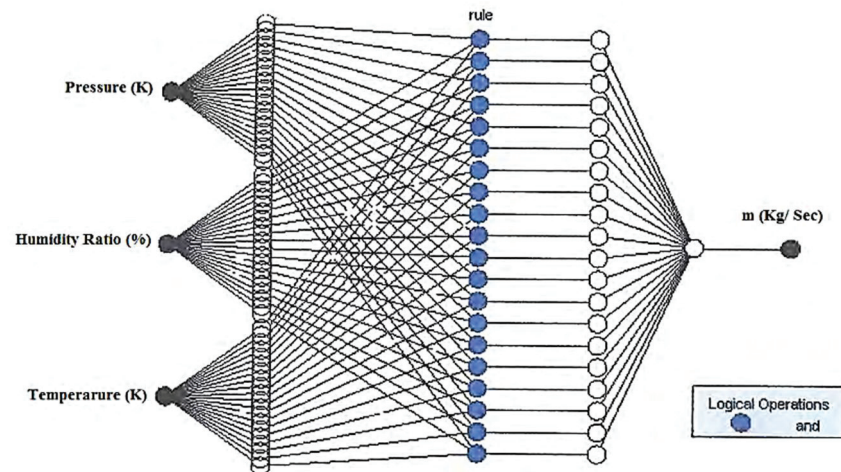


Figure 4.6. ANFIS structure for water mass flow rate
(Source: Al-Jarrah and Al-Jarrah, 2013)

The study showed that the ANFIS predictions for heat transfer rate and mass flow rate have a very low root mean square error (RMSE) with a moderate mean relative error (MRE) of 2.3% and 3% respectively. Marvuglia et al. (2014) coupled ANN and FL controllers for thermal comfort control in an office building. The authors used ANFIS controller with HVAC systems due to the advantage of being characterized using linguistic rules instead of complex analytical expressions.

ANFIS controllers can help HVAC systems to maintain thermal comfort while enhancing energy savings (Lindelöf et al., 2015). However, training stage of the controller can be computationally heavy and the controller requires classification of many physical parameters.

4.2.4. Model Predictive Controllers

The literature proposes several studies on MPCs for HVAC systems (Ma et al., 2011; Karlsson and Hagentoft, 2011; Ma et al., 2012; Ascione et al., 2016; Stauffer et

al., 2017). In particular, for HVAC systems, different formulations of cost functions and constraints have been analyzed to minimize the consumption or to guarantee a desired comfort level. Lü et al. (2007) controlled the AHU for regulating the dry bulb temperature which was set to 26°C (Fig. 4.7). The feedback regulation part was designed to be added to the general predictive functional control to compensate uncertainties of predictive model. The measurement signals for the experiments were the water and airflow rates, on-coil air dry-bulb/wet-bulb temperature, cooling coil inlet and outlet water temperature. The authors demonstrated that compared with the conventional PID controller, the fuzzy predictive controller technology has advantageous dynamical performance of less overshoot and shorter setting time.

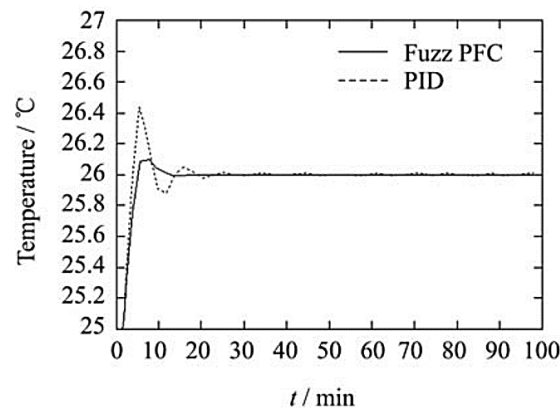


Figure 4.7. Comparison of PID and fuzzy-MPC of an AHU system (Source: Lü et al., 2007)

In 2010, Morosan et al. (2010) studied a similar a predictive control structure for thermal regulation in buildings (Fig. 4.8). To have a better comparison of the control methods, the study imposed for the classic on/off and P/PI controllers. The MPC scheme reduced the energy consumption by 5.5% while improving thermal comfort by 36.7%.

MPC strategy can be used for zone temperature control for thermal comfort in buildings (Sirocky et al., 2011; Privara et al., 2011; Castilla et al., 2014; Hilliard et al., 2017). Privara et al. (2011) succeeded to achieve 29% decrease in energy consumption with MPC whilst maintaining same thermal comfort compared to the conventional control methods. Researchers compared MPC also with other expert systems. For instance, Xi et al. (2007) compared MPC with ANN controller and concluded that MPC improved settling time by 25%.

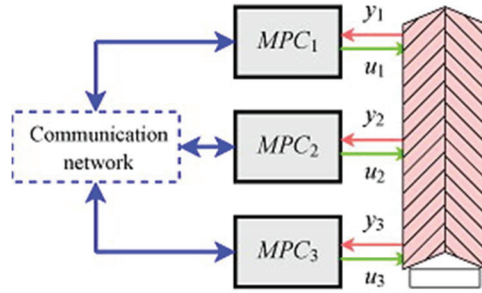


Figure 4.8. MPC scheme for HVAC systems
(Source: Morosan et al., 2010)

Molina et al. (2011) used optimized MPC for energy saving in HVAC systems as well. The study reduced operational costs by 30% compared to non-optimized MPC. In another study by Castilla et al. (2017), MPC implemented in order to control thermal comfort (Fig. 4.9). A non-linear MPC was designed for a biblio-climatic building and the results were compared with conventional controller. The results showed that MPC was able to maintain thermal comfort inside a comfort zone even in the presence of disturbances, and to reduce the energy consumption by 53% in comparison with PID controller.

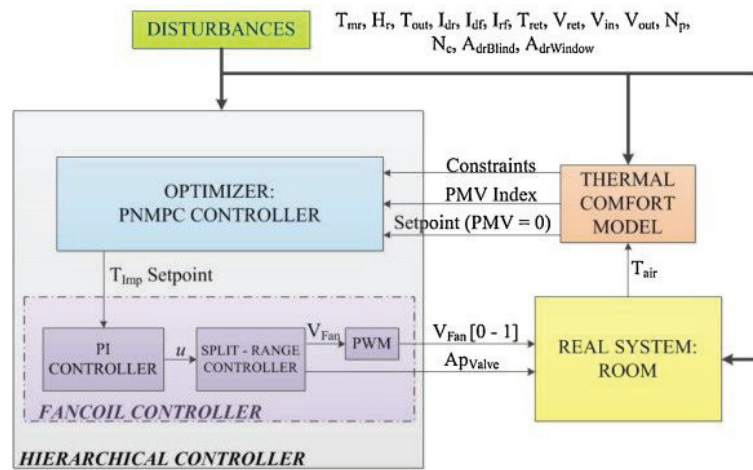


Figure 4.9. MPC control system for thermal comfort
(Source: Castilla et al., 2017)

Yang et al. (2018) applied MPC to building automation in order to control thermal comfort. The controller proposed to develop a PMV index by using indoor air temperature, mean radiant temperature and humidity. Compared to the conventional on/off controller, the MPC controller achieved 19.4% of energy savings whilst keeping the PMV index within an acceptable comfort range. The advantages of MPCs are the

fact that they allow the current sampling time to be optimized while keeping future sampling times in account, moreover, MPCs anticipate future events and can take control actions accordingly. However, MPC requires building models in terms of equipment and dynamics. Consequently, such controllers may not be suitable for large buildings. Table 4.1 depicts advantages and disadvantages of HVAC control systems.

Table 4.1. Comparison of HVAC control systems
(Source: Turhan and Gökçen Akkurt, 2018)

Type of controller	Method	Year	Output variable	Advantages	Disadvantages	References
CONVENTIONAL CONTROLLERS	On/off	1930s	Temperature	Simple and common	No feedback	Harrold and Lush, 1998; Calvino et al., 2010; Mirinijad et al., 2012
	PID-type	1980s	Temperature	Easy to operate	Do not produce fast response suffer a problem of overshoot Large settling time	Kulkarni and Hong, 2004; Masato et al., 1994; Geng and Geary, 1993; Craig and Russell, 2001
AI-BASED CONTROLLERS	ANN	1990s	Thermal comfort	Requires mathematical model of both HVAC system and thermal comfort sensation	Difficult to find proper construction of layers and neuron numbers	Kanarachos and Geramanis, 1998; Ferreira et al., 2012; Krarti, 2003; Liang and Du, 2005
	FL	1990s	Thermal comfort	Preferable for HVAC systems that are hard to model mathematically	Requires time to construct rules	Zhou et al., 2000; He et al., 2005; Gouda and Danaher, 2011

(cont. on next page)

Table 4.1. (Cont.)

Type of controller	Method	Year	Output variable	Advantages	Disadvantages	References
AI-BASED CONTROLLERS	ANFIS	1990s	Thermal comfort	Self-learning ability Simple structure	Combination of ANN and FL	Soyguder and Alli, 2009; Marvuglia et al., 2014; Turhan et al., 2017
	MPC	2000s	Thermal comfort	Anticipate future events Optimization procedure	Require building models Difficult to apply in larger buildings	Ascione et al., 2016; Ma et al., 2011; Pedersen et al., 2017

4.3. Personalized Thermal Comfort Controllers

Although the control algorithms of conventional HVAC systems are directly applicable, they do not detect occupant-building interactions. Furthermore, individual differences are neglected in conventional PMV-PPD method. However, studies in the literature show that individual differences such as gender and age are significant on thermal comfort (Humphreys and Hancock, 2007; Indrigandi and Rao, 2014). Conventional HVAC system controllers merely regulate the indoor air temperature where thermostats are used for the feedback control of temperature. But the controllers do not take into account the occupant's thermal comfort. On the other hand, AI-based controllers calculate a unique standardized thermal sensation or operative temperature for all occupants instead of taking into account individual differences. Therefore, researchers have started exploring the ways and methods to make HVAC systems adaptive to the occupant's thermal sensation and individual differences instead of using average models.

This section focuses on wireless multi-sensors studies used for thermal comfort control. To reduce HVAC energy consumption, previous studies have proposed using wireless occupancy sensors or even cameras for occupancy based actuation showing energy savings up to 42% (Feldmeir, 2009; Li et al., 2011; Brooks et al., 2014; Ranjan and Scott, 2016; Ghahramani et al., 2018) In 2003, Lin et al. (2003) developed a

thermal comfort control model by using multi-sensors. The study addressed this multi-sensor, single-actuator control problem which was solved by a computer program and optimization technique. In the study, each room equipped with multisensors and a sensor network and the controller operated only on the temperature reading from the room sensors. As a conclusion, the authors demonstrated that the comfort-optimal strategy reduces energy consumption by 4% while reducing PDD from 30% to 20%. In 2009, Feldmeir (2009) created a novel air-conditioning control system which aimed at personalized environments. The author developed an extremely low power, light weight, wireless sensor which can measure temperature, humidity, activity and light level directly on the occupant's body (Fig. 4.10). The measured data were then used to immediately infer occupant thermal comfort and to control HVAC system in order to minimize both cost and thermal discomfort. The proposed controller decreased energy consumption by 3% which represented the direct result of improving occupant's thermal comfort.



Figure 4.10. Sensors worn by an occupant
(Source: Feldmeir, 2009)

Similarly, in 2009, Watanabe et al. (2009) used a chair with local heating and cooling strips and fans to ensure personalized thermal comfort (Fig. 4.11). Experiments were conducted in a climate chamber during summer with seven healthy male college

students. Authors concluded that even at a room temperature of 30°C, the occupants were able to create acceptable thermal environments by using the chairs with fans.



Figure 4.11. Personalized thermal comfort controller as a chair
(Source: Watanabe et al., 2009)

Occupancy measurements play an important role to achieve energy saving by detecting the absence/presence of the occupant. In 2011, Li et al. (2011) studied radio-frequency identification (RFID)-based location sensor to measure occupancy presence. The RFID based location sensor which has two AA batteries and two antennas sent signals to the reader and thus the authors succeeded to know the location of the occupant. Hence, the study demonstrated that RFID based location sensors could be used for energy-efficient driven HVAC systems. In another study by Erickson et al. (2013), power-efficient occupancy-based energy management system was developed. The HVAC system was controlled based on actual occupancy levels and utilizes a purpose-built wireless network of camera sensors with a parallel network of Passive Infrared (PIR) sensors to sense the presence of occupants to obtain the optimal personalized thermal comfort (Fig. 4.12). The authors succeeded to save 26% of energy consumption with occupancy based HVAC controller.

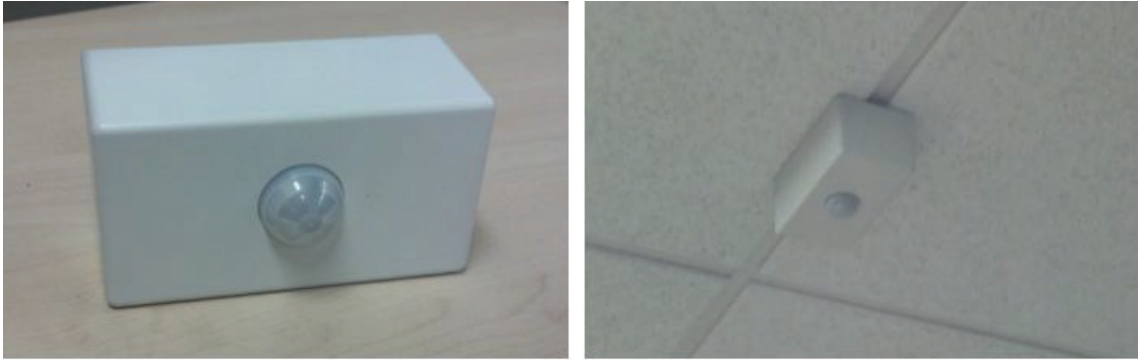


Figure 4.12. PIR sensors used for occupancy detection
(Source: Erickson et al., 2013)

Additionally, in 2014, Brooks et al. (2014) used motion detectors with low-cost, wireless sensor nodes (Fig. 4.13). A building in University of Florida campus which uses 3 AHUs was selected as a test chamber. The controller used wireless sensor network, a software infrastructure for data management and control execution (MATLAB) and a control algorithm for computing commands. In the study, real-time measurements were used as thermal comfort controller. A PIR sensor (for measuring occupant presence), a CO₂ sensor (for indoor air quality) and a T/RH sensor were deployed with a microprocessor. Even though the study did not take into account CO₂ sensor in the control algorithm, the experiments showed that the controller achieved 37% energy saving without sacrificing thermal comfort.

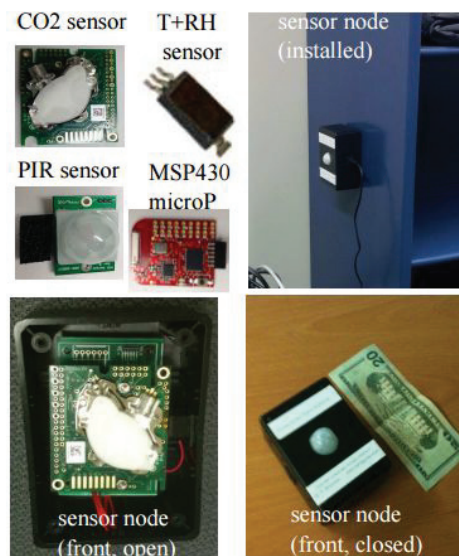
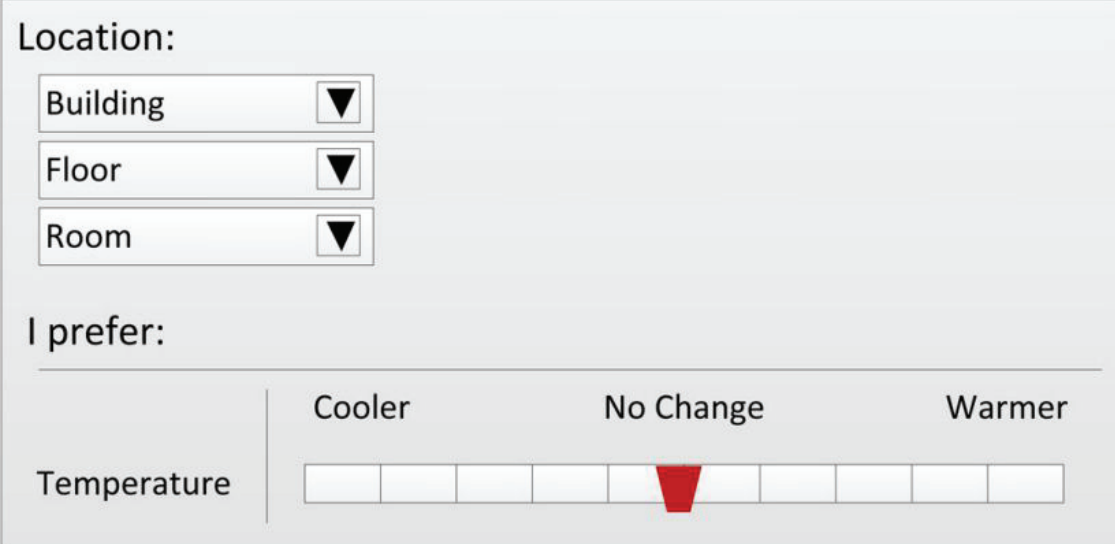


Figure 4.13. Wireless sensors for thermal comfort measurement
(Source: Brooks et al., 2014)

A number of studies on personalized thermal comfort prefer to use surveys or mobile phone applications instead of/along with sensor measurements. In 2014, Jazizadeh et al. (2014) implemented occupant thermal comfort profiles to the HVAC control logic. The estimation of the profiles was done by FL approach. The controller used user interference and thermal preference scale which is shown in Fig. 4.14. The study used participatory sensing approach which relies on computing devices such as notebooks and mobile phones. Occupants reported their preferences under different indoor environmental conditions through the user interface. Thus, the controller learned occupants thermal comfort profiles which will be used in HVAC operations. Moreover, the results showed a 39% reduction in daily average airflow rate when the HVAC system used personalized thermal comfort driven controller.



The figure shows a user interface for setting thermal preferences. It is divided into two main sections: 'Location:' and 'I prefer:'. The 'Location:' section contains three dropdown menus for 'Building', 'Floor', and 'Room'. The 'I prefer:' section features a horizontal scale with three labels: 'Cooler', 'No Change', and 'Warmer'. Below these labels is a row of ten rectangular boxes. A red downward-pointing triangle is positioned in the fifth box from the left, indicating the current preference level.

Figure 4.14. Components of user interface and thermal preference scale
(Source: Jazizadeh et al., 2014)

Ranjan and Scott (2016) used thermographic imaging technique for personalized thermal comfort control. The controller used real-time thermal preferences of the occupants by machine learning model (Fig. 4.15). The authors indicated that energy could be saved if realtime thermal preferences were used rather than using standard air temperature based control in HVAC systems.

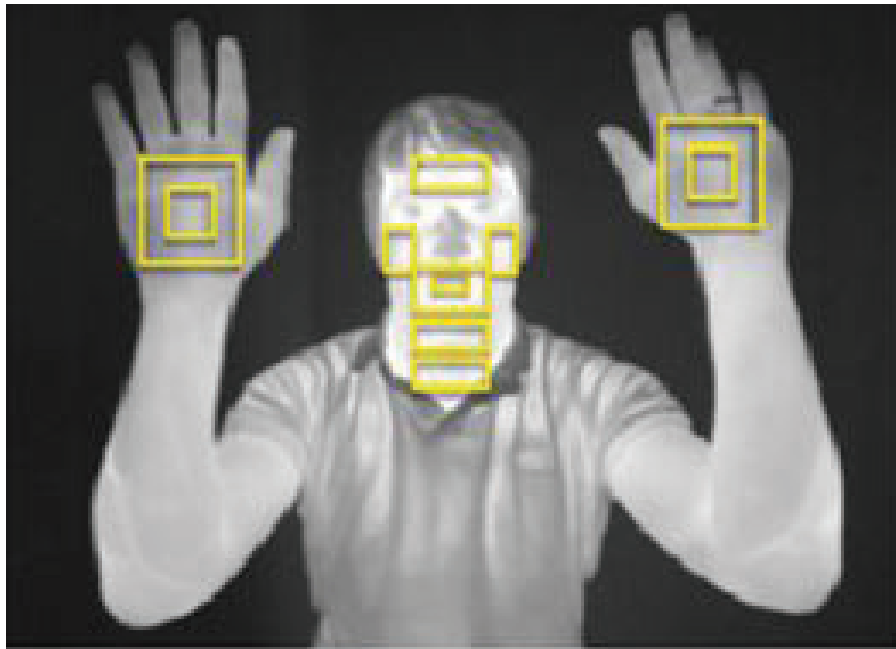


Figure 4.15. Thermographic data collection points
(Source: Ranjan and Scott, 2016)

In addition, Lopez et al. (2016) achieved personalized thermal comfort by heating wrist instead of heating the whole thermal environment (Fig. 4.16). The controller measured temperature at index finger, palm and back of the hand and controlled the set-point temperature of HVAC system. The authors indicated that the personalized thermal comfort controller which consumes lower energy consumption could be used instead of conventional control systems.

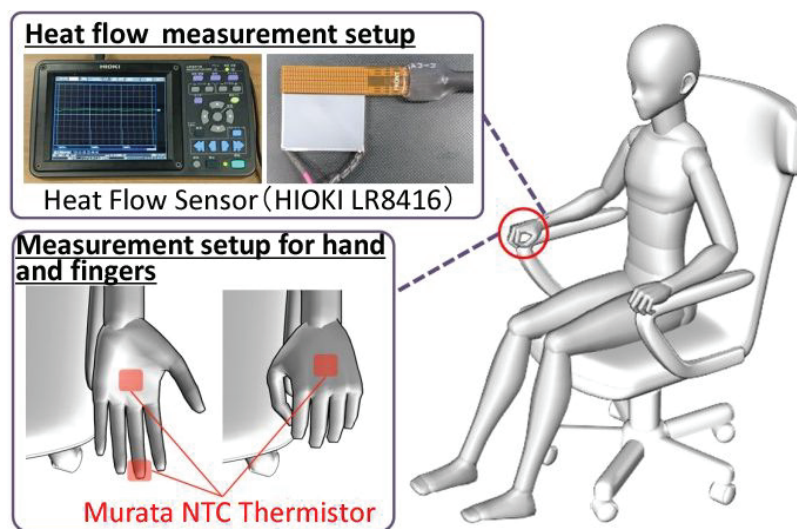


Figure 4.16. Sensor placement for personalized thermal comfort controllers
(Source: Lopez et al., 2016)

Similarly, Ghahramani et al. (2018) utilized infrared thermography with the help of sensors which is installed on eyeglass frame (Fig. 4.17). The authors proposed a hidden Markov model learning approach to capture dynamic thermal comfort of occupants. Surveys were conducted for four days at the same time with the measurements and the proposed learning algorithm predicted uncomfortable conditions with an accuracy of 82.8%. The authors concluded that real-time measurements of personalized thermal comfort allow HVAC system controllers to optimize energy consumption while ensuring better thermal comfort.



Figure 4.17. The infrared sensing system installed on an eyeglass frame
(Source: Ghahramani et al., 2018)

Personalized thermal comfort controllers are also used for industrial applications. Learning thermostats adopts thermal preferences of occupants to temperature changes (Fig. 4.18). The occupant easily changes the room temperature from the smart thermostat and the thermostat programs itself after a week training period. Moreover, the thermostat wants to know the occupant's schedule thus understands the presence/absence of occupants so that saves the energy.

Local body temperature can be more useful than core body temperatures for personalized thermal comfort controllers (Feldmeir, 2009; Rahman and Scott, 2016). For this reason, some companies use wearable smart thermostats (Fig. 4.19). The occupants press “hot (red color in wrist thermostat)” or “cold (blue color in wrist

thermostat)” button whenever they feel uncomfortable. The wrist thermostat uses Peltier Effect (Wang et al., 2018) and activates a comforting wave of cooling or heating on wrists.



Figure 4.18. Learning thermostats
(Source: Google Nest, 2018)



Figure 4.19. Personal wristband thermostat
(Source: Embrlabs, 2018)

The recent literature showed that personalized thermal comfort controllers can achieve individual thermal comfort and energy saving. However, these control systems are still expensive because of the high number of pricey sensors. Many sensing systems are not easy-to-use by the occupants since dense sensing systems make personalized thermal comfort controllers complicated. Moreover, the programming of such a large sensor network becomes the most complicating issue.

4.4. Studies on Exergetic Thermal Comfort

Many authors used human body exergy balance calculation to find the relationship between HBexC and thermal comfort. Shukuya (2013) calculated HBexC by using exergy balance equation and indicated that the minimum rate gives the neutral thermal comfort. Isawa et al. (2013) showed indication of correlations between thermal comfort and HBexC. Similar to the Shukuya's work, the authors concluded that the lowest exergy consumption occurred at thermal neutrality ($PMV=0$). Prek (2005) used thermal sensation votes (Actual Mean Vote) and found that minimum exergy consumption rates were near neutral thermal sensation votes. The author indicated that there are a limited number of combinations of T_i and MRT which gives the minimum HBexC value. In another study by Prek and Butala (2017), the HBexC method was compared with PMV method and it was indicated that the Second Law determines thermal comfort more accurately than the First Law. Batato et al. (1990) applied human body exergy analysis and concluded that the metabolism produces the same exergy and energy magnitude; however, the energy losses to the environment significantly exceed the exergy losses. Simone et al. (2011) used several sets of the thermal sensation data from previous studies to the HBexC. The authors found that there is a second-order polynomial relationship between thermal sensation votes and HBexC rate.

Caliskan (2013) performed energy and exergy analyses to the human body for summer period for Izmir/Turkey. Exergy consumption rate were found as 2.56 W/m^2 with PMV value of 0.028. The author recommended that the analysis should be done with different climatic conditions and large data sets. No studies were found using large data sets and both heating and cooling periods for investigating the relationship between HBexC and thermal comfort in Turkey.

This thesis is distinguished from past work by various aspects. A novel personalized thermal comfort driven controller (PTC-DC) (software and hardware) for air-conditioning systems is developed without any retrofitting at HVAC system components. The developed control algorithm uses simple and easy-to-understand fuzzy logic rules and operates an air-conditioner automatically according to the thermal preferences of an occupant decreasing energy consumption compared with conventional air-conditioner with PID controller. This technique could be generalized to other HVAC systems. Furthermore, the thesis is tried to correlate IAQ parameters with thermal comfort. Based on the author's knowledge there exist a few studies on the impact of IAQ parameters on thermal comfort in the literature (Noh et al, 2007; Grathier et al., 2015) without any successful correlation. The developed control algorithm of PTC-DC takes IAQ parameters (O_2 and CO_2 concentration levels) into account as well as thermal comfort parameters. Moreover, this thesis investigates exergetic approach of thermal comfort along with energetic approach. The relationship between HBexC rate and thermal comfort for both heating and cooling periods is shown for Izmir/Turkey.

CHAPTER 5

METARIALS AND METHODS

The overall process of the methodology can be summarized in three major parts. The first part gives the development procedure of PTC-DC while part two includes measurements of environmental parameters and tests of PTC-DC. Assesment of the results of Part 1 and 2 is presented in the third part. Fig. 5.1 illustrates the flow chart of the methodology.

Development of PTC-DC

In the first part, the control algorithm of PTC-DC is developed and written with C programming language. Afterwards, a wireless sensor network is deployed to objective data (T_i , T_o , RH_o , RH_i , O_2 and CO_2 concentrations). In addition, the mobile application is developed to obtain subjective data (AMV and clo value) while fuzzy logic estimation model is developed to predict thermal preferences of occupants. The details are provided in Section 5.2.

Measurements

A measurement campaign is designed based on occupant thermal preferences. An office building in Izmir Institute of Technology, Izmir/Turkey is selected as a case building for measurements and application of developed PTC-DC. The PTC-DC is trained in the case building for one day and after training period, the controller is operated according to occupant's thermal preferences, automatically. Simultaneously, PTC-DC is validated with the help of PMV and HOBO sensors (INNOVA, 2018; Onset, 2018) (Section 5.3).

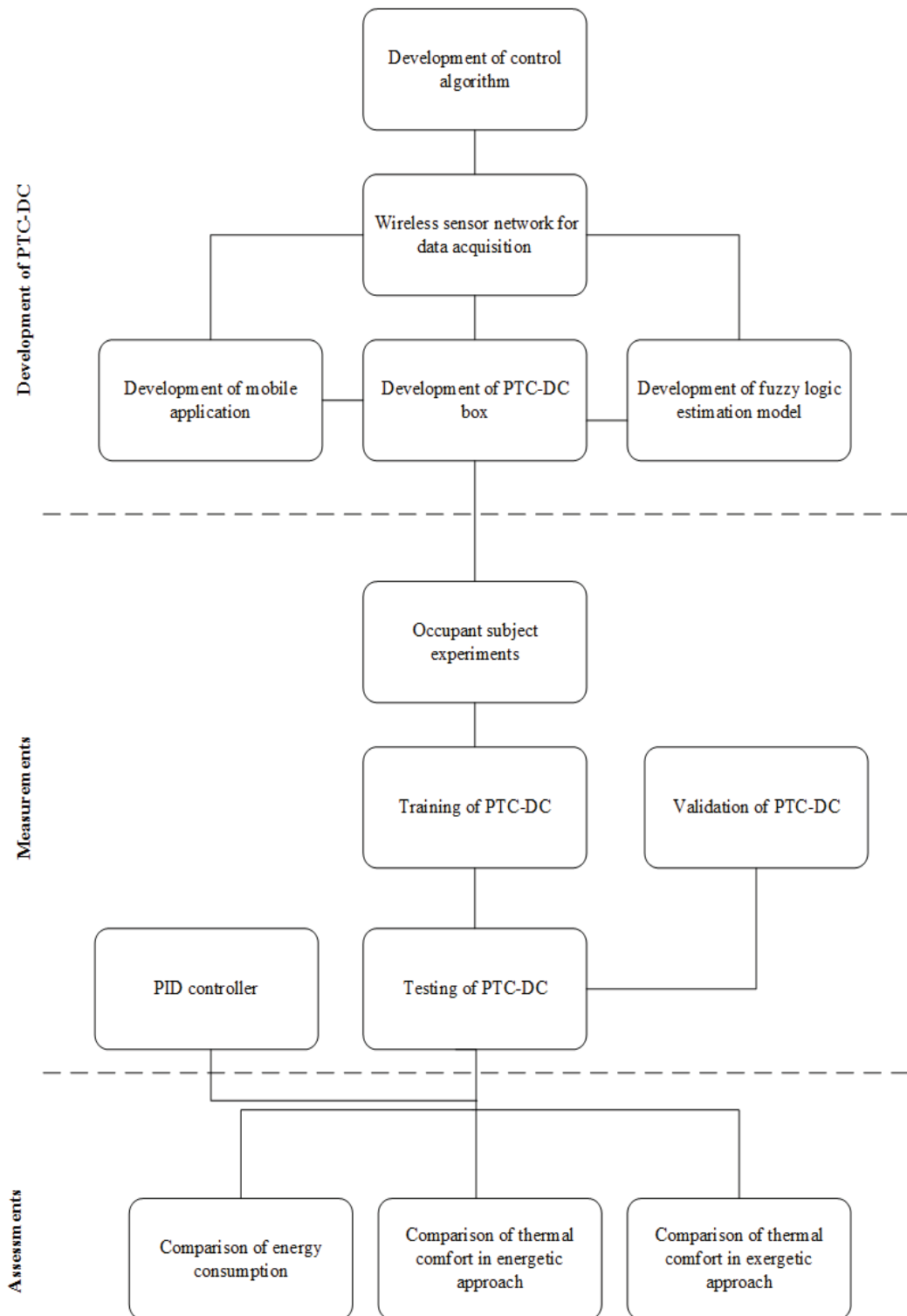


Figure 5.1. Overview of the methodology

Assessment

The goal of the third part is to evaluate the measurements and the performance of the developed PTC-DC. In this last part, PTC-DC is compared with a conventional controller in terms of energy consumption as well as energetic and exergetic approaches of thermal comfort. The assessment techniques are provided in Section 5.4.

5.1. Case Building

The case building is located in Izmir Institute of Technology Campus Izmir/Turkey at latitude 38.3°N and longitude 26.6°E (Fig. 5.2) which has a typical Mediterranean climate called as “temperate humid”. The monthly average minimum temperatures vary between 6-8°C for winter and $\geq 25^{\circ}\text{C}$ for summer (Turkish State Meteorological Service, 2018). The heating period is from November to May whilst cooling period is from May to October.



Figure 5.2. Location of Izmir (left) and case building (right)

The case building consists of two office rooms which have a total dimension of 6m (width) x 6m (depth) x 2.8m (height) and is faced outside with six windows and four external walls. Two rooms are separated with a well-insulated internal wall. However, the internal door is kept open during the measurements. The outer views of the case building are shown in Fig. 5.3.

The external walls of the case building consist of cement plastering, pumice concrete and cement screed. The building is constructed on a soil-filled ground. The innermost layers of the ground are cast concrete, floor screed and limestone. Layers of the roof consist of plasterboard, air gap, glass wool and asphalt. All the window frames

are PVC with double glazing (13 mm air gap). Similarly, the external door and internal door have PVC frame (Fig. 5.4).



Figure 5.3. Surroundings of the case building (left) and case building-outer view (right)



Figure 5.4. The configuration of door (left) and windows (right)

The airtightness of the building is assumed as 0.5 ACH which is a moderate rate for natural ventilated, non-shielded single-family buildings (ISO 13790, 2008). Overall heat transfer coefficients and thicknesses of the walls, floor, doors and windows of the case building are given in Table 5.1.

Indoor environment of the case building is controlled by an air-conditioner with a set-temperature of 22°C from 09.00 a.m to 12:30 p.m and 13:30 p.m to 17:00 p.m during weekdays (Fig. 5.5). The specification of the air-conditioner is given in Table 5.2.

Table 5.1. Overall heat transfer coefficients and thicknesses of the walls, floor, doors and windows of the case building

Parameter	Thickness (m)	U value (W/m²K)
External walls	0.25	0.84
Roof	0.36	2.93
Floor	0.19	2.07
Partition wall	0.25	0.84
Windows	-	1.924
Doors	-	1.9

Table 5.2. Specifications of air-conditioner

Capacity	Cooling	kW	3.25
	Heating		3.95
Dehumidification		lt/h	1.8
Volume flow-rate		m ³ /h	540
Energy Supply		V/W/Hz	230/1/50
Compressor power	Cooling	kW	1.35
	Heating		1.28
COP	Cooling	-	2.40
	Heating		3.08
Fan speed level	Low, medium, high		
Remote controller unit	38 kHz		

The case building is ventilated naturally twice a day for 15 minutes at 09:00-09:15 and 13:30-13:45. A personal computer (70 W) exists in the case building and two fluorescent lamps (50 W each) are used for lighting.



Figure 5.5. Inside of case building (left) and split type air-conditioner used in the case building (right)

5.2. Development of PTC-DC

The development of PTC-DC involves following processes including:

- Software development
- Mobile application development
- Hardware development

The PTC-DC algorithm is shown in Fig. 5.6.

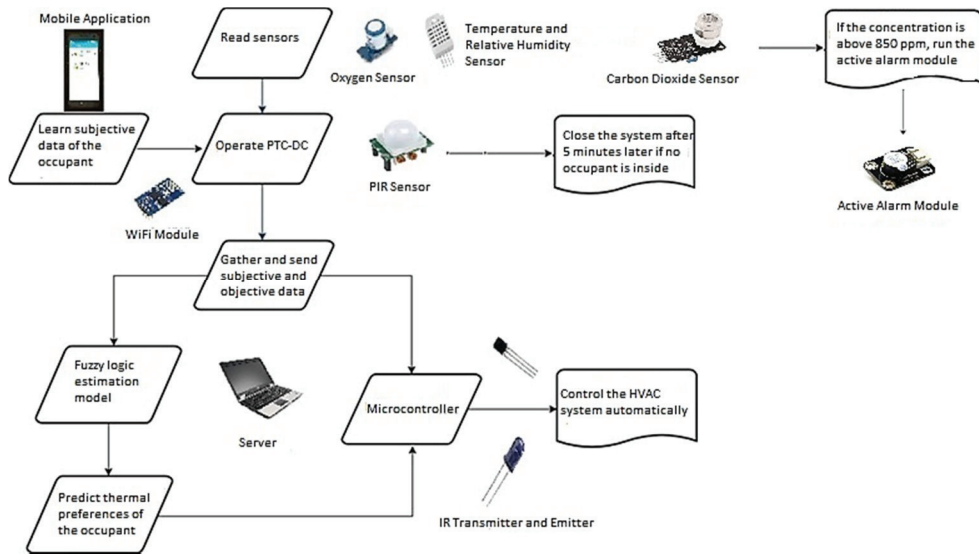


Figure 5.6. Algorithm of PTC-DC

5.2.1. Development of PTC-DC software

The PTC-DC uses a novel control algorithm to obtain personalized thermal comfort. The control algorithm is implemented in C programming language and the script is stored in the server of PTC-DC. The PTC-DC software combines the IR codes of the air-conditioner, fuzzy logic estimation model, subjective and objective data obtained from mobile application and objective sensors, respectively. The PTC-DC uses the previously demodulated IR codes of remote controller of air-conditioner. The novel control algorithm uses FL estimation model to predict occupant's thermal preferences. The reason for choosing FL algorithm for PTC-DC is simplicity (Munataka, 1998; Luger, 2009; Tayfur, 2012). The FL algorithm does not require complex mathematical models and it is more effective due to the fuzzy nature of thermal comfort. The FL estimation model uses two inputs (air temperature and AMV) and two outputs (set-temperature and fan speed). The first input "air temperature" is obtained from T&RH measurements whereas AMV is taken from the mobile application. The PTC-DC uses fuzzy logic model with membership functions created with MATLAB (2016) environment. Table 5.3 shows the division of input and output parameters into fuzzy sets membership functions whilst Fig. 5.7 depicts the membership functions used in the fuzzy logic model of the controller.

Fuzzy rule sets permit the interaction of the membership functions of the fuzzy logic model.

The FL algorithm is constructed with Mamdani fuzzy inference system (Mamdani and Assilian, 1975) and defuzzified with centroid method. The model is trained for one day and after one-day training period, PTC-DC predicts set-temperature and fan speed of air-conditioner according to thermal preferences of the occupants. The accuracy of the FL model outputs affects the efficiency of PTC-DC. Performance of model is characterized by multiple correlation coefficient (R^2) as given in (5.1).

Table 5.3. Division of thermal perception index range into fuzzy sets membership function

Input variables	Linguistic terms	Membership function type	Fuzzy sets (a,b,c)
Indoor air temperature	Low (L)	Trapezoid	$\infty, 20, 22$
	Medium (M)	Triangular	$20, 22, 24$
	High (H)	Trapezoid	$22, 24, \infty$
AMV	Too Cold (TC)	Trapezoid	$\infty, -1, -0.5$
	Cold (C)	Triangular	$-1, -0.5, 0$
	Neutral (N)	Triangular	$-0.5, 0, 0.5$
	Hot (H)	Triangular	$0, 0.5, 1$
	Too Hot (TH)	Trapezoid	$0.5, 1, \infty$
Output variables	Linguistic terms	Membership function type	Fuzzy sets (a,b,c)
Set-temperature	Low (L)	Trapezoid	$\infty, 20, 22$
	Medium (M)	Triangular	$20, 22, 24$
	High (H)	Trapezoid	$22, 24, \infty$
Fan speed	Low (L)	Trapezoid	$\infty, 1, 1.5$
	Medium (M)	Triangular	$1, 1.5, 2$
	High (H)	Trapezoid	$1.5, 2, \infty$

$$R^2 = \frac{\sum(y_i - \hat{y})^2}{\sum(\hat{y} - y)^2} \quad (5.1)$$

where y_i is measurements and y is the standard deviation whilst \hat{y} is the fuzzy logic estimation model output.

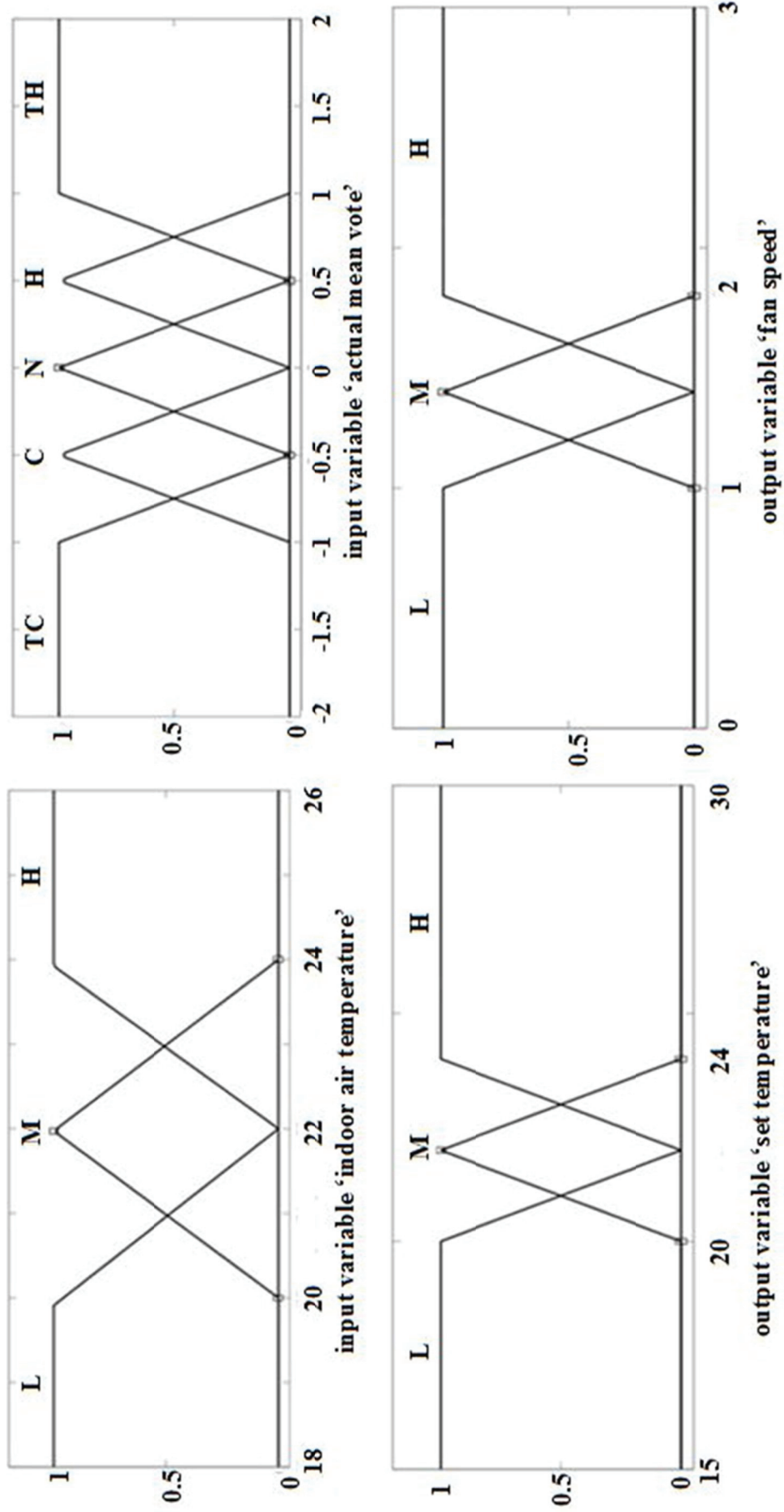


Figure 5.7. Membership functions used for the development of PTC-DC

5.2.2. Mobile application development

The mobile application has been developed as applications for Android-based smartphones and the values are stored in a web server. The mobile application adopts preferences of occupants regarding comfort by inherently incorporating the sensor data and the feedbacks of the occupant with ambient conditions. The application allows occupants to express their preferences according to ambient conditions that have the greatest impact on building energy consumption and occupant's thermal comfort. The mobile application described in the thesis focuses on the comfort preferences as a perceptible parameter for occupants to express their perceptions regarding their thermal comfort and to actuate the air-conditioner according to fuzzy logic estimation model results. In order to train PTC-DC, the occupant is asked to enter name and garment once a day and thermal preferences and whether the occupant is satisfied or not with the fan speed when the occupant feels any discomfort with the environment. The mobile application calculates clothing insulation of occupant by adding garments in Table 3.2.

5.2.3. Development of PTC-DC hardware

The components of PTC-DC hardware are;

- Sensors (3 items) (temperature and relative humidity, oxygen sensor, and passive-infrared sensors)
- Wi-Fi module (1 item)
- Infrared (IR) transmitter and receiver (1 item)
- Microcontroller (1 item)
- Server (1 item)

The PTC-DC stores data transferred from mobile application and sensors, learns thermal preference of the occupant and then predicts the future desired thermal comfort preferences of the occupant following one-day training period by using a fuzzy logic estimation model.

5.2.3.1. Components of PTC-DC hardware

PTC-DC uses sensors to collect objective data. The T&RH sensor provides T&RH data to the PTC-DC, while O₂ and CO₂ sensors measure O₂ and CO₂ concentration values, respectively.

Temperature/Relative Humidity Sensor

The DHT22 (AM2302) sensor is a basic, low-cost and pre-calibrated digital T&RH sensor (Aosong Electronics, 2018). It uses a capacitive humidity sensor and a thermistor to measure the surrounding air, and spits out a digital signal on the data pin. Although DTH11 is the most commonly used T&RH sensor in the literature (Tianlung, 2010; Saha et al., 2018; Kalaiarasi et al., 2018), DHT22 is more precise and accurate and works in a larger range of T&RH. On the other hand, it is more expensive with a larger size.

The DHT22 sensor is connected to an Arduino Mega board (Arduino, 2018), which reads the measured T&RH data and transmits the data to a PC via a USB cable or Wi-Fi module at one second intervals.

In order to make the readings even more precise, the DHT22 sensor was calibrated with a HOBO sensor (Onset, 2018) and (5.2) and (5.3) were obtained:

$$T_{\text{dht22}} = 1.0078 \times T_{\text{hobo}} \text{ (}^\circ\text{C)} \quad (5.2)$$

$$\text{RH}_{\text{dht22}} = 0.9356 \times \text{RH}_{\text{hobo}} \text{ (RH}\%) \quad (5.3)$$

Oxygen Sensor

The PTC-DC includes a Grove-Gas Sensor (O₂) to measure the oxygen concentration in air (SeedStudio, 2018). The O₂ sensor is an organic reaction module and provides a little current while putting the current in the air. Thus, an external power is not needed for this sensor.

Carbondioxide Sensor and Active Alarm Module

A CO₂ sensor, MG-811 (Hanwei Electronics, 2018), is used in order to measure CO₂ concentration in the case building. The ASHRAE 62 (2016) specifies a CO₂ concentration threshold of 1000 ppm for educational and office buildings. In the literature, there exist a number of studies that are concerned with the effects of CO₂ concentration on the health and productivity of occupants in office buildings and these studies set a limit of 850 ppm to provide an alert to the occupants (Persily, 1997; Rice, 2003; Toksoy, 2015; Hossein Sagheby, 2018). The PTC-DC uses DFR0032 active alarm module (DFRobot Electronics, 2018) and warns the occupant by a beep alert whenever the CO₂ concentration raises above 850 ppm. Furthermore, the PTC-DC displays “open the window” message on the main screen. Once CO₂ concentration drops below 850 ppm, the alert and message will vanish.

Passive Infrared Sensor

Passive Infrared (PIR) sensors are used to detect motion based on the infrared heat in the buildings. The PIR sensors are tuned to detect IR wavelength which only emanates when a human being arrives in proximity. Since these sensors do not have an infrared source of their own, they are also termed as passive. The PTC-DC uses HC-SR501PIR sensor (SunRom Electronics, 2018). When an occupant enters/leaves the case building, the PIR sensor sends the signal to server as occupied/unoccupied. The main problem of PIR sensors is when the tracked occupant is staying without motion. In such moments, PIR sensor may not be actually facing towards the occupant. Therefore, the control algorithm is introduced with a 5 minute measurement delay.

Wi-Fi Module

ESP8266-type Wi-Fi module that follows TCP/IP protocol is used to transfer data from mobile application to the server (Espressive Systems, 2018). The module has high storage capacity that allows to be integrated with many sensors.




IR Transmitter and Receiver

The IR transmitter and receiver are used for the communication between PTC-DC and air-conditioner. The system uses DP1838 IR receiver which is small size, light-weight and consumes low energy (DaSheng Electronics, 2018). A PIN diode and a preamplifier are assembled on lead frame, the epoxy package contains an IR filter. The demodulated output signal is directly connected to a microcontroller for decoding.

A 5 mm led is used as an IR transmitter to send the required signal to the air-conditioner in the PTC-DC algorithm (Everlight Electronics, 2018). PTC-DC sends IR signals to the air-conditioner with the help of IR transmitter according to fuzzy logic estimation model results.



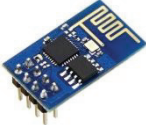




The list of all components used in PTC-DC and their specification are summarised in Table 5.4.

Table 5.4. Specifications of all components used for PTC-DC hardware

Sensors	Sensor types	Aim of usage	Specifications	
			Measurement range	Sensitivity
	DHT 22	Temperature and relative humidity	T: -40÷80 °C RH: 0÷100 %RH	RH: ±%3 (max. %5) T: < ±1°C
	HC-SR501	Infrared motion	3÷5 m	Angle: 140°
	Grove-Gas	Oxygen concentration	%0÷25 (Volumetric)	(-20÷40°C): <%0.1 (Volumetric)

(cont. on next page)

Table 5.4. (Cont.)

	DP1838	IR receiver, communication	10 m	Wave lenght: 940 nm
	5 mm LED	IR transmitter, communication	10 m	Wave lenght: 940 nm
	ESP8266	Wi-Fi module, communication	2 ms	Power consumption<1.0 mW
	MG 811	Carbondioxide concentration	350-10000 ppm	±20 ppm
	DFR0032	Active alarm module	-	-
	INNOVA 1221	PMV measurement	T: -20÷100 °C	0.1 °C
	HOBO	T&RH	T: 0°C to 50°C RH: 10-90%	±0.35°C ±2.5% RH

Microcontroller

The PTC-DC uses Arduino Mega as microcontroller (Arduino, 2018). Arduino Mega is an Arduino card that uses the ATmega2560 base which has 54 digital inputs, an USB connection and an adaptor input (Fig. 5.8). The microcontroller executes arithmetic and logical operations required for the operation of the PTC-DC. The

controller can be connected to a server via USB cable to introduce PTC-DC control algorithm.

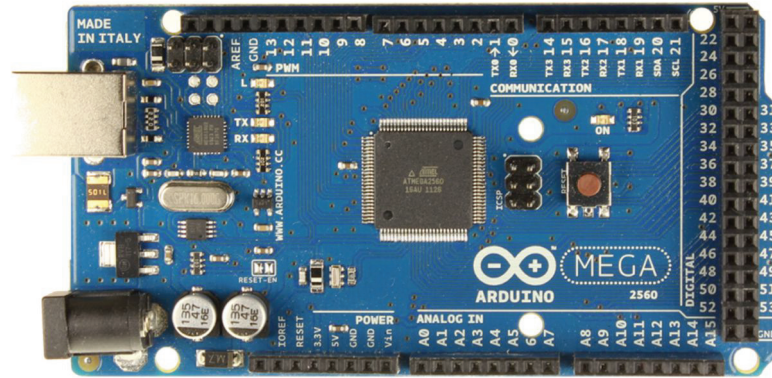


Figure 5.8. Microcontroller for PTC-DC
(Source: Arduino, 2018)

Codes are generated to communicate with the devices. There exist two functions in a C programming code: `setup()` and `loop()`. `setup()` function programmes the codes for microcontroller which is executed when the Arduino Mega is initiated or resetted. After initialization, the microcontroller goes to the loop mode, in which it executes the function `loop()` forever. Arduino Mega is started by setting up a serial communication socket to the PC by calling the `Serial.begin(9600)` line. The parameter 9600 is the baud rate of the serial line. To communicate with the sensors, the libraries of each sensors must be initialized.

Server

The server is used to collect and process data coming from the mobile application, observe the data coming from objective sensors and running the fuzzy logic estimation model. The server of PTC-DC is a PC with an Intel i5-4200U with 1.6 GHz with turbo boost up to 2.6 GHz processor and 4GB of RAM, running Windows 10 edition. Table 5.5 depicts minimum hardware and software requirements in order to operate PTC-DC.

Table 5.5. Minimum requirements for PTC-DC

Hardware requirements	Software requirements
Microsoft Windows 7 or above	Visual Studio 2010 and Net Framework 4*
Intel@Core 5, 1.6 GHz or or faster processor	Arduino IDE**
At least 4 dedicated USB 2.0 bus	C IDE***
Wi-Fi serial transceiver module	* to develop software environment ** to communicate between the PTC-DC and the Arduino microcontroller *** to run the PTC-DC
4 GB Ram	

5.3. Measurements

The PTC-DC is tested from July 3rd, 2017 to November 1st, 2018 and energy consumption and thermal comfort of occupant are compared with conventional PID controller of the air-conditioner in the case building with a male occupant. Physical data of the occupant is shown in Table 5.6.

Table 5.6. Physical data of the occupant

Gender	Age	Height	Weight	Skin surface
Male	33	190 m	82 kg	2.09 m ²

The PTC-DC and PID controller was operated alternating days in order to minimize environmental parameter changes that affect thermal comfort. In addition, the case building is monitored with a PMV sensor to verify the results (Fig. 5.9). T_o , RH_o , T_i and RH_i values are also recorded during the measurement campaign via HOBO sensors (Onset, 2018). The specifications of PMV and HOBO sensors can be found in Table 5.4.



Figure 5.9. The PMV sensor used for measuring the PMV
(Source: INNOVA, 2018)

In addition, a three phase-power analyser was installed to air-conditioner in order to measure energy consumption in kWh (Fig. 5.10). The power analyser was connected to a PC in order to store the data in server of PTC-DC for the comparison. The specification of the power analyser is shown in Table 5.7.



Figure 5.10. Power analyser to measure energy consumption of air-conditioner
(Source: Extech, 2018)

Table 5.7. Specifications of power analyser

Instrument	Measurable parameters	Specification range	Accuracy
EXTECH 3-phase power analyser	Volt, Ampers, kW, kWh, pf, Hz	0-50°C 0-80 RH%	±2% for kWh

5.4. Assessment of PTC-DC

In order to evaluate the performance of the proposed control algorithm, the PTC-DC and PID control of the air-conditioner in the case building was operated alternating days from July 3rd, 2017 through November 1st, 2018. During the operations of the control systems, objective and subjective measurements were conducted as given in the previous sections. The collected data was used to compare the PTC-DC and PID operations in terms of thermal comfort and energy consumption.

Evaluation for Energy Consumption

The PTC-DC was compared with conventional controller in terms of heating, cooling and total energy consumptions. Recalling that the case building was occupied from 09.00 am to 17.00 pm, the assessments of the controllers were done between these hours. Data were collected every day and averaged over a day.

Evaluation for Thermal Comfort

The PTC-DC was analysed in terms of energetic and exergetic thermal comfort approaches. For energetic approach, during operation of both control systems, the AMV of the occupant was collected from mobile application with one-hour intervals based on occupation schedule, then, daily averaged AMV values were plotted and compared for v.1 and v.2 on heating and cooling periods.

The exergetic analysis were applied to the human body system for measured data including heating and cooling periods. The calculations were made with a human-body exergy balance contour calculation tool developed by Asada (2009) which uses six parameters given in Chapter 1-Introduction. These parameters are inputs of the tool which calculates different combinations of T_i and MRT. Daily HBexC rates were calculated and plotted for both PID and PTC-DC controllers. In addition to comparison of the controllers, HBexC rate as a function of T_i and MRT was plotted for the occupant.

Further experiments were run in order to investigate the effect of CO₂ concentration on AMV for both PID controller and PTC-DC. The objective values were set as constant during the experiment days and the occupant was asked to use mobile application in every 5 minutes.

CHAPTER 6

RESULTS AND DISCUSSION

6.1. PTC-DC Software Development

While air-conditioner is operated for a set-temperature of 22°C and mostly constant fan speed at existing PID control, PTC-DC predicts and automatically adjusts set-temperature (v.1) and fan speed (v.2) according to thermal preferences of the occupant (Fig. 6.1).

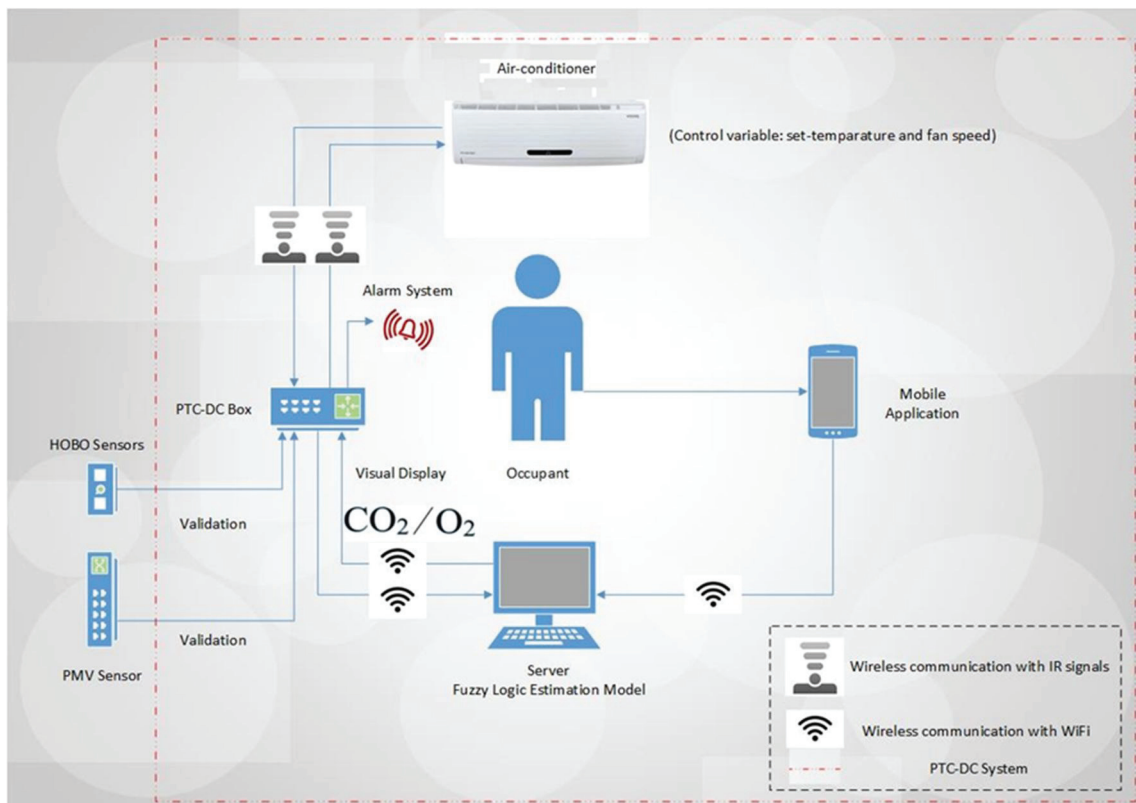


Figure 6.1. Schema of the developed PTC-DC software

The PTC-DC uses C programming language including FL estimation model. The model uses objective data which are sensor-based measurements and subjective data which are obtained from mobile application. According to the results of fuzzy logic

estimation model, the PTC-DC predicts thermal preferences of the occupant, then, the IR transmitter transmits signals that can change the set-temperature and fan speed of the air-conditioner. According to Table 5.3, 135 fuzzy rules are constructed and an example set is given in Table 6.1.

IF indoor air temperature is *low* (L) and AMV is *too cold* (TC) THEN set-temperature is *High* (H) and fan speed is *High* (H) (6.1)

Table 6.1. An example set of 135 fuzzy rules

Indoor air temperature	AMV	Set-temperature	Fan speed
L	TC	H	H
M	C	H	M
M	N	M	M
H	H	M	L
M	TH	L	L
H	TH	L	L

The PTC-DC can be used for any air-conditioner. First, the controller demodulates IR codes of air-conditioner via IR receiver, then, uses these codes to send required signals to the air-conditioner with the help of IR transmitter. Fig. 6.2 shows the screenshot of the first part of PTC-DC programming.

Two versions of PTC-DC, Version 1 (v.1) and Version 2 (v.2) are developed in the thesis. In the first stage, PTC-DC (v.1) is developed to control set-temperature of air-conditioner according to thermal preferences of the occupant. Following the successful operation of (v.1), another version (v.2) is developed in order to improve thermal comfort of the occupant by controlling fan speed along with set-temperature. Furthermore, the O₂ sensor, which was modified and used in (v.1), is not used in (v.2) algorithm, however, it can be monitored on the main screen of PTC-DC server. Instead of O₂ sensor, a CO₂ sensor and an active alarm module are added to (v.2). The differences between (v.1) and (v.2) are given in Table 6.2.

```

void setup() {
  Serial.begin(115200);
  Serial.println("PTC-DC is starting");
  pinMode(46, OUTPUT);
  dht.begin();
  TCNT5 = 0x0000;
  OCR5A = 0x00D0;
}

void loop()
{
  unsigned char data[15]={0x14,0x63,0x00,0x10,0x10,0xFC,0x08,0x30,0x61,0x00,0x00,0x00,0x00,0x30};
  unsigned char data_off[6]={0x14,0x63,0x00,0x10,0x10,0x02};
  unsigned char i;
  unsigned char j;
  unsigned char a;
  unsigned char binary;

  if(CONTROL==0){
    float Vout =0;
    Vout = readO2Vout();
    float h = dht.readHumidity();
    // Read temperature as Celsius (the default)
    float t = dht.readTemperature();
    // Read temperature as Fahrenheit (isFahrenheit = true)
    float f = dht.readTemperature(true);
  }
}

```

Figure 6.2. Screenshot of PTC-DC programming

Table 6.2. Comparison of Version 1 and 2 of PTC-DC

	PTC-DC (v.1)	PTC-DC (v.2)
Temperature/RH sensor	√	√
PIR sensor	√	√
Oxygen sensor	√	√
Carbon dioxide sensor	X	√
Active alarm module	X	√
IR transmitter and receiver	√	√
Wi-Fi module	√	√
Interfaces in mobile application	<i>Name, garments,AMV</i>	<i>Name,garments,AMV, fan speed</i>
Control outputs	<i>Set-temperature</i>	<i>Set-temperature and fan speed</i>

6.2. Mobile Application Development

Mobile application is used to obtain thermal preferences of the occupant. Fig. 6.3 depicts the screenshots of mobile application which is used by PTC-DC. The interface design of mobile application is limited to four questions in order to have a successful participatory sensing approach and avoid being complicated for occupants. In the first interface, application asks the name of the occupant in order to understand which thermal preferences belong which occupants in case there are more than one occupant. Then, thermal preferences (AMV) of the occupant are asked. The interface of the mobile application is originally designed using ASHRAE sensation scale (2017) incorporating five degrees as too cold, cold, neutral, hot and too hot for simplicity. This phenomenon is also used by other researchers (Wong and Khoo, 2003; Humpreys and Hancock, 2007; Jazizadeh et al., 2014). At the third interface, occupant satisfaction of the fan speed is asked as satisfactory, stronger or weaker fan speed preferences. In addition, the occupant is asked to report the garments by selecting clothings on the last interface so that the mobile application easily calculates the clothing value according to ASHRAE (2017). All collected data during the day are used to determine AMV value and thermal preferences of the occupant. Then, the data is transferred to the server via Wi-Fi module and processed in fuzzy logic estimation model. After one-day training period, the PTC-DC is operated automatically. However, the PTC-DC must be re-trained for each period.

The developed mobile application can be downloaded freely from “Google Play Store”.

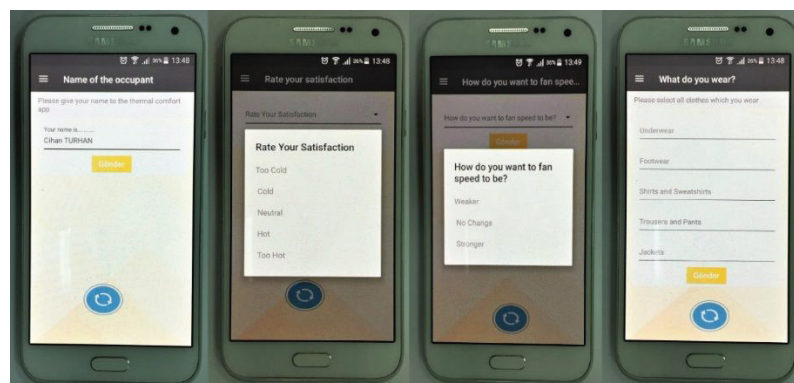


Figure 6.3. Screenshots of mobile application used by PTC-DC

6.3. PTC-DC Hardware Development

The components of hardware are collected in a box. The box consists of a Wi-Fi module to communicate with the mobile application, an IR transmitter and IR receiver to communicate with the air-conditioner, a CO₂ sensor to measure CO₂ concentration, a O₂ sensor to measure oxygen concentration, a temperature and relative humidity sensor, a PIR sensor to detect the absence/presence of the occupant, an active alarm module to warn when the CO₂ concentration is above 850 ppm and an EEPROM to store the data. In addition, resistances are used to prevent overvoltage burns and noises in the system. In order to produce PTC-DC box, the cables and sensors must be connected according to the wiring and sensor diagram in Appendix A. PTC-DC box can be placed on a desk so that the sensors are close to the occupant. In this way, accuracy of the measurements will increase and the maximum thermal comfort would be obtained. The box is powered by a DC adaptor or 12 V battery.

After the wiring and sensor connections, the PTC-DC is packed in a storage box. The PTC-DC box can be produced by any 3D printer according to the technical drawing given in Fig. 6.4 and three-view drawing in Fig. 6.5.



Figure 6.4. Technical drawing of PTC-DC, front (left), back (right)

The produced PTC-DC box is 343 gr with a dimension of 170 mm x 130 mm x 45 mm. T&RH sensor, CO₂ sensor and PIR sensor are placed on the box so that the sensors are not affected by internal heat while active alarm module is placed inside the box (Fig. 6.6 and Fig. 6.7). The legs are added to situate the box easily on a table where it can both detect the occupant and control the air-conditioner from maximum 10 m. The average power consumption of PTC-DC is 7.4 W. The power consumption of PTC-

DC is mainly a result of computation, sensing and Wi-Fi communications. All sensors and modules were awake during the measurement process.

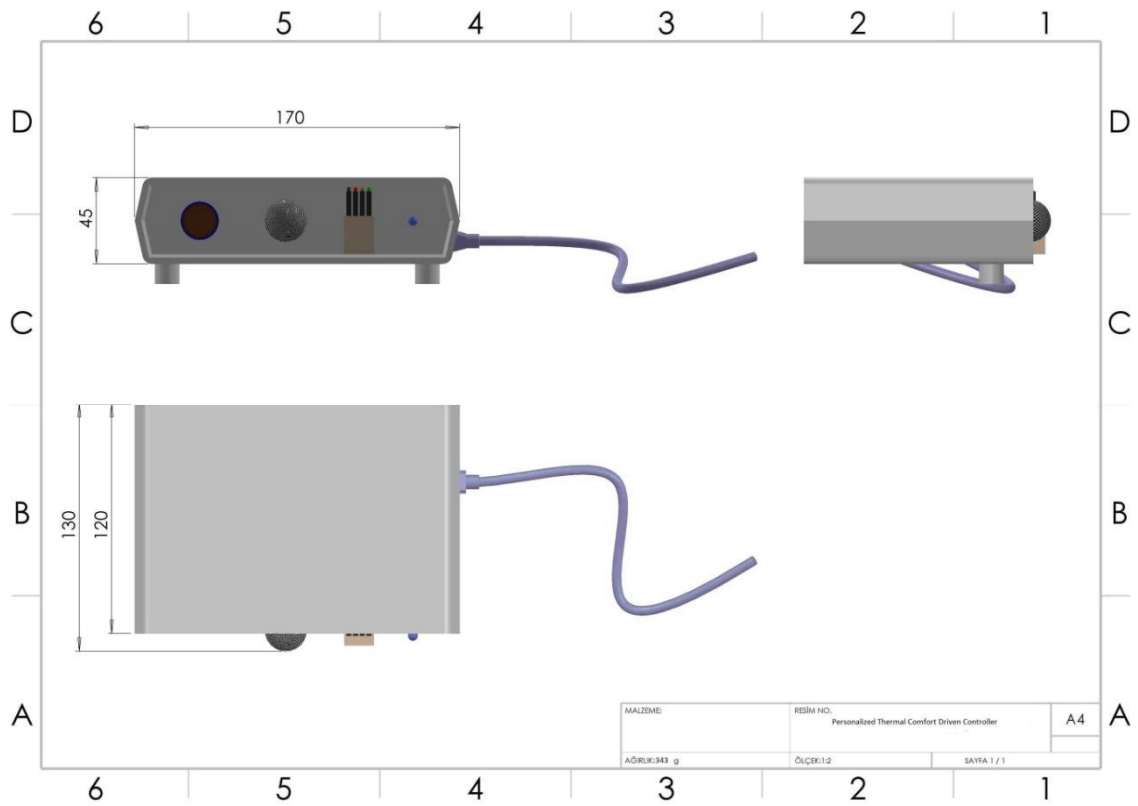


Figure 6.5. Three-view drawing of PTC-DC



Figure 6.6. Front view of the prototype of PTC-DC

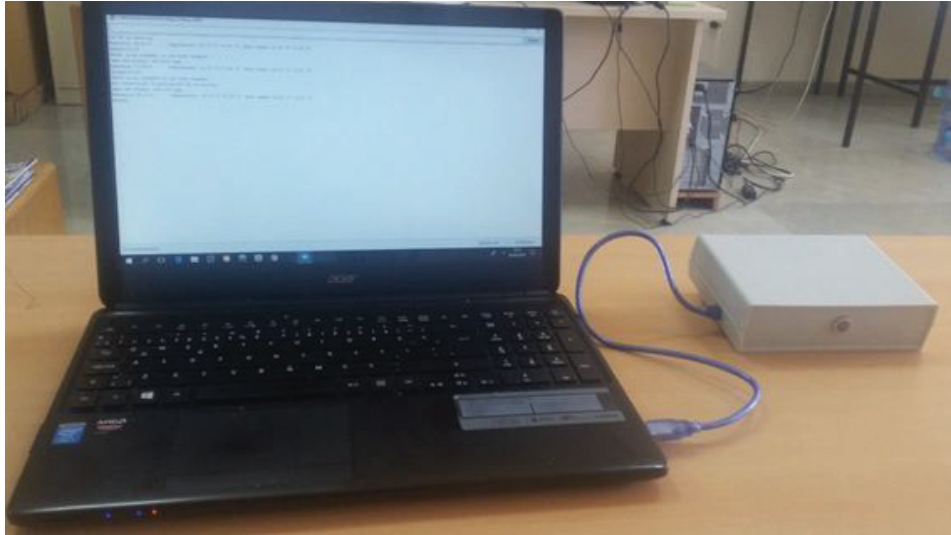


Figure 6.7. Back view of the prototype of PTC-DC

Developed PTC-DC communicates with the occupant via main screen on the server (Fig. 6.8). By this screen, occupant can follow operation steps, objective data, presense/absence of the occupant in the building and display messages of the controller (for instance; open the window, PTC-DC is operating etc.).

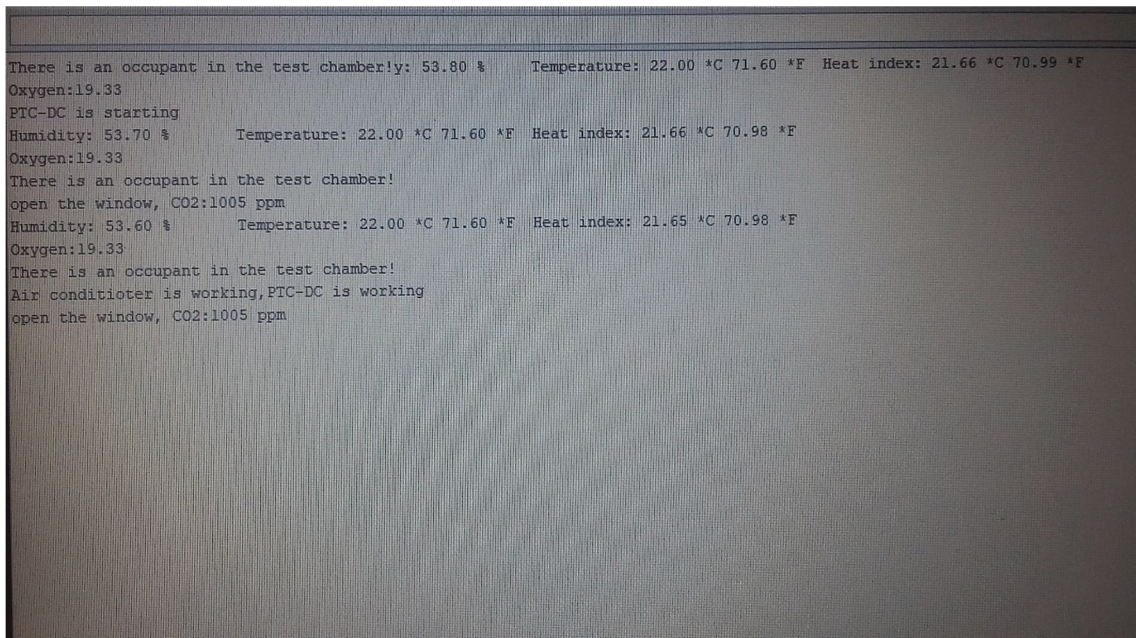


Figure 6.8. The main screen of PTC-DC

6.4. Assessment of PTC-DC

The PTC-DC is operated from July 3rd, 2017 and March 8st, 2018 for v.1 and from March 8st, 2018 and November 1st, 2018 for v.2. During the operations, measurements are taken as given in Section 5 in detail. Table 6.3 shows total measurement days, minimum, maximum and mean outdoor temperatures, set-temperature of PID controller and preferred temperature of PTC-DC for heating and cooling periods.

Table 6.3. Total measurement, outdoor and preferred temperatures for measurement period

		v.1		v.2		
		PID controller	PTC-DC	PID controller	PTC-DC	
Total measurement days	heating	46	46	18	18	
	cooling	40	40	67	67	
T_o (°C)	heating	min	5	5	17	16
		max	20	21	24	22
		mean	13	13	19	19
	cooling	min	22	22	21	20
		max	38	37	38	38
		mean	30	31	30	30
Preferred temperature (°C)	heating	22	21.9-22.6	22	21.7-22.8	
	cooling	22	22.2-23.8	22	22.1-23.6	

The occupant is asked to use mobile application for one day to obtain AMV values. Due to the seasonal changes, the occupant is asked to use mobile application to train the fuzzy logic estimation model for heating and cooling periods, respectively (Table 6.4). Following the training period, the PTC-DC is operated automatically according to the thermal preferences of the occupant. The FL estimation model has close matches with the measurement results within R² of 0.89 and 0.86 for set-temperature and fan speed outputs, respectively.

Table 6.4. Training dates for PTC-DC

Training Period	PTC-DC (v.1)	PTC-DC (v.2)
Cooling	July, 2 nd , 2017	May, 1 st , 2018
Heating	November, 1 st , 2017	March, 7 th , 2018

Clothing value (clo) is calculated from mobile application of PTC-DC as 0.79 and 0.54 for heating and cooling periods, respectively. The metabolic rate of the occupant is chosen to be 1 met ($M = 58 \text{ W/m}^2$) corresponding to normal work when sitting in an office (ASHRAE, 2017). The PTC-DC and PID controllers are operated in alternating days in order to minimize environmental parameter changes that affect thermal comfort.

6.4.1. Evaluation of energy consumption

Power consumption of controllers changes during different periods of operation. During transition period which is between turn-on and steady-state operation, power consumption is high. The reasons of high power consumption are high current flow while turning the air-conditioner on and pressure of the gas in air-conditioner which are initially out of equilibrium. When a system reaches to steady-state condition, power consumption drops down (Aswani et al., 2012). To be able to determine the transition period, power consumptions in the first 100 minutes of the operation are plotted for PTC-DC and PID controller (Fig. 6.9). The figure indicates that approximately first one hour is the transition region and power consumption is higher than steady-state operation.

Fig. 6.10 gives the energy consumption of the PTC-DC (v.1) and PID controllers with respect to heating, cooling and total measurement periods. The figure shows transition period and steady-state operation together. Total energy consumption for more than one-year period is 374.9 kWh for PID controller and 357.7 kWh for PTC-DC (v.1).

It is worth to note that total energy consumption decreased almost by 6% for both PID controller and PTC-DC when transition period was disregarded. The PTC-DC decreased energy consumption by 4.6% and 10.9% for heating and cooling periods, respectively. Moreover, total energy consumption was decreased by 7.4% compared to PID controller.

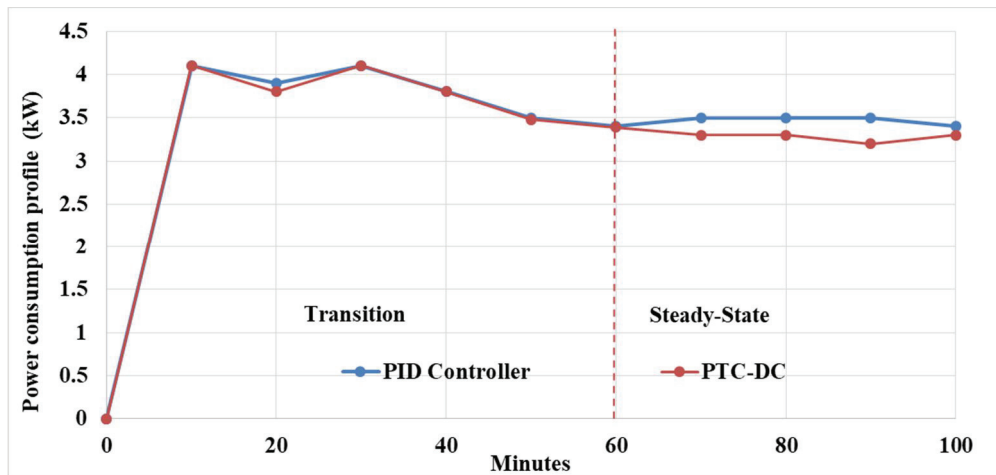


Figure 6.9. Power consumption profile of transition and steady-state conditions

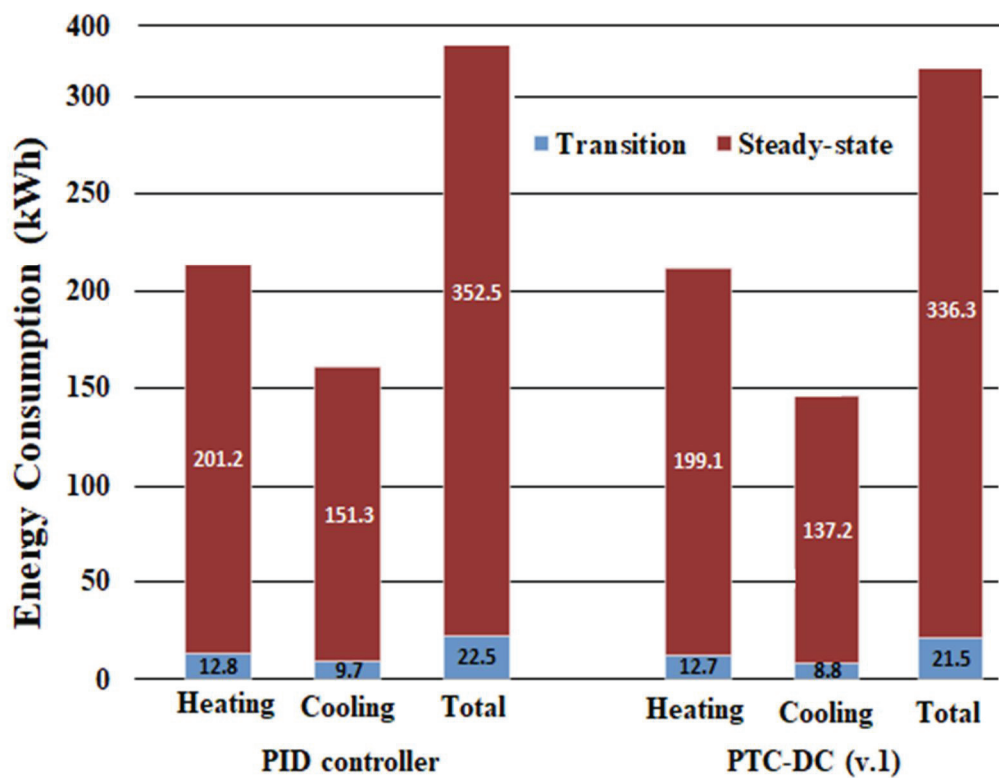


Figure 6.10. Comparison of energy consumption for PID controller and PTC-DC (v.1)

Fig. 6.11 exhibits energy consumption of the PTC-DC (v.2) with PID controller for heating, cooling and total measurement periods. Energy consumptions of transition

and steady-state periods are also shown in the graph. PID controller consumes 317.6 kWh while energy consumption is 284.6 kWh for PTC-DC (v.2). Compared to the PID controller, the PTC-DC (v.2) decreases the energy consumption by 10.3% and 13.7% for heating and cooling periods, respectively. However, total energy consumption decreased by 13.2% compared to PID controller excluding the transition period.

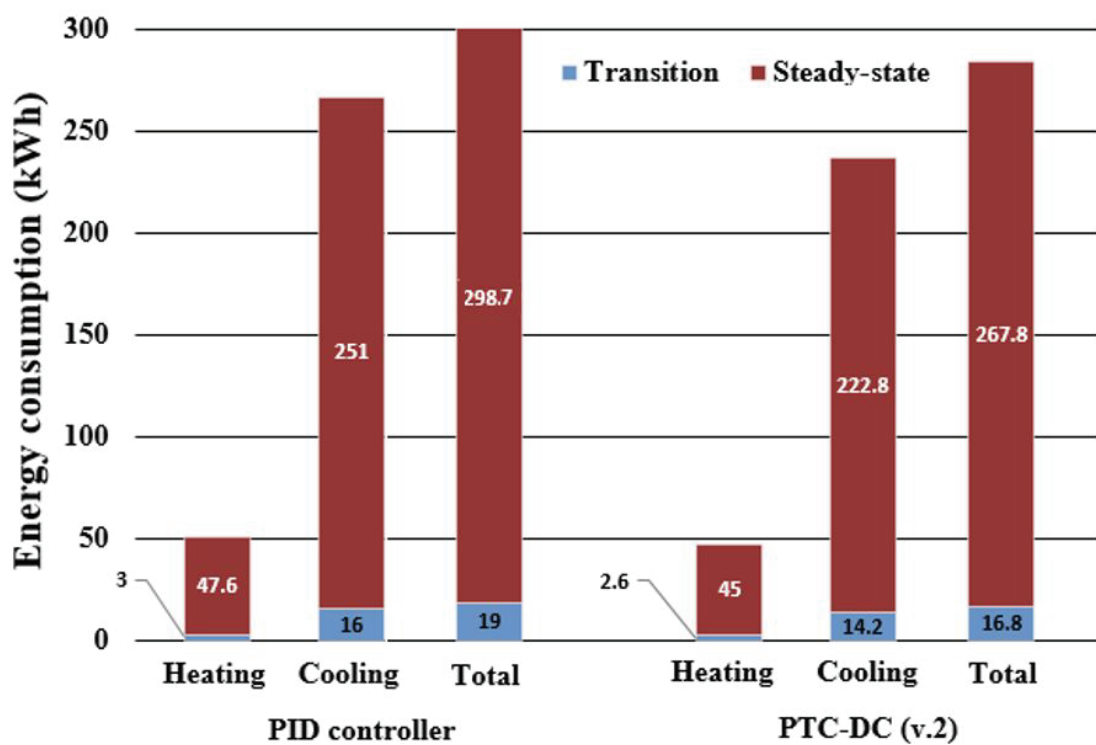


Figure 6.11. Comparison of energy consumption for PID controller and PTC-DC (v.2)

Figures 6.10-6.11 indicate that PTC-DC provides a considerable energy savings over PID controller of a single air-conditioner under given conditions and saving rates obtained at heating, cooling and total measurement periods are summarised in Table 6.5. Total energy consumption was decreased by 7.4% and 13.2% for PTC-DC (v.1) and PTC-DC (v.2), respectively. Considering the seasons, energy savings in the cooling period are higher than the heating period. Even though compressor power consumption is lower in heating period, energy consumption of PTC-DC is higher in the heating period than cooling period. One of the reason could be the sensor locations which are closer to the north facade. Another reason could be the occupant's thermal perception and the adaptation to the climate. Adaptation is defined as "*the gradual lessening of the response to repeated environmental stimulation*" (Brager and de Dear, 1998). The case

building is located at temperate climate with hot and humid summers and mild winters. The occupant could prefer higher temperatures at both heating/cooling periods beyond ASHRAE 55 comfort scale (Humpreys, 1996; Heideri and Sharples, 2002; Indrigandi and Rao, 2010). Therefore, preferred higher set-temperatures cause an increase in energy consumption in winter while a decrease is encountered in summer.

Table 6.5. Summary of energy consumption saving of PTC-DC compared to PID controller (excluding the first one hour)

PTC-DC	Energy saving (%)		
	Heating	Cooling	Total
(v.1)	4.6	10.9	7.4
(v.2)	10.3	13.7	13.2

Compared to PTC-DC (v.1), PTC-DC (v.2) increases energy savings by 5.6% and 2.8% for heating and cooling seasons, respectively. For total measurement period, v.2 increases energy savings by 5.8%. The reason of higher energy savings for v.2 is controlling of fan speed alongside the set-temperature according to thermal preferences of the occupant.

6.4.2. Evaluation of thermal comfort

Energetic approach

Fig. 6.12 depicts the comparison of AMV values for both PID controller and PTC-DC (v.1) for the measurement period of 86 days in total. According to ASHRAE 55 (2017), the range of ± 0.5 PMV (less than 10% PPD) is accepted as comfortable zone (blue area). The purple lines (secondary y-axis) show T_o while black and red lines represent AMV values with PID controller and PTC-DC (v.1), respectively.

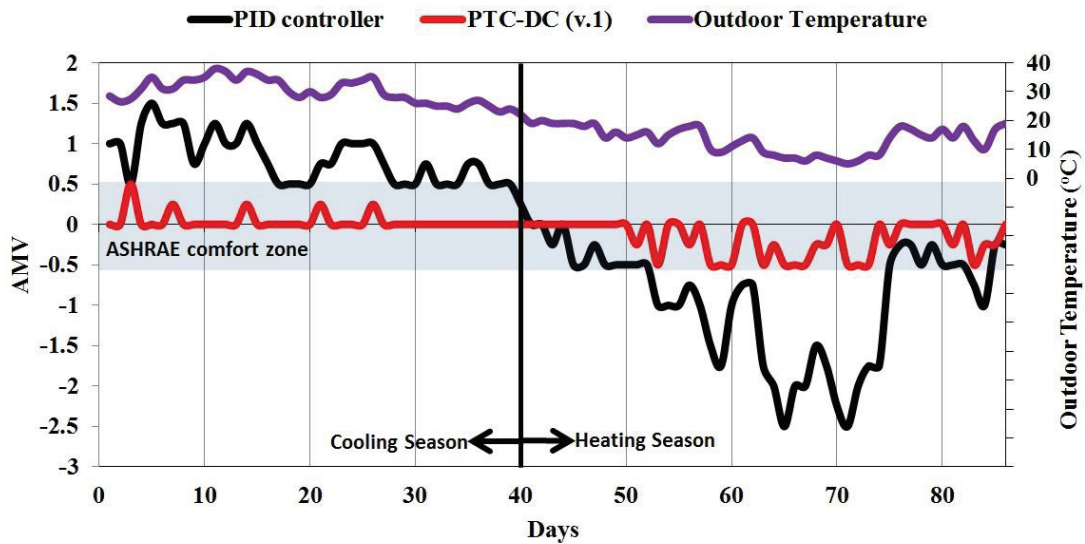


Figure 6.12. AMV comparison for PID controller and PTC-DC (v.1)

While PID controller remains in the ASHRAE 55 comfort zone in 40% of total measurement period, it does not satisfy neutral thermal comfort ($AMV=0$) for 95% in the same period. However, AMV values of the occupant are generally zero in 88% of total days during PTC-DC (v.1) operation. It is worth to note that outdoor temperatures of the days which PTC-DC (v.1) does not satisfy $AMV=0$ value are extremely higher or lower than the rest of the period (Fig. 6.12). The outdoor temperature varies in the range of 5-21°C and 22-37°C for heating and cooling periods, respectively.

ISO 7730 (ISO, 2005) provides criteria for thermal comfort based on PMV and PPD indices. However, in the study, Actual Percentage of Dissatisfied (APD) is used instead of PPD since AMV is obtained as subjective data. APD gives the percentage of dissatisfied occupants from indoor environment. Fig. 6.13 shows APD values of PID controller and PTC-DC (v.1). It can be seen that APD values of PTC-DC (v.1) are between 5% and 10% for the total measurement period. However, APD values of PID controller reaches to 90%. The PTC-DC (v.1) reduces the actual percentage of dissatisfied occupants by 88%.

Fig. 6.14 compares AMV values of PID controller and PTC-DC (v.2). The PTC-DC (v.2) satisfies neutral thermal comfort in 92% of total measurement period whilst PID controller remains on the $AMV=0$ value only for 6% of total days.

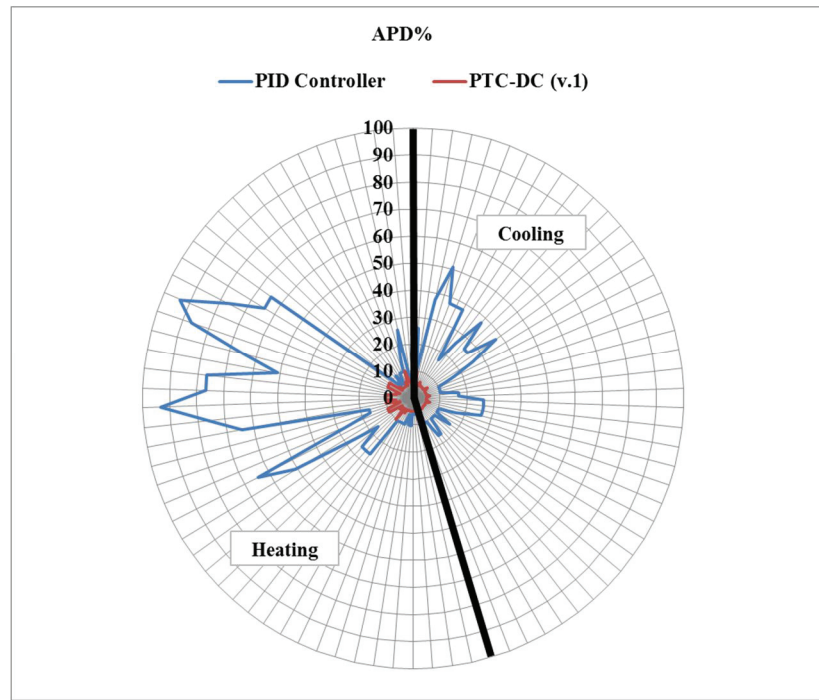


Figure 6.13. APD comparison for PID controller and PTC-DC (v.1) for the total measurement period

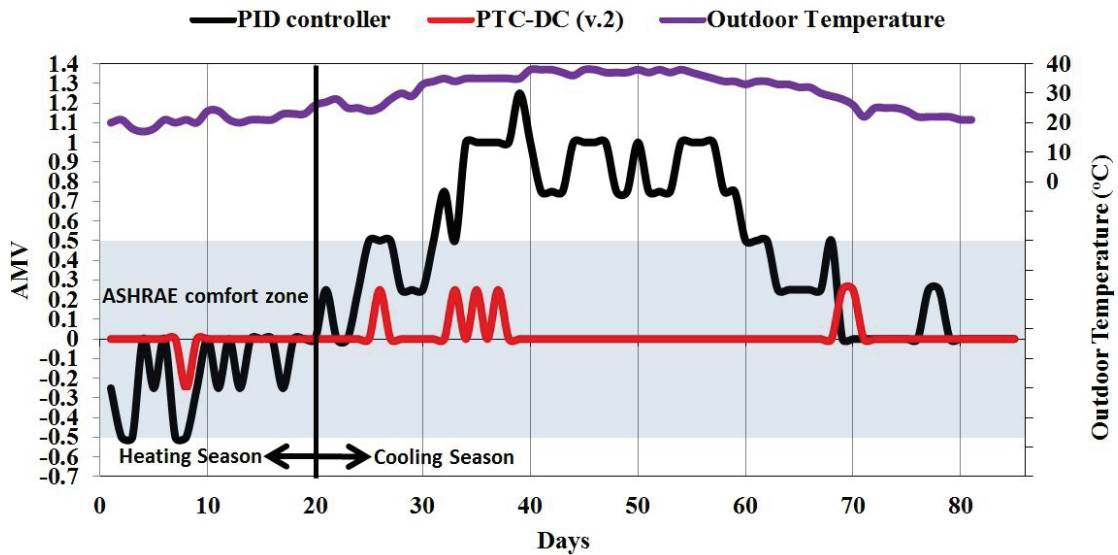


Figure 6.14. AMV comparison for PID controller and PTC-DC (v.2)

Fig. 6.15 compares APD values of PID controller and PTC-DC (v.2). APD values of the PTC-DC (v.2) are around 5% which is the lowest bound of the APD index

values. However, APD values of PID controller reach nearly 40%. The reason of lower APD values in heating period than in cooling period is outdoor temperatures that vary in the range of 16-22°C for PTC-DC (v.2). The outdoor temperatures for heating period of v.2 are warmer than v.1. Another reason could be the shorter measurement period of v.2 than v.1 for heating period. The PTC-DC (v.2) is tested for the heating period of total 18 days. Table 6.5 summarizes the decrease of APD for v.1 and v.2 compared to PID controller. The PTC-DC (v.2) decreases APD by 87.5%.

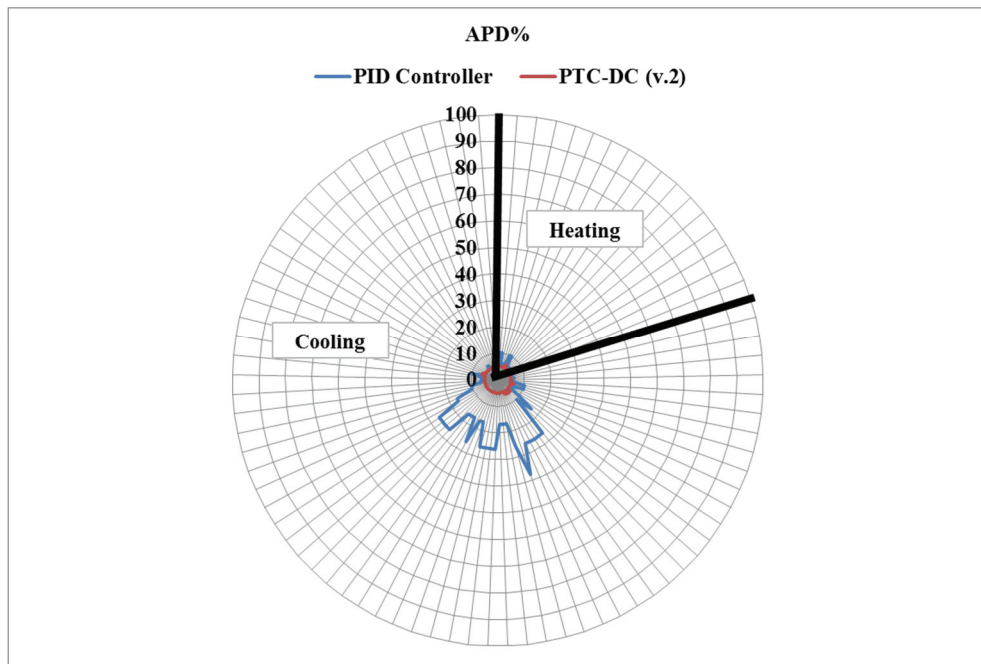


Figure 6.15. APD comparison for PID controller and PTC-DC (v.2) for the total measurement period

Table 6.6. Decrease in APD values compared to PID controller

PTC-DC	Decrease of APD (%)		
	Heating	Cooling	Total
(v.1)	91.0	86.0	88.0
(v.2)	52.1	88.1	87.5

Fig. 6.16 depicts the change of AMV values with respect to T_i and MRT. The green line shows the combinations of the T_i and MRT where neutral thermal comfort

(AMV=0) is obtained. As can be seen from the figure that there are many combinations of T_i and MRT values which give AMV=0 in energetic approach.

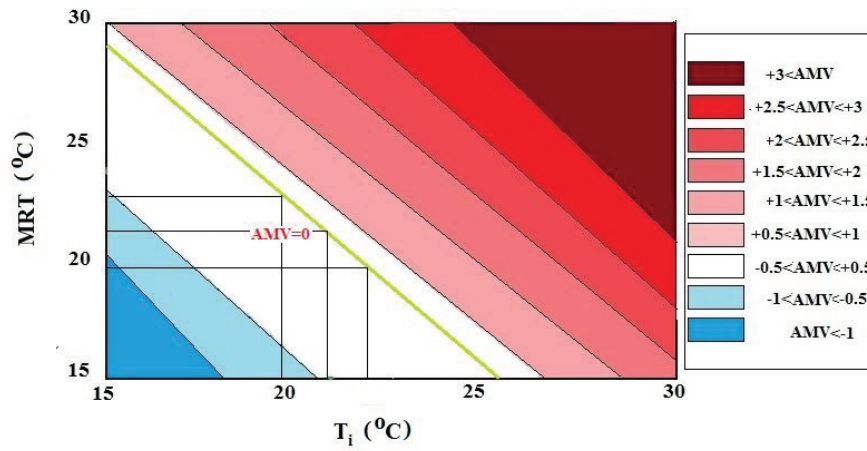


Figure 6.16. AMV value in dependence on T_i and MRT

Fig. 6.17 depicts the effect of CO₂ concentration on AMV for PID controller for one-day measurement period. Since PID controller cannot measure CO₂ concentration, the occupant prefers to open the windows twice a day at 09:00-09:15 and 13:30-13:45. However, at the end of the office hours CO₂ concentration is measured above the threshold (>1000 ppm). As a result, the occupant feels warmer when CO₂ concentration increases. In other words, AMV increases from 0 to +0.5 with a 441 ppm increase in CO₂ concentration.

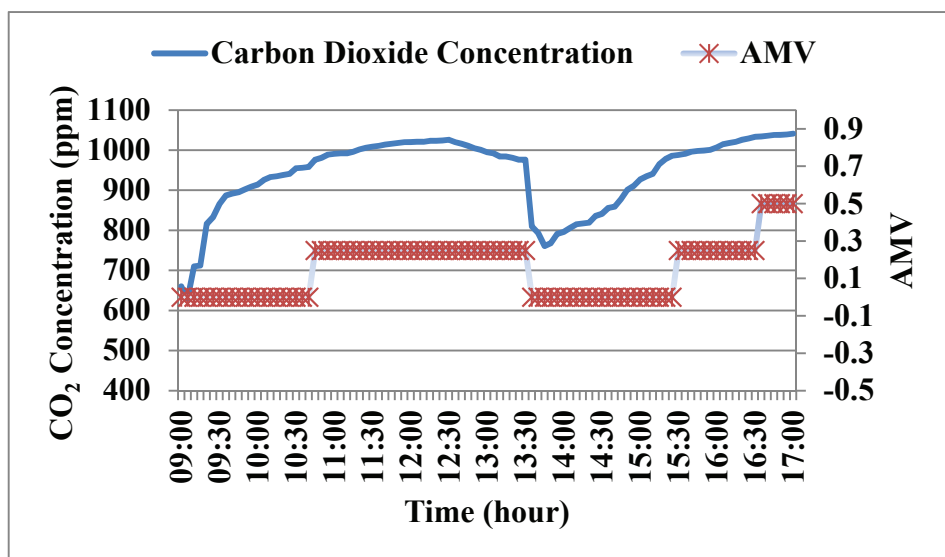


Figure 6.17. The effect of carbon dioxide concentration on AMV for PID controller

The effect of CO₂ concentration on AMV for PTC-DC (v.2) is shown in Fig. 6.18. The occupant prefers to open windows for 5 minutes when PTC-DC (v.2) gives an alert and displays “open the window” message on the screen indicating CO₂ concentration is above 850 ppm. Thus, the PTC-DC (v.2) prevents increase in CO₂ concentration and has been able to keep the occupant’s AMV mostly at neutral AMV. The results showed that IAQ parameters should be taken into account on thermal comfort.

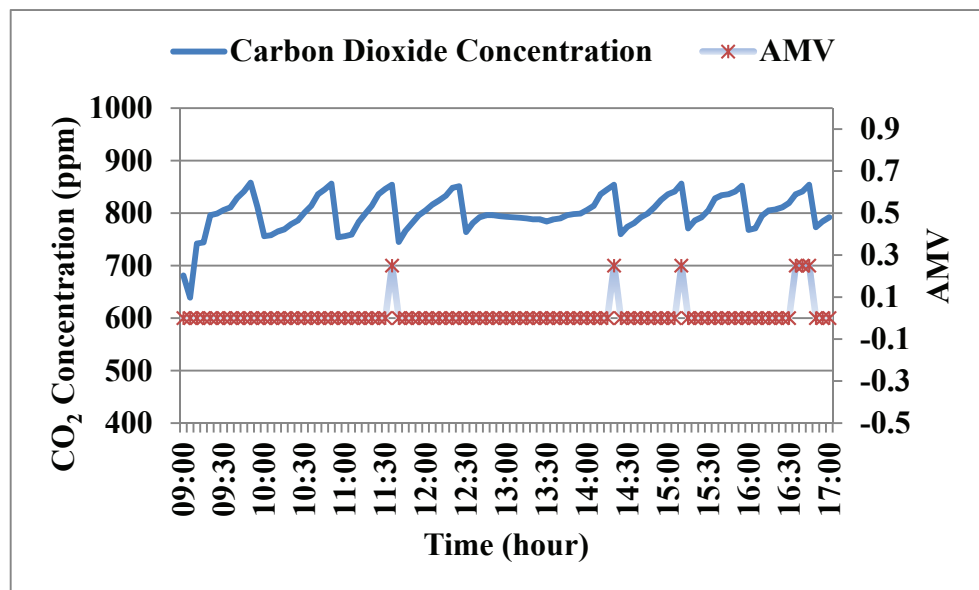


Figure 6.18. The effect of carbon dioxide concentration on AMV for PTC-DC (v.2)

Exergetic approach

The performance of the developed PTC-DC was assessed with exergetic approach of thermal comfort. The calculations were made with a human-body exergy balance contour calculation tool developed by Asada (2010) which uses six parameters (T_o , RH_o , T_i , RH_i , MRT and v_a) as inputs and calculates output values for different combinations of T_i and MRT . Recalling that the minimum HBexC rate gives the neutral thermal comfort, the results are summarized in Table 6.7 for PID controller, PTC-DC (v.1) and PTC-DC (v.2) presenting the input and output values at the points where HBexC rates are minimum. Additionally, measured PMV and AMV values are given in

the table. Simone et al. (2011) indicated that the control systems should provide thermal comfort with the lowest possible HBexC rate.

Table 6.7. Calculated and measured parameters which give minimum HBexC rates

Controller	PID	PTC-DC (v.1)	PTC-DC (v.2)
T _i (°C)	20.1	21.6	21.8
MRT (°C)	22.5	23.1	23.2
MRT- T _i (°C)	2.4	1.5	1.4
HBexC rate (W/m ²)	3.05	2.67	2.41
PMV	0.26	0.17	0.15
AMV	0	0	0

Based on the calculations, the PTC-DC provides lower HBexC rate compared to PID controller as 2.41 W/m² (v.2) and 2.67 W/m² (v.1), and 3.05 W/m², respectively. The results shows that PTC-DC provides lower HBexC rate compared to PID controller.

The combinations of T_i and MRT are 20.1°C and 22.5°C in PID controller while these values are 21.6°C and 23.1°C in PTC-DC (v.1) and 21.8°C and 23.2°C in PTC-DC (v.2). Walikewitz et al. (2015) concluded that the differences between T_i and MRT influence thermal comfort due to the heat stress on human body. These findings indicate that PTC-DC decreases the difference between T_i and MRT which satisfies better thermal comfort (Table 6.7).

The results also showed that there is a gap between AMV and PMV. PMV values were on slightly warm side and calculated as 0.26 and 0.17 for PID controller and PTC-DC (v.1), respectively. In addition, PMV value decreased from 0.17 to 0.15 for PTC-DC (v.2). The results of PMV calculations indicated that PTC-DC (v.2) satisfied better indoor environment compared to v.1.

Fig. 6.19 compares HBexC rate and MRT for both PID controller and PTC-DC. When MRT increases, HBexC rate decreases until MRT is reached the neutral temperature where AMV is zero. Then, HBexC rate shows an increasing trend for both PID controller and PTC-DC. The figure is in a good agreement with the literature (Isawa et al., 2003; Shukuya, 2013; Prek and Butala, 2017). However, the PTC-DC (v.2) gives the lowest HBexC rate values at all MRT values.

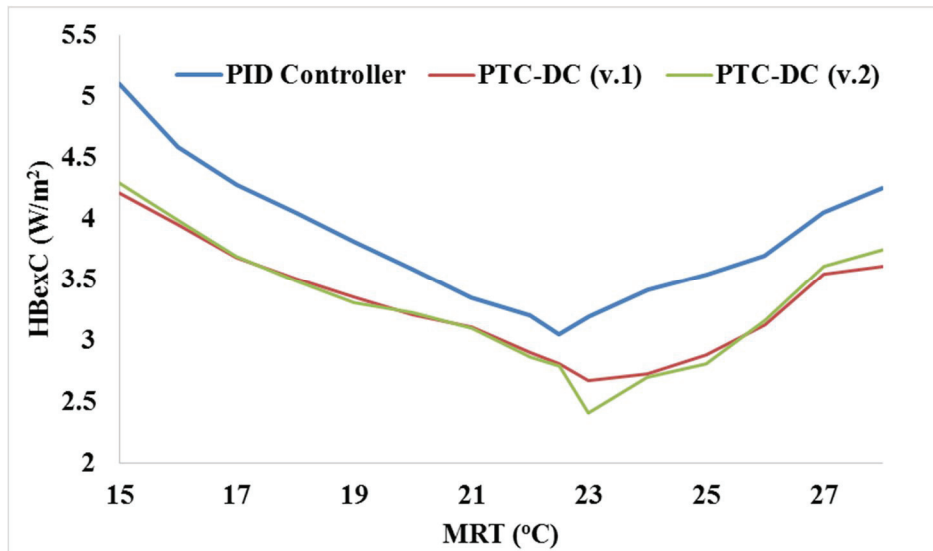


Figure 6.19. Comparison of PID and PTC-DC with respect to HBexC and MRT

The HBexC rate with the combination of T_i and MRT of an occupant in an office building in temperate climate zone is plotted in the Matlab (2016) environment for heating and cooling periods, respectively. Fine lines with numbers depict HBexC rate whilst the neutral AMV value is shown with red with respect to T_i and MRT on the graph. Fig. 6.20 shows the HBexC rate of an occupant in the case building for winter period. Environmental conditions and personal parameters are kept constant in order to plot HBexC rate with respect to T_i and MRT ($v_a=0.1$ m/s, $RH_i=50\%$, $met=1$, $clo=0.79$). The lowest HBexC rate was obtained as 2.68 with a combination of $T_i=22.7^\circ\text{C}$ and $MRT=24.1^\circ\text{C}$ (PTC-DC (v.2)).

Similarly, the HBexC rate for cooling period were plotted for constant values of $v_a=0.1$ m/s, $RH_i=55\%$, $met=1$ and $clo=0.54$ (Fig. 6.21). The lowest exergy consumption rate emerges at the point, where T_i and MRT equal to 21.8°C and 23.2°C (PTC-DC (v.2)), respectively. The slope of the curves depicts the interaction of the T_i and MRT on HBexC rate. Similar to the studies in Shukuya (2009) and Prek and Butola (2017), there is a trend for HBexC rate to be minimum when MRT is higher than T_i . Negative values range of AMV values are towards the lower left corner from zero AMV value when the T_i and MRT are lowered and the occupant feel cooler. Similarly, when T_i and MRT are increased, the AMV values are positive which indicate that the occupant feels warmer. In addition, Fig. 6.20 and 6.21 show that the difference between T_i and MRT is

low since v_a is kept below 0.2 m/s during the experiments. This means that the impact of T_i is greater than MRT on HBexC rate.

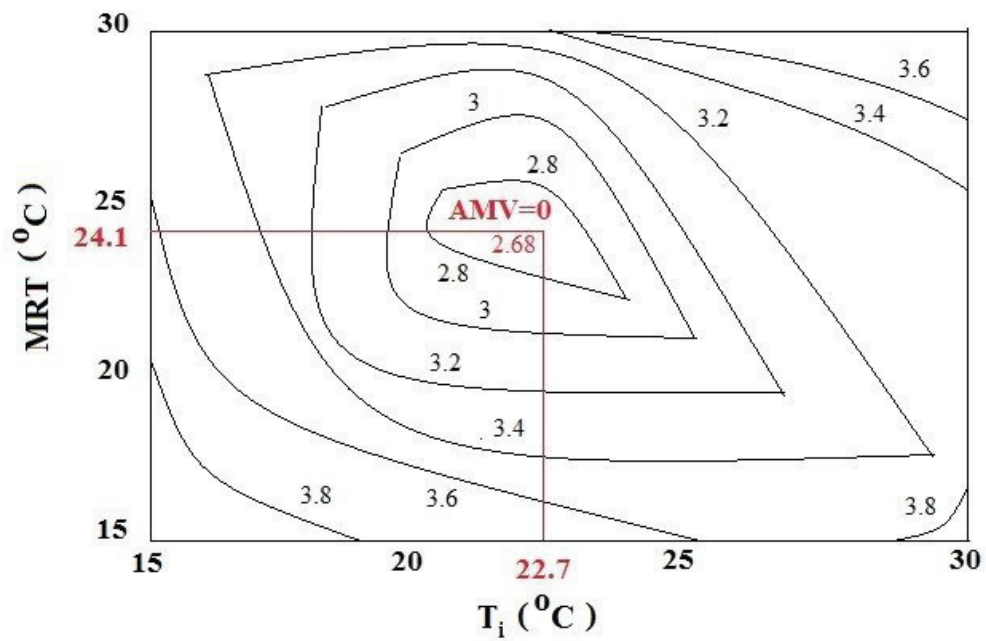


Figure 6.20. HBexC rate-heating period

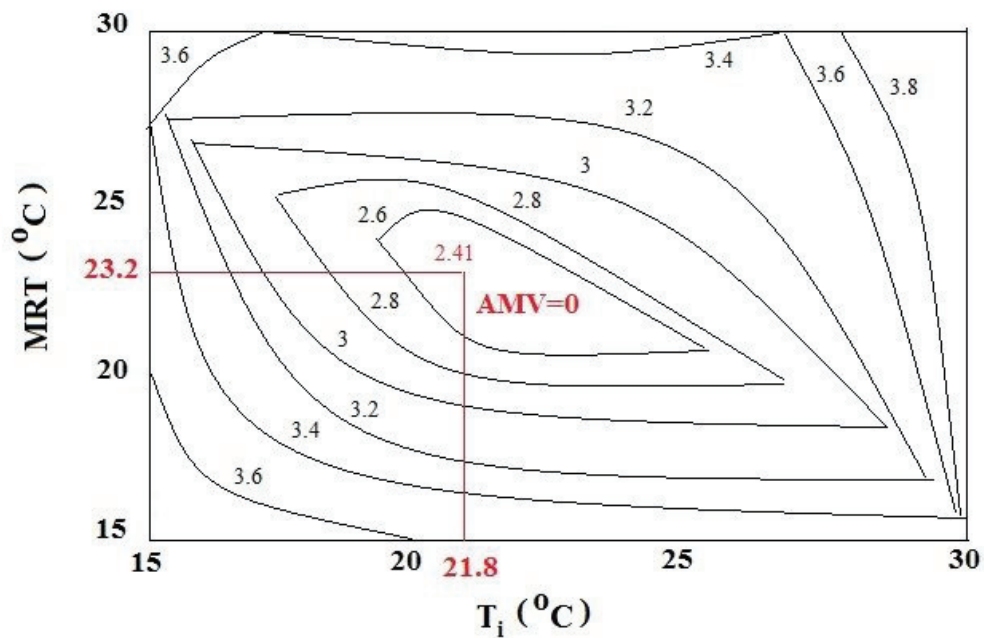


Figure 6.21. HBexC rate-cooling period

Exergetic approach gives one combination of T_i and MRT which satisfies neutral thermal comfort (Fig. 6.20-6.21). However, there are many combinations of T_i and MRT in energetic approach (Fig. 6.16).

The exergy balance based on (3.9) is conducted for various cases. Fig. 6.22 demonstrates an example for environmental conditions of $T_i=21.8^\circ\text{C}$ and $\text{RH}_i=55\%$ which gives the minimum HBexC rate on 12th of June, 2018. For an exergy input of 100%, exergy consumed, which represents HBexC rate, constitutes 60% while outgoing exergy (convection+exhaled&sweat+warm radiation) has a share of 40%. The shares of exergy flows vary with environmental conditions while outgoing exergy flows are more significant on thermal comfort (Shukuya, 2009; Prek, 2005; Prek and Butola, 2017).

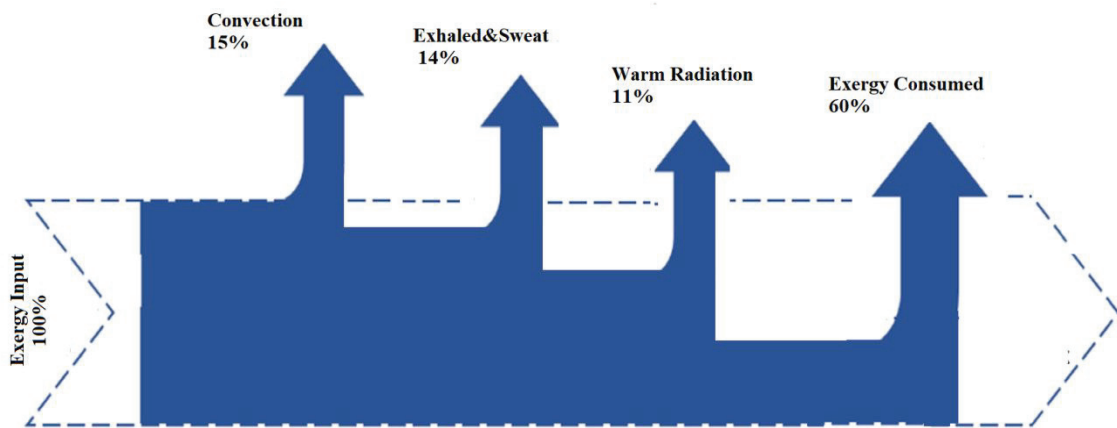


Figure 6.22. Variation of outgoing exergy calculated for the conditions of $T_i=21.8^\circ\text{C}$ and $\text{RH}_i=55\%$ on 12th of June, 2018

The results showed that the PTC-DC achieved better thermal comfort and decreased total energy consumption compared to PID controller. Main findings of the study can be summarised as follows.

- Since the “neutral” thermal comfort is preferred by the occupants in the office buildings, PTC-DC achieves better thermal comfort.
- The PTC-DC decreases the number of percentage of dissatisfied occupants by 88% and 87.5% for (v.1) and (v2), respectively.
- The PTC-DC (v.2) decreases energy consumption by 13.2% compared to the PID controller for total measurement period.

- The PTC-DC uses thermal preference of the occupant for thermal comfort whilst PID controller only regulates indoor air temperature.
- The sensors of PTC-DC could be situated close to the occupant which have the possibility of being more accurate than the thermostat of the PID controller.
- The PTC-DC uses passive-infrared (PIR) sensor to detect the office building whether if it is occupied or unoccupied. It turns the air-conditioner off if the office is unoccupied.
- The PTC-DC measures O₂ and CO₂ concentrations and takes into account these measurements to obtain better thermal comfort.
- The PTC-DC warns the occupant when CO₂ concentration drops under 850 ppm. So that PTC-DC satisfies indoor air quality every time.
- The PTC-DC automatically turns on/off the air-conditioner, sets air temperature and fan speed according to the thermal preferences of the occupant.

CHAPTER 7

CONCLUSIONS

This thesis presents the development of a novel energy-efficient personalized thermal comfort driven controller (PTC-DC) algorithm and prototype, the tests of the prototype with an air-conditioner in a case building and the comparison of the prototype with a PID controller based on energetic and exergetic approaches of thermal comfort and energy consumption.

An office building located in Izmir Institute of Technology, İzmir/Turkey is selected as case building. The prototype of PTC-DC which uses a novel control algorithm is installed at the case building and used to control an air-conditioner. The PTC-DC is tested between 03.07.2018 and 01.11.2018 and compared with the PID controller of the air-conditioner in terms of energy saving and both energetic and exergetic approaches of thermal comfort. In addition, the effect of CO₂ concentration on AMV values is evaluated for both PID controller and PTC-DC.

The PID controller satisfies neutral thermal comfort for only 6% of total measurement days. However, AMV=0 for 88% and 92% of total measurement days for PTC-DC (v.1) and PTC-DC (v.2), respectively. Compared to PTC-DC (v.1), PTC-DC (v.2) increases thermal comfort by 4% for total measurement period. From energy consumption point of view, PTC-DC (v.1) decreased energy consumption by 7.4% compared to PID controller. With enhancements in PTC-DC (v.2), energy saving reached to 13.2%. Moreover, PTC-DC (v.2) prevents the increase of CO₂ concentration which is a further improvement in thermal comfort.

A number of personalized thermal comfort systems are commercially available, but these are expensive and not easy-to-use by occupants. The PTC-DC uses cost-effective wireless sensors and simple fuzzy logic rules to obtain occupant's personalized thermal comfort level.

The PTC-DC can be improved further with controllable windows by servomotors. In this way, the system becomes occupant-free. Similarly, a Heat Recovery Ventilation (HRV) system can be integrated into the PTC-DC control system. For a heating period, HRV system takes fresh air from outside and gives pre-heated fresh air

inside the building. Thus, CO₂ concentration can be decreased automatically whenever it reaches 850 ppm. Furthermore, HRV system increases energy savings by pre-heating and pre-cooling the outside air (Güngör et al., 2018). Wi-Fi module of PTC-DC can also be used to communicate between HRV system and PTC-DC.

The PTC-DC uses fuzzy logic estimation model to predict thermal preferences of the occupants. The ANN approach could be used in the algorithm, however, training process of the model is computationally heavy burden. Moreover, the model requires big data sets. Similarly, MPC requires large optimization procedures which makes the model unsuitable to use in a real-time measurement system like PTC-DC. Furthermore, the MPC requires dynamic models of HVAC system and thermal sensation to predict thermal preferences of the occupant. The advantage of selecting fuzzy logic approach for PTC-DC is simplicity. The model does not require complex mathematical systems and big data sets. The PTC-DC can predict thermal preferences of the occupant with imprecise and incomplete data with the help of fuzzy logic. Moreover, there is no need to re-train the model when a new data or rule is added to the system.

Mobile application of PTC-DC provides a standardized and systematic method for assessing thermal preferences of occupants. In the thesis, the mobile application is used with one occupant. However, the average response rate is significant for large groups to obtain AMV via mobile application. The occupants should be encouraged to conduct a greater response in order to increase the accuracy of the PTC-DC.

The PTC-DC calculates clothing value of the occupant for heating and cooling periods, respectively. However, occupants have the flexibility to change their personal parameters in order to improve thermal comfort. The occupants can arrange their garments from the interface of mobile application to re-calculate clothing value but it is worth to say that the processing of large data sets can become computationally heavy. Instead, image-processing which can directly calculates clothing value from the temperature of the clothes can be used for PTC-DC.

In the thesis, the effect of IAQ parameters on thermal comfort is investigated for one-day measurement period. However, the results should be validated with larger data sets and longer periods.

The PTC-DC box will be improved such as decreasing the dimensions and adding image-processing sensors.

The PTC-DC is tested with an adult-male occupant in a relatively small office building. However, personalized thermal comfort varies greatly depending upon gender,

age, behaviour and location. As future works, PTC-DC will be tested in larger office buildings in different climatic zones with a variety of occupants.

REFERENCES

- Abdo-Allah, A., Iqbal, T., & Pope, K. (2018). Modeling, Analysis and Design of a Fuzzy Logic Controller for an AHU in the S.J.Carew Building at Memorial University, *Journal of Energy*, 2018, 1-11.
- Aesong Electronics (2018, April 15). Retrived from <https://www.sparkfun.com/datasheets/Sensors/Temperature/DHT22.pdf>
- Afram, A., & Sharifi, F.J. (2017). Supervisory model predictive controller (MPC) for residential HVAC systems: Implementation and experimentation on archetype sustainable house in Toronto, *Energy and Buildings*, 154, 268-282.
- Ahn, J., Chung, D.H., & Cho, S. (2017). Performance analysis of space heating smart control models for energy and control effectiveness in five different climate zones, *Building and Environment*, 115, 316-331.
- Ahn, J., Cho Dae, S., & Chung, H. (2017). Analysis of energy and control efficiencies of fuzzy logic and artificial neural network technologies in the heating energy supply system responding to the changes of user demands, *Applied Energy*, 190, 222-231.
- Alcal'a, R., Benitez, J.M., Casillas, J., Cordo'n, O., & Pe'rez, R. (2013). Fuzzy control of HVAC systems optimized by genetic algorithms, *Applied Intelligence*, 18, 155-177.
- Al-Jarrah, R., & Al-Jarrah, M. A. (2013). Developed adaptive neuro-fuzzy algorithm to control air conditioning system at different pressures, *International Journal of Engineering, Science and Technology*, 5 (4), 43-59.
- Anastasiadi, C., & Dounis, A.I. (2018). Co-simulation of fuzzy control in buildings and the HVAC system using BCVTB, *Advances in Building Energy Research*, 12 (2), 195-216.
- Arduino Mega (2018, April 14). Retrieved from <https://www.arduino.cc/en/uploads/Main/arduino-mega2560.pdf>
- Asada, H. (2010). Introduction to the tool to calculate human body exergy consumption for contour plot. The tool itself is developed by Hideo Asada, Toshiya Iwamatsu, and Masanori Shukuya.
- Ascione, F., Bianco, N., De Stasio, C., & Mauro, G.M. (2016). Simulation-based model predictive control by the multi-objective optimization of building energy performance and thermal comfort, *Energy and Buildings*, 111 , 131-144.
- ASHRAE 55 (2017). Thermal Environmental Conditions for Human Occupancy.

- ASHRAE 62 (2016). Ventilation for Acceptable Indoor Air Quality.
- ASHRAE (2017). Fundamentals Chapter 9: Thermal Comfort, American Society of Heating, Refrigerating and Air-Conditioning Engineers, Inc.
- Aswani, A., Master, N., Taneja, J., Culler, D., & Tomlin, C. (2012). Reducing Transient and Steady State Electricity Consumption in HVAC Using Learning-Based Model-Predictive Control, *In: Proceedings of IEEE*, 100 (1), 240-253.
- Atmaca A. (2016). Life cycle assessment and cost analysis of residential buildings in south east of Turkey: part 1—review and methodology, *International Journal of Life Cycle Assessments*, 21, 831-846.
- Bai, J., & Zhang, X. (2007). A new adaptive PI controller and its application in HVAC systems, *Energy Conversion and Management*, 48 (4), 1043-1054.
- Baia, J., Wang, S., & Zhang, X. (2008). Development of an adaptive Smith predictor-based self-tuning PI controller for an HVAC system in a test room, *Energy and Buildings*, 40 (12), 2244-2252.
- Batato, M, Borel, L, Deriaz, O, & Jequier, E. (1990). Analyse exergetique theorique et experimentale du corps humain, *Entropie*, 26 (153-154),120-130.
- Bedford, R.E., Bonnier, G., Maas, H., & Pavese, F. (1990). Recommended values of temperature on the International Temperature Scale of 1990 for a selected set of secondary reference points, *Metrologia*, 33 (2), 133.
- Berglund, L., Gonzales, R., & Gaffe, A. (1990). Predicted human performance decrement from thermal discomfort and ET*. *In: 5th International Conference on Indoor Air Quality and Climate*, 215–220, Toronto, Canada.
- Bermejo, P., Redondo, L., de la Ossa, L., Rodr'iguez, D., Flores, J., Urea, C., G'ameza, J.A., & Puerta, J.M. (2012). Design and simulation of a thermal comfort adaptive system based on fuzzy logic and on-line learning, *Energy and Buildings*, 49, 367–379.
- Bi, Q., Cai, W.J., Wang, Q.G., Hang, C.C, Lee, E.L, Sun, Y., Liu, K.D., Zhang, Y., & Zou, B. (2000). Advanced controller auto-tuning and its application in HVAC systems, *Control Engineering Practice*, 8 ,633-644.
- Brager, G., Fountain, M., Benton, C., Arens, E.A., & Bauman, F. (1993). A comparison of methods for assessing thermal sensation and acceptability in the field, *In Thermal Comfort: Past, Present and Future*, UK.
- Brager, G., & de Dear, R.J. (1998). Thermal adaptation in the built environment: a literature review, *Energy and Buildings*, 27 , 83–96.
- Brooks, J., Goyal, S., Subramany, R., Lin, Y., Middelkoop, T., Arpan, L., Carloni, L., & Barooah, P. (2014). An experimental Investigation of Occupancy-Based Energy-

Efficient Control of Commercial Building Indoor Climate, *In: 53rd IEEE Conference on Decision and Control*, 5680-5685, Los Angeles, California, USA.

- Calvino, F., Gennusa, M.L., Morale, M., Rizzo, G., & Scaccianoce, G. (2010). Comparing different control strategies for indoor thermal comfort aimed at the evaluation of the energy cost of quality of building, *Applied Thermal Engineering*, 30, 2386–2395.
- Castilla, M.; Alvarez, J.D., Normey-Rico, J.E., ; & Rodriguez, F. (2014). Thermal comfort control using a non-linear MPC strategy: A real case of study in a bioclimatic building, *Journal of Process Control*, 24 (6), 703-713.
- Chen, X., Wang, Q., & Srebric, J. (2016). Occupant feedback based model predictive control for thermal comfort and energy optimization: A chamber experimental evaluation, *Applied Energy*, 164, 341-351.
- Chinnakani, K., Krishnamurthy, A., & Moyne, J. (2011). Comparison of Energy Consumption in HVAC Systems Using Simple ON-OFF, Intelligent ON-OFF and Optimal Controllers, *2011 IEEE Power and Energy Society General Meeting*, 24-29 July, 2011, Michigan, USA.
- Chua, K.J, Ho, J.C, & Chou, S.K (2007). A comparative study of different control strategies for indoor air humidity, *Energy and Buildings*, 39, 537-545.
- Cooper (2018, May 19). Retrieved from <https://engfac.cooper.edu/melody/417>
- Craig, W.A., & Jr. Russell, E.T. (2001). A comparison of traditional and adaptive control strategies for systems with time delay, *ISA Transactions*, 40, 353-368.
- Cucchiella, F., D'Adamo, I., Gastaldi, M., & Miliacca, M. (2018). Efficiency and allocation of emission allowances and energy consumption over more sustainable European economies, *Journal of Cleaner Production*, 182, 805-817.
- Çalışkan, H. (2013). Energetic and exergetic comparison of the human body for the summer season, *Energy Conversion and Management*, 76, 169-176.
- Çengel, Y., & Boles, M.B., *Thermodynamics: An Engineering Approach*, Eight Edition, McGraw-Hill Press, 2015.
- Dai, Y., Jiang, Z., Shen, Q., Chen, P., Wang, S., & Jiang Y. (2016). A decentralized algorithm for optimal distribution in HVAC systems, *Building and Environment*, 95, 21-31.
- Dar, U.I., Georges, L., Sartori, I., & Novakovic, V. (2015). Influence of occupant's behaviour on heating needs and energy system performance: A case of well-insulated detached houses in cold climates, *Building and Simulation*, 8, 499-513.
- DaSheng Electronics, DP 1838 Datasheet (2018, April 10). Retrieved from https://img.ozdisan.com/ETicaret_Dosya/433900_2764891.PDF

- Dehghani, A., & Khodadadi, H. (2017). Designing a Neuro-Fuzzy PID Controller Based on Smith Predictor for Heating System, *In: 17th International Conference on Control, Automation and Systems (ICCAS 2017)*, 18-21 October, 15-20, Jeju, Korea.
- DFRobot Electronics, DFR0032 Datasheet (2018, May 3). Retrived from <https://www.robotmesh.com/df-robot/digital-buzzer-module>.
- Dong, B., & Lam, K.P. (2014). A real-time model predictive control for building heating and cooling systems based on the occupancy behaviour pattern detection and local weather forecasting, *Building and Simulations*, 7, 89-106.
- Dong, W. , & Xinhua, P. (2004). Application of PMV Comfort Index to HVAC System Control, *Journal of Beijing Institute of Civil Engineering and Architecture*, 20 (1), 51-56.
- Dounis, A.I, & Caraiscos, C. (2009). Advanced control system engineering for energy and comfort management in a building environment-a review, *Renewable and Sustainable Energy Reviews*, 13 (6-7), 1246-1261.
- E.U. Commission, Energy Efficiency Directive (2018, November 7). Retrieved from http://ec.europa.eu/energy/efficiency/eed/eed_en.htm
- E.U.Parliament, E.U.Council, On the Energy Performance of Buildings, June 2017.
- Embrlabs (2018, June 25). Retrieved from <https://embrlabs.com/>
- EnergyPlus 7 (2011), US DOE.
- EPBD (2018), Directive (EU) 2018/844 of the European Parliament and of the Council (2018). Support for setting up a smart readiness indicator for buildings and related impact assessment, Final Report, August 2018, Brussels, Switzerland.
- Erfani, A., Rajabi-Ghahnaviyeh, A., & Boroushaki, M. (2018). Design and construction of a non-linear model predictive controller for building's cooling system, *Building and Environment*, 133, 237-245.
- Erham, E., Markus, A., & Sopianti, W.P. (2018). Design of a new on-off controller based on Arduino UNO R3 with application to Window A/C, *IPTEK Journal of Proceedings Series*, 174-182.
- Erickson, V.A, Achleiter, S., & Cerpa, A.E. (2013). POEM: Power-efficient Occupancy-based Energy Management System, *In: 2013 ACM/IEEE International Conference on Information Processing in Sensor Networks (IPSN)*, 15-17 April, Berlin, Germany.
- Espressive Systems, ESP 8266 Wi-Fi Module Datasheet (2018, April 7). Retrieved from https://www.espressif.com/sites/default/files/documentation/0a-esp8266ex_datasheet_en.pdf

- Everlight Electronics, LED IR Transmitter Datasheet (2018, April 5). Retrieved from http://www1.futureelectronics.com/doc/EVERLIGHT%C2%A0/334-15__T1C1-4WYA.pdf
- Extech, Power Analyser Datasheet (2018, April 10). Retrieved from <http://www.extech.com/display/?id=14185>
- Fanger P., Thermal Comfort, Copenhagen: Danish Technical Press, 1970.
- Feldmeier M.C. (2009). Personalized Building Comfort Control, PhD Thesis, Massachusetts Institute of Technology.
- Ferreira, P.M., Ruano, A.E., Silva, S., & Conceição, E.Z.E (2012). Neural network based predictive control for thermal comfort and energy saving in public buildings, *Energy and Buildings*, 55, 238-251.
- Gagge, A.P., Fobelets, A.P., & Berglund, L.G. (1986). A standard predictive index of human response to the thermal environment, *ASHRAE Transactions*, 91 (2B) 709–731.
- Garnier, A. , Eynard, J., Caussanel, M., & Grieu, S., Predictive control of multizone HVAC systems in non-residential buildings. *In: 19th World Congress The international federation of Automatic control*, August 24-29, 2014, Capetown, South Africa.
- Geng, G., & Geary, G.M. (1993). The application of PI control and Smith predictors in an air-handling plant, *In: Second IEEE Conference on Control Applications*, 1-5.
- Ghahramani, A., Castro, G., Karvigh, S.A., & Becerik-Gerber, B. (2018). Towards Unsupervised Learning of Thermal Comfort Using Infrared Thermography. *Applied Energy*, 211, 41-49.
- Grathier, S., Liu, B., Huebner, G., Shipworth, D., Investigating the effect of CO₂ concentration on reported thermal comfort, CISBAT 2015, Lausanne, Switzerland, 2015.
- Griffiths, I.D, & McIntyre, A.D. (1974). Sensitivity to Temporal Variations in Thermal Conditions, *Ergonomics*, 17 (4), 499-507.
- Google Nest (2018, April 5). Retrieved from <https://nest.com/>
- Gou, W., & Zhou, M. (2009). Technologies toward Thermal Comfort-based Energy-efficient HVAC Systems: A Review, *In: Proceedings of the IEEE International Conference on Systems, Man and Cybernetics*, 3883-3888, USA.
- Gouda, M.M, & Danaher, S. (2011). Thermal comfort based fuzzy logic controller, *Building Services Engineering Research and Technology*, 22 (4), 227-253.

- Guillemin, A, & Morel, N. (2002). Experimental results of a self-adaptive integrated control system in buildings: A pilot study, *Solar Energy*, 72 (5), 397-403.
- Güngör, Ş., Barış, T., & Karadeniz, Z.H. (2018). Thermal characterization of a heat exchanger optimized for additive manufacturing, *In: 7th Rostocker International Conference: THERMAM 2018*, 26-27 July, 1-7, 2018, Germany.
- Hagras, H. (2008). Employing computational intelligence to generate more intelligent and energy efficient living spaces, *International Journal of Automation and Computing*, 5, 1–9.
- Hamdi, M., & Lachiver, G. (1998), Fuzzy control system based on the human sensation of thermal comfort, *In: IEEE International Conference on Fuzzy Systems*, 1, 487 – 492.
- Hang, T., Sarah, C., Lange, T., D'Oca, S., Yan, D., & Corgnati, S.P. (2016), Advances in research and application of energy-related occupant behavior in buildings, *Energy and Buildings*, 116, 694-702.
- Hang, L., & Kim, D.H. (2018). Enhanced Model-Based Predictive Control System Based on Fuzzy Logic for Maintaining Thermal Comfort in IoT Smart Space, *Applied Science*, 8, 1031.
- Hanwei Electronics, MG811 Carbon Dioxide Sensor Datasheet (2018, April 22).
Retrieved from
http://www.datasheet.hk/view_download.php?id=1167564&file=0079\mg811_741654.pdf
- Harrold, M.V., & Lush, D.M. (1988). Automatic controls in building services, *IEEE Proceedings*, 135 (3), 105-133.
- He, M., Cai, W.J., & Li, S.Y. (2005). Multiply fuzzy model-based temperature predictive control for HVAC systems, *Information Science*, 169 (1-2), 155-174.
- Heideri, S. & Sharples, S. (2002). A comparative analysis of short-term and long-term thermal comfort surveys in Iran, *Energy and Buildings*, 34, 607-614.
- Hilliard, T., Swan, L., & Qin, Z. (2017). Experimental implementation of whole building MPC with zone based thermal comfort adjustments, *Building and Environment*, 125, 326-338.
- Hirota, K., & Pedrycz, W. (1991). Fuzzy logic neural networks: Design and computations. *In: International Joint Conference on Neural Networks*, 152-157, Singapore.
- Holland, J.H., *Adaptation in neural and artificial systems*, Ann Arbor: University of Michigan Press, 1975.

- Homod, R. Z. (2018), Analysis and optimization of HVAC control systems based on energy and performance considerations for smart buildings, *Renewable Energy*, 126, 49-64.
- Hossein Sagheby, S. (2018). Active Room-Human Feedback System: Design and Discussion, *REHVA Journals*, 58-61.
- Humphreys, M.A. (1996). Thermal comfort temperatures world-wide-the current position, *Renewable Energy*, 7, 139-144.
- Humphreys, M.A. & Hancock, M. (2007). Do People Like to Feel ‘Neutral’? Exploring the Variation of the Desired Thermal Sensation on the ASHRAE Scale, *Energy and Buildings*, 39, 867–874.
- Hussain, S., Gabbar, H.A, Bondarenko, D., Musharavati, F., & Pokharel, S. (2014). Comfort-based fuzzy control optimization for energy conservation in HVAC systems, *Control Engineering Practice*, 32, 172-182.
- Indrigandi, M. & Rao, K.D. (2010). Effect of age, gender, economic group and tenure on thermal comfort: A field study in residential buildings in hot and dry climate with seasonal variations, *Energy and Buildings*, 42 (3), 273-281.
- INNOVA (2018), Thermal Comfort Sensor, LumaSense Technologies.
- Isawa, K., Shukuya, M., & Komizo, T. (2013). Human-body exergy consumption varying with the combination of room air and mean radiant temperatures, *Journal of Environmental Engineering*, 70, 29-35.
- ISO 7730 (2005a), Moderate thermal environments-determination of the PMV and PPD indices and specification of the conditions for thermal comfort, International Standards Organization, Geneva.
- ISO 10551 (1995). Ergonomics of the thermal environment assessment of the influence of the thermal environment using subjective judgement scales. Geneva: International Standardization Organization.
- ISO 13790 (former 832) (2008). Thermal performance of buildings—calculation of energy use for heating.
- Işık, E., & Inallı, M. (2018). Artificial neural networks and adaptive neuro-fuzzy inference systems approaches to forecast the meteorological data for HVAC: The case of cities for Turkey, *Energy*, 154, 7-16.
- Jang, J.S.R. (1993)., ANFIS: adaptive network-based fuzzy inference systems, *In: IEEE International Conference on Systems, Man and Cybernetics*, 23 (3) 665-685, USA.
- Jawed, A., Larjiani, H., Wixted, A., & Emmanuel, R. (2017). Random neural networks based cognitive controller for HVAC in non-domestic buildings using LoRa, *In:*

*16th International Conference on Cognitive Informatics & Cognitive Computing (ICCI*CC)*, 26-28 July 2017, Calgary, Canada.

- Jazizadeh, F., Ghahramani, A., Becerik-Gerber, B., Kichkaylo, T., & Orosz, M. (2014). User-led decentralized thermal comfort driven HVAC operations for improved efficiency in office buildings, *Energy and Buildings*, 70, 398-410.
- Jazizadeh, F., & Jung, W. (2018). Personalized thermal comfort inference using RGB video images for distributed HVAC control, *Applied Energy*, 220, 829-841.
- Jian, W., & Wenjian, C. (2000). Development of an adaptive neuro-fuzzy method for supply air pressure control in HVAC system, *Systems, Man, and Cybernetics*, In: *2000 IEEE International Conference on Acoustics, Speech, and Signal Processing*, 5, 3806-3809, Istanbul, Turkey.
- Kalaiarasi, S., Gautam, S., Behera, A., & Mewara, M. (2018). Arduino Based Temperature and Humidity Sensor, *Journal of Network Communications and Emerging Technologies (JNCET)*, 8 (4), 329-331.
- Kanarachos, A., & Geramanis, K. (1998). Multivariable control of single zone hydronic heating systems with neural networks, *Energy Conversion Management*, 13 (13), 1317-1336.
- Kang, J., & Park S. (2000), Integrated comfort sensing system on indoor climate, *Sensors and Actuators A*, 82, 302–307.
- Karlsson, H., & Hagentoft, C.E. (2011). Application of model based predictive control for water-based floor heating in low energy buildings, *Building and Environment*, 46, 556-569.
- Kim, J. J. (2004). Arch 315 Environmental Technology I - Lecture Note, TCAUP, University of Michigan.
- Kolokotsa, D., Niachou, K., Geros, V., Kalaitzakis, K., Stavrakakis G.S, & Santamouris M. (2005). Implementantion of an integrated indoor environment and energy management system, *Energy and Buildings*, 37, 93-99.
- Krarti M. (2003). An overview of artificial intelligence-based methods for building energy systems, *Journal of Solar Energy Engineering*, 125 (3), 331-342.
- Kulkarni, A.D, (2001). Computer Vision and Fuzzy-Neural Systems, Printice Hall, New Jersey, USA.
- Kulkarni, M. R., & Hong, F. (2004). Energy optimal control of a residential space-conditioning system based on sensible heat transfer modeling, *Building and Environment*, 39 (1), 31-38.
- Kumar, R., Aggarwal, R.K., & Sharma, J.D. (2013). Estimation of total energy load of building using Artificial Neural Network, *Energy and Environmental Engineering*, 1 (2), 25–35.

- Kumar, P., & Singh, K.P. (2013), Comparative analysis of air conditional system using PID and neural network controller, *International Journal of Scientific and Research Publications*, 3(8), 1-6.
- Lan, L., Wargocki, P., & Lian, Z.W. (2011). Quantitative measurement of productivity loss due to thermal discomfort, *Energy and Buildings*, 43, 1057–1062.
- Li, N. Li, S., Becerik-Gerber, B., & Çalış, G. (2011). Design and Evaluation of Algorithm and Deployment Parameters for an RFID-Based Indoor Location Sensing Solution, *Computing in Civil Engineering*, 77-84.
- Liang, J., & Du, R. (2005). Thermal comfort control based on neural network for HVAC application, *In: Proceedings of 2005 IEEE Conference on Control Applications*, 819-824, Sydney, Australia
- Lightfootmechanical (2018, April 18). Retrived from <https://lightfootmechanical.com/new-construction/>
- Lin, C., Federspiel, C., & Auslander, D. (2003). Multi-Sensor single-actuator control of HVAC systems, *In: International Conference for Enhanced Building Operations*, Berkeley, California, USA.
- Lindelöf, D., Afshari, H., Alisafae, M., Biswas, J., Caban, M., Mocellin, X., & Viaene, J. (2015), Field tests of an adaptive, model-predictive heating controller for residential buildings, *Energy and Buildings*, 99 (1), 292-302.
- Lopez, G., Tokuda, T., & Isoyama, N. (2016). Development of a Wrist-Band Type Device for Low-Energy Consumption and Personalized Thermal Comfort, *In: 11th France-Japan & 9th Europe-Asia Congress on Mechatronics (MECATRONICS)*, 15-17 June 2016, Compiègne, France.
- Luger, F.G., (2009). *Artificial Intelligence; Structures and Strategies for Complex Problem Solving*, Pearson Addison-Wesley, London, UK.
- Lü, H., Jia, L., Kong, S., & Zhang, Z. (2007). Predictive functional control based on fuzzy T-S model for HVAC systems temperature control, *Journal of Control Theory and Applications*, 5, 94-98.
- Ma, J., Quin, J., Salsbury, T., & Xu, P. (2011). Demand reduction in building energy systems based on economic model predictive control, *Chemical Engineering Science*, 67, 92-100.
- Ma, Y., Borrelli, F., Hency, B., Coffey, B., Benga, S., & Haves, P. (2012). Model predictive control for the operation of building cooling systems, *IEEE Transaction Control System Technology*, 20, 796-803.
- Macarulla, M., Casals, M., Forcada, N., and Gangolells, M. (2017). Implementation of predictive control in a commercial building energy management system using neural networks. *Energy and Buildings*, 151, 511–519

- Magnier, L., & Haghghat, F. (2010). Multiobjective optimization of building design using TRNSYS simulations, genetic algorithm, and Artificial Neural Network, *Building and Environment*, 45 (3), 739–746.
- Mamdani, E.H , & Assilian, S. (1975). An experiment in linguistic synthesis with a fuzzy logic controller, *International Journal of Man-Machine Studies*, 7, 1-13.
- Marvuglia, A., Messineo, A., & Nicolosi, G. (2014). Coupling a neural network temperature predictor and a fuzzy logic controller to perform thermal comfort regulation in an office building, *Building and Environment*, 72, 287-299.
- Masato, K.,Tadahiko, M., Yoshiaki, K., & Takanori, Y., Hashimoto, Y., Kamimura, K., Kurosu, S. (1994). Design and tuning of robust PID controller for HVAC systems, *ASHRAE Transactions*, 105 , 154.
- MATLAB (2016). Version 2016 ed.,The Mathworks.
- May-Ostendorp, P., Henze, P.G., Corbin, C.D., Rajagopalan, B., Felsmann,C. (2011). Model-predictive control of mixed-mode buildings with rule extraction, *Building and Environment*, 46(2), 428-437.
- McIntyre, D.A. (1980). Indoor climate, Applied Science Publishers Ltd., London, UK.
- Metcalf, M. & Reid, J. (1992), Fortran 90 Explained. Oxford University Press. ISBN: 0-19-853772-7.
- Metrel (2018, April 28). Retrieved from <https://www.metrel.co.uk>
- Mirinejad, H., Welsh, K.C., & Spicer, L. (2012). A Review of Intelligent Control Techniques in HVAC Systems, *IEEE Energytech*, 1-5.
- Molina, D., Lu, C., Sherman, V., & Harley, R. (2011). Model predictive and genetic algorithm based optimization of residential temperature control in the presence of time-varying electricity prices, *In: Industrial Applications Annual Meeting (IAS)*, 17, Orlando, Florida, USA.
- Moon, J., Jung, S.K, Kim, Y., & Han, S.H. (2011). Comparative study of artificial intelligence based building thermal control- Application of fuzzy, adaptive neuro-fuzzy inference system and artificial neural network, *Applied Thermal Engineering*, 31 (14-15), 2422-2429.
- Morel, N., Bauer, M., El-Khoury, E., & Krauss, J. (2000). Neurobat, a predictive and adaptive heating control system using artificial networks, *International Journal of Solar Energy*, 21, 161-201.
- Morosan, P.D, Bourdais, R., Dumur, D., & Buisson, J. (2010). Building temperature regulation using a distributed model predictive control, *Energy and Buildings*, 42, 1445-1452.

- Mosbybuildingarts (2018, May 5). Retrieved from <http://www.mosbybuildingarts.com/blog/2010/11/24/buying-the-right-hvac-system/>
- Mohsenizadeh, N., Swaroop, D., & Bhattacharyya, S.P. (2011), Synthesis of PID controllers with guaranteed non-overshooting transient response, 50th IEEE Conference on Decision and Control and European Control Conference, 12-15 December 2011, Orlando, Florida, USA.
- Munakata, T. (1998). *Fundamentals of the New Artificial Intelligence: Beyond Traditional Paradigms*, Springer-Verlag, New York, USA.
- Nall, D. H. (2014). Looking across the water: Climate-adaptive buildings in the United States & Europe. *The Construction Specifier*, 57, 50 – 56
- Nassif N. (2014). Modeling and optimization of HVAC systems using artificial neural network and genetic algorithm, *Building Simulation*, 7, 237–245.
- Nassif, N., Moujaes, S., & Zaheeruddin M. (2008). Self-Tuning Dynamic Models of HVAC System Components, *Energy and Buildings*, 40 (9), 1709-1720.
- Nicol, J.F., & Humphreys, M.A. (2002). Adaptive thermal comfort and sustainable thermal standards for buildings, *Energy and Buildings*, 34(6), 563-572.
- Noh, K.C., Jang, J.S., & Oh, M.D. (2007). Thermal comfort and indoor air quality in the lecture room with 4-way cassette air-conditioner and mixing ventilation system, *Building and Environment*, 42 (2), 689-698.
- Nowak, M., & Urbaniak, A. (2011). Utilization of intelligent control algorithms for thermal comfort optimization and energy saving, *In: 12th International Carpathian Control Conference (ICCC)*, 270 – 274, Velke Karlovice, Czech Republic.
- Onset Dataloggers (2018, April 4). Retrieved from <https://www.onsetcomp.com/products/sensors/t-dci-f300-1x3>
- Pedersen, T.H., Knudsen, M.D., Hedegaard, R.E., & Petersen, S. (2017). Handling thermal comfort in economic model predictive control schemes for demand response, *Energy Procedia*, 122, 985-990.
- Persily, A. (1997). Evaluating building IAQ and ventilation with indoor carbon dioxide, *ASHRAE Transactions*, 103 (2), 1-5.
- Prek, M. (2005). Thermodynamic analysis of human heat and mass transfer and their impact on thermal comfort, *International Journal of Heat and Mass Transfer*, 48, 731-739.
- Prek, M., & Butala, V. (2017). Comparison between Fanger's thermal comfort model and human exergy loss, *Energy*, 138, 228-237.

- Privara, S., Siroky, J., Ferkl, L., & Cigler, J. (2011). Model predictive control of a building heating system: The first experience, *Energy and Buildings*, 43, 564-572.
- Ramteke, S., & Parvat, B. (2015). Temperature Control in HVAC Application using PID and Self-Tuning Adaptive Controller, *International Journal of Emerging Trends in Science and Technology*, 2 (2), 1819-1825.
- Ranjan, J., & Scott, J. (2016). ThermalSense: Determining Dynamic Thermal Comfort Preferences Using Thermographic Imaging, *In: ACM International Joint Conference on Pervasive and Ubiquitous Computing*, 1212-1222, Heidelberg, Germany.
- Reena, K.E.M., Mathew, A.T., & Jacop, L. (2018). A flexible control strategy for energy and comfort aware HVAC in buildings, *Building and Environment*, 145,330-342.
- Rice, S. (2003). Health effects of acute and prolonged CO₂ exposure in normal and sensitive populations, *In: 2nd Annual Conference on Carbon Sequestration*, Virginia, USA.
- Rossiter, J.A. (2005). *Model-Based Predictive Control*, CRC Press, Washington, USA.
- Saha, A.K., Sircar, S., Chatterjee, P., Dutta, S., Mitra, A., Chatterjee, A., Chattopadhyay, S.P., & Saha, H.N. (2018). A raspberry Pi controlled cloud based air and sound pollution monitoring system with temperature and humidity sensing, *In: 2018 IEEE 8th Annual Computing and Communication Workshop and Conference (CCWC)*,8-10 June, 607-611, Las Vegas, USA.
- Scheatzle, D. G. (1991). The Development of PMV-Based Control for a Residence in a Hot Arid Climate, *ASHRAE Transactions*, 97 (2),1-5.
- SeedStudio, Grove-Gas Sensor Datasheet (2018, April 14). Retrieved from <https://www.mpja.com/download/31227sc.pdf>
- Seppänen, O.A. , Fisk, W.J. & Mendell, M.J. (1999). Association of ventilation rates and CO₂ concentrations with health and other responses in commercial and institutional buildings, *Indoor Air*, 9, 252–274.
- Shukuya, M. (2013). *Exergy: Theory and Applications in the Built Environment*; Springer: Berlin, Germany.
- Shukuya, M., Saito, M., Isawa, K., Iwamatsu, T., & Asada, H. (2009). Human-body exergy balance and thermal comfort, Working Report of IEA/ECBCS/Annex 49.
- Simone, A., Kolarik, J., Iwamatsu, T., Asada, H., Dovjak, H., Schellen, L., Shukuya, M., & Olesen, B.W. (2011). A relation between calculated human body exergy consumption rate and subjectively assessed thermal comfort, *Energy and Buildings*, 43, 1–9.

- Siroky, J., Olderwurtel, F., Cigler, J., & Privara, S. (2011). Experimental analysis of model predictive control for an energy efficient building heating system, *Applied Energy*, 88, 3079-3087.
- Spengler, J. D., Samet, J. M., & McCarthy, J. F. (2001). Indoor Air Quality Handbook, Chapter 15 Thermal Comfort Concepts and Guidelines, McGraw-Hill.
- Stauffer, Y., Olivero, E., Onillon, E., Mahmed, C., & Lindelof, D. (2017). NeuroCool: field tests of an adaptive, model-predictive controller for HVAC systems, *Energy Procedia*, 122, 127-132.
- Soyguder, S., & Alli, H. (2009). An expert system for the humidity and temperature control in HVAC systems using ANFIS and optimization with Fuzzy Modelling Approach, *Energy and Buildings*, 41 (8), 814-822.
- Soyguder, S., Karaköse, M., & Alli, H. (2009). Design and simulation of self-tuning PID-type fuzzy adaptive control for an expert HVAC system, *Expert Systems with Applications*, 36 (3), 4566-4573.
- SunRom Electronics (2018, April 5). Retrieved from <https://www.mpja.com/download/31227sc.pdf>
- Takagi, T., & Sugeno, M. (1985). Fuzzy identification systems and its applications to modelling and control, *IEEE Transactions on System Man and Cybernetics*, 15, 116-132.
- Tayfur, G. (2012) ,Soft computing methods in water research engineering, WIT Press Southampton, UK.
- Tianlung, N. (2010). Application of Single Bus Sensor DHT11 in Temperature Humidity Measure and Control System, *Microcontrollers & Embedded Systems*,6, 1-15.
- Toksoy, M. (2015). Okullarda İç Hava Kalitesi ve Yönetimi: Günümüz Bilgi ve Pratiği”, MMO, TESKON 2015, In: *12. Ulusal Tesisat Mühendisliği Kongresi* Tepekule, 8 -11 Nisan 2015, İzmir, Türkiye.
- TUIK, Turkish Statistical Institute (2018, May 3). Retrieved from <http://tuik.gov.tr/UstMenu.do?metod=temelist>
- Turhan, C., Simani, S., Zajic, I., & Gökçen Akkurt, G. (2017). Performance analysis of data-driven and model-based control strategies applied to a thermal unit model, *Energies*, 10 (1), 67.
- Turhan, C., & Gökçen Akkurt, G. (2018), Personalized Thermal Comfort Driven Control Techniques in Hvac Systems, In: *13th International HVAC+R & Sanitary Technology Symposium*, 12-14 April 2018, 239-246, Istanbul, Turkey.

- Turhan, C., Kazanasmaz, T., Uygun, İ.E., Ekmen, K.E., & Gökçen Akkurt, G. (2014). Comparative study of a building energy performance software (KEP-IYTE-ESS) and ANN-based building heat load estimation, *Energy and Buildings*, 85, 115-125.
- Turhan, C., Simani, S., Zajic, I., & Gökçen Akkurt, G. (2015). Application and comparison of temperature control strategies to a heating element nonlinear model, *In: The International Conference on Systems Engineering*, August 2015, Coventry, UK.
- Turkish State Meteorological Service (2018 November 1). Retrieved from <https://mgm.gov.tr/eng/forecast-cities.aspx?m=IZMIR>
- Walikewitz, N., Janicke, B., Langner, M., Meier, F., & Endlicher, W. (2015). The difference between the mean radiant temperature and the air temperature within indoor environments: A case study during summer conditions, *Building and Environment*, 84, 151-161.
- Vernier (2018, July 26). Retrieved from <https://www.vernier.com/products/sensors/rh-bta/>
- Wang, G. , & Dai, Y. (2004). Intelligent control of room temperature with variable frequency central air-conditioning, *Journal of Shandong Univeristy of Technology (Sci & Tech)*, 18 (1), 76-81.
- Wang., Z., Lou, M., Zhang, H., & Liu, S. (2018). The Effect of a Low-Energy Wearable Thermal Device on Human Comfort, *In: The 15th Conference of the International Society of Indoor Air Quality & Climate (ISIAQ)*, 22-27 July 2018, Philadelphia, PA, USA.
- Wang, J.J., Zhang, C., Jing, Y., & An, D. (2007). Study of Neural Network PID Control in Variable frequency Air-conditioning System, *In: IEEE International Conference on Control and Automation WeCP-10*, Guangzhou, China.
- Watanabe, S., Shimomura, T., & Miyazaki, H. (2009). Thermal Evaluation of a Chair with Fans as an Individually Controlled System, *Building and Environment*, Vol. 44, 1392-1398.
- Wong, N.H, & Khoo, S.S. (2003). Thermal comfort in classrooms in the tropics, *Energy and Buildings*, 35, 337-351.
- Xi, X.C, Poo, A.N, & Chou, S.K. (2007). Support vector regression model predictive control on HVAC plant, *Control Engineering Practice*, 15, 897-908.
- Yan, H., Pan, Y., Li, Z., & Deng, S. (2018). Further development of a thermal comfort based fuzzy logic controller for a direct expansion air conditioning system, *Applied Energy*, 219, 312-324.
- Yang, S., Wan, M.P., Feng Ng, B., Zhang, T., Babu, S., Zhang, Z., Chen, W., & Dubey, S. (2018). A state-space thermal model incorporating humidity and thermal

comfort for model predictive control in buildings, *Energy and Buildings*, 170, 25-39.

Zadeh, L.A., (1965). Fuzzy sets, *Information and Control*, 8, 338-352.

Zhang, D., Huang, X., Gao, D., Cui, X., & Cai, N. (2018). Experimental study on control performance comparison between model predictive control and proportion-integral-derivative control for radiant ceiling cooling integrated with underfloor ventilation system, *Applied Thermal Engineering*, 143, 130-136.

Zhou, X., Wang, Y., Zhou, Z., & Xiao, B. (2000). Simulation study of fuzzy control based on the variable flow in inverter air conditioner, *Fluid Machinery*, 28 (7), 42-49.

APPENDIX A

THE WIRE DIAGRAM OF PTC-DC

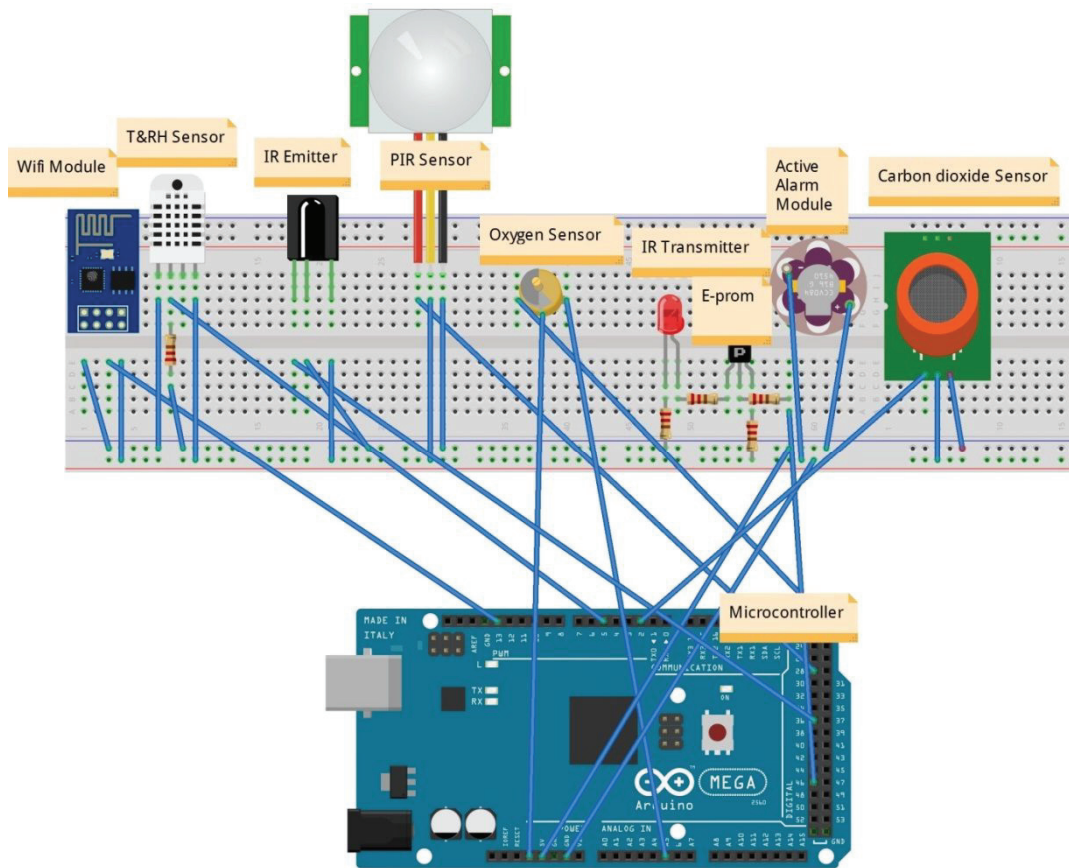


Figure A1- The wire diagram of PTC-DC

VITA

Cihan TURHAN, borned in 1985 in Manisa-TURKEY. After he graduated from Industrial Engineering Department in 2008, he got M.Sc. degree in 2012 from Energy MSc Programme of Izmir Institute of Technology. Between the years of 2008-2018, he worked as a research assistant at Mechanical Engineering Department of Izmir Institute of Technology. He joined a six-month project in 2014 at Ferrara, Italy, and studied with Assist. Dr. Silvio Simani on performance analysis of HVAC (Heating, Ventilating and Air-conditioning) controllers. His research fields are building energy efficiency, advanced HVAC controllers, artificial intelligence for buildings and thermal comfort.

Some of his publications are listed below:

Selected Journal Papers:

1. **Turhan, C.**, Kazanasmaz, T., Erlalitepe Uygun, İ., Ekmen, K.E., & Gökçen Akkurt, G. (2014). Comparative study of a building energy performance software (KEP-IYTEE-ESS) and ANN-based heat load estimation, *Energy and Buildings*, Vol. 85, Pages 115-125.
2. Kazanasmaz, T., Erlalitepe Uygun, İ., Gökçen Akkurt, G., **Turhan, C.**, & Ekmen, K.E. (2014). On The Relation Between Architectural Considerations And Heating Energy Performance Of Turkish Residential Buildings In Izmir, *Energy and Buildings*, Vol.72, 38-50.
3. **Turhan, C.**, Kazanasmaz, T., & Gökçen Akkurt, G. (2017). Performance indices of soft computing models to predict the heat load of buildings in terms of architectural indicators, *Journal of Thermal Engineering*, Vol. 3, No. 4, Special Issue 5, pp. 1358-1374.
4. **Turhan, C.**, Simani, S., Zajic, I., & Gokcen Akkurt, G. (2017). Performance Analysis of Data-Driven and Model-Based Control Strategies Applied to a Thermal Unit Model, *Energies*, Vol.10, 67.
5. **Turhan, C.**, & Gökçen Akkurt, G. (2018). Assessment of Thermal Comfort Preferences in Mediterranean Climate: A University Office Building Case, *Thermal Science*, Vol.22 (5), 2177 – 2187.